DEVELOPMENT OF A TRAFFIC-ACTUATED
SIGNAL TIMING PREDICTION MODEL

By

PEI-SUNG LIN

A DISSERTATION PRESENTED TO THE GRADUATE SCHOOL
OF THE UNIVERSITY OF FLORIDA IN PARTIAL FULFILLMENT
OF THE REQUIREMENT FOR THE DEGREE OF
DOCTOR OF PHILOSOPHY

UNIVERSITY OF FLORIDA

1995

ACKNOWLEDGMENTS

This dissertation cannot be accomplished without the assistance of many people. I wish to express my sincerest thanks to my supervisory committee, dear friends and lovely family who helped make it possible.

First, I would like to express my extreme gratitude to professor Kenneth G. Courage, chairman of my supervisory committee, for giving me the opportunity to pursue my graduate studies under his enthusiastic guidance. He not only provided me the financial assistance but also gave me many levels of support. Every time when I face any difficulty in research, he has always inspired me with his ingenious idea. His lofty standard has always been a source of motivation to me. I will never forget what he has done for me during my studies.

Dr. Charles E. Wallace is the Director of Transportation Research Center. Under his leadership, I felt very warm in my mind when I was in this big family. Although Dr. Wallace was very busy, he always made time for me. He has provided his professional guidance to my research and lofty standard to my dissertation. I deeply believe his comments on my dissertation will be beneficial for my professional career. For this, I am eternally grateful.

Dr. Joseph A. Wattleworth served as one of my committee member. Although he has been retired, his assistance and personal support are sincerely appreciated.

Dr. Sherman X. Bai has been a source of inspiration and motivation. His technical support and personal caring were really invaluable to the success of this research. He has

TABLE OF CONTENTS

LIST OF TABLES

LIST OF FIGURES

Abstract of Dissertation Presented to the Graduate School
of the University of Florida in Partial Fulfillment of the
Requirements for the Degree of Doctor of Philosophy

DEVELOPMENT OF A TRAFFIC-ACTUATED
SIGNAL TIMING PREDICTION MODEL

By

Pei-Sung Lin

December, 1995

Chairman: Kenneth G. Courage
Major Department: Civil Engineering

The Highway Capacity Manual (HCM) provides a methodology in Chapter 9 to

estimate the capacity and level of service at a signalized intersection as a function of the traffic

characteristics and the signal timing. At traffic-actuated intersections, the signal timing

changes from cycle to cycle in response to traffic demand. An accurate prediction of average

phase times and cycle length is required to assess the performance of intersections controlled

by traffic-actuated signals. The current technique in Appendix II of HCM Chapter 9 for this

purpose has not been well accepted.

This dissertation describes a more comprehensive methodology and a more

satisfactory analytical model to predict traffic-actuated signal timing for both isolated and

coordinated modes. The proposed methodology and model have been verified by simulation

augmented by limited field studies. The results are very encouraging with respect to their

general reliability and their compatibility with the current HCM Chapter 9 structure. The techniques developed in this study would provide an important contribution to the methodology of traffic engineering for traffic-actuated signal timing prediction and improve the analytical treatment of traffic-actuated control in the HCM Chapter 9.

CHAPTER 1
INTRODUCTION

The concepts of capacity and level of service (LOS) are central to the analysis of a signalized intersection. Level of service is expressed as a letter grade from A through F that describes the quality of performance of a signalized intersection from the driver's perspective. It is evaluated based on the average stopped delay per vehicle for various movements within the intersection. The 1985 Highway Capacity Manual (HCM) [1] prescribes a methodology in Chapter 9 (Signalized Intersections) to estimate the LOS as a function of the traffic characteristics and the signal timing.

Intersection traffic control is characterized as "pretimed" if a predetermined timing plan is repeated cyclically or "traffic-actuated" if the operation varies from cycle to cycle in response to information from traffic detectors on the roadway. Pretimed control is usually appropriate for constant traffic demand, while traffic-actuated control is better suited to variable traffic demand. Pretimed control is much easier to analyze, but traffic-actuated control offers more in the way of performance to the motorist.

Whether an isolated actuated controlled intersection or a set of coordinated actuated intersections, the operational performance largely depends on traffic patterns and the actuated controller parameters to be discussed in this dissertation. A well-designed actuated control plan that responds appropriately to traffic demand can significantly reduce delay and fuel

1

consumption. More advanced forms of adaptive traffic control strategies were introduced recently, but the traffic-actuated control concepts still play a very important role today. Because of its superiority, traffic-actuated control has become the predominant mode throughout the U.S.A. in spite of its analytical complexity.

Many traffic-related measures at a signalized intersection, such as intersection capacity, vehicle delay and queue length, are determined by the phase times and cycle length. For traffic-actuated control, the phase times and corresponding cycle length vary from cycle to cycle in response to the traffic demand. Therefore, it becomes desirable to predict the average phase times and cycle length for traffic-actuated control which are the main inputs in the procedure contained in the HCM Chapter 9 for the computation of intersection capacity and vehicle delay.

Improvement of the analytical treatment of traffic-actuated control presented in the HCM Chapter 9 is the subject of this dissertation. An enhanced analytical model will be proposed and tested.

Problem Statement

Capacity and delay are two major measures of effectiveness for the analysis of a signalized intersection. The procedure contained in Chapter 9 of the HCM is used almost as a standard to estimate the intersection capacity and vehicle delay. For traffic-actuated operation, accurate estimates of intersection capacity and vehicle delay must rely on accurate estimates of the signal timing. However, the primary technique, presented in an appendix to HCM Chapter 9, to predict the signal timing for traffic-actuated operation has been the subject of much criticism in the literature [2, 3, 4, 5, 6].

This technique is based on the simple assumption that a traffic-actuated controller will maintain a high degree of saturation (95% in the HCM Chapter 9 procedure) on the critical approach to each phase. It does not consider any controller parameter that influences the signal timing in field. This has created many questions in the literature regarding the validity of the assumption and the simplistic nature of the technique. Therefore, the main deficiency of the technique in the appendix to HCM Chapter 9 comes from improper analytical treatment of traffic-actuated control.

Some analytical work has been done on estimating individual phase lengths for traffic-actuated operation [2, 6, 7, 8, 9, 10], but a method for treating the entire phase sequence, given a specified set of traffic volumes, controller parameters and detector placements, does not exist. Simulation is currently the most reliable method for determining the signal timing. Simulation is a powerful tool, but its application is best suited to situations that do not lend themselves to analytical treatment. Furthermore, the signal timing prediction based on simulation is time consuming.

Therefore, the development of a practical analytical technique to predict traffic-actuated signal timing is very desirable. Such a technique would provide an important contribution to the methodology of traffic engineering and improve the analytical treatment of traffic-actuated control in the HCM Chapter 9.

In this case, there are three major questions with the development of the traffic-actuated signal timing prediction model. The first question is whether the model can improve the analytical treatment of traffic-actuated control in the HCM Chapter 9 procedure on signal timing prediction. The proposed methodology must be in a form that can be incorporated

into the HCM Chapter 9 procedure. The second one is whether the model can treat the entire phase sequence for a specified set of traffic volumes, actuated controller parameters, intersection configuration and detector placements. The third question is whether the model can accurately and quickly predict the signal timing for traffic-actuated operation.

Objectives

The signal timing of a traffic-actuated signal will vary from cycle to cycle in response to traffic demand. The goal of this research is to develop an analytical model to accurately predict the average signal timing for traffic-actuated intersection for both isolated and coordinated modes. Although performance measures (delay, stops, queue length, fuel consumption, etc.) are sensitive to actuated controller parameters, it is necessary to note that this study does not include the development of an optimization methodology of the actuated controller parameters. The specific objectives of the research are stated as follows:

1. Review the literature that deals with the subject of traffic-actuated control, particularly related to signal timing prediction and vehicle delay estimation.

2. Develop a model to improve the analytical treatment of traffic-actuated control in the HCM Chapter 9 on signal timing prediction and present the methodology in a form that may be incorporated into the HCM Chapter 9 procedure.

3. Assure that the developed analytical model can predict the average phase times and corresponding cycle length for a specified set of traffic volumes, controller settings, intersection configuration and detector placements.

4. Test and evaluate the analytical model using simulation and limited field data to assess its accuracy and feasibility of implementation.

Organization

This dissertation includes seven chapters that are devoted to developing an analytical model to predict the signal timing for traffic-actuated control. The first chapter provides a general introduction to the dissertation topic, problem statement and research objectives.

The next two chapters describe the development of the proposed analytical model. Chapter 2 presents the background knowledge required for the analytical model development and a preliminary model that deals with protected movements from exclusive lanes only. Chapter 3 extends the methodology developed in Chapter 2 to include shared lanes, permitted left turns and compound left turn protections (permitted plus protected phasing and protected plus permitted phasing).

The implementation of the proposed analytical model and procedure in a computer program to predict traffic-actuated signal timing is addressed in Chapter 4. The computational process of this program is also presented.

The comparisons of predicted phase times between the proposed analytical model and simulation and field data are presented in Chapter 5. An intensive evaluation is also made on the comparison of vehicular arrivals at the stopline produced by simulation and the proposed analytical model.

Chapter 6 presents several refinements of the proposed analytical model to achieve a stronger capability on the phase time prediction. Uniform delay formulations developed in this study for traffic-actuated control are shown in the appendix. The final conclusions and recommendations are stated in Chapter 7.

CHAPTER 2
BACKGROUND

Introduction

There has been a substantial amount of research conducted on traffic-actuated control which provides essential information for traffic-actuated operating characteristics and signal timing prediction. This chapter first reviews past and current research on the traffic-actuated control followed by the presentation of a preliminary model structure of phase time prediction for fully-actuated operation. Each traffic control concept or theory that has contributed to the model development is addressed separately. Next, two simulation models, TRAF-NETSIM (NETSIM) and EVIPAS, which have been adopted by this study as evaluation tools for the proposed analytical model, are introduced. Finally, a preliminary consideration of signal timing prediction for semi-actuated traffic signal coordination is described. Further model development and implementation for traffic-actuated signal timing prediction will be mostly based on the background knowledge presented in this chapter.

Literature Review

Traffic-actuated control has been used since in the early 1930s. Whether an isolated actuated controlled intersection or a set of coordinated actuated intersections, the operational performance is largely determined by the traffic arrival patterns and actuated controller parameters. The arrival patterns refers to the arrival headway distributions. The basic

actuated controller parameters include the minimum green time, maximum green time and allowable gap settings (vehicle interval or unit extension). A well-designed actuated control plan that responds appropriately to traffic demand can significantly reduce delay and fuel consumption. Therefore, shortly after actuated signal control was first introduced, researchers began to study the influence of traffic arrival patterns and departure characteristics at a signalized intersection with traffic-actuated control. Many researchers also focused on the optimization of controller settings, detector placement, and the relationship among them. Recently, some researchers began to develop models to predict traffic-actuated signal timing for the purpose of more accurate capacity computation and delay estimation.

Review of past and current research is an area which definitely merits attention. There has been a substantial amount of research conducted on traffic-actuated control which will contribute to this dissertation.

The development of a traffic-actuated signal timing prediction model is the subject of this study. Thus, the major emphasis of this literature review is on the traffic-actuated control that particularly is related to operation characteristics, vehicle arrival headway distributions and signal timing prediction models. The procedure contained in the HCM Chapter 9 is used almost as a standard to analyze signalized intersection capacity and level of service, so the literature review also covers the methodology for both capacity computation and delay estimation. One item that needs to be reviewed carefully is a new program called EVIPAS. The EVIPAS model is an optimization program which is able to analyze and determine the optimal settings of controller parameters for traffic-actuated control. The results of the testing efforts on EVIPAS are report in this chapter.

The main topics of the literature review include

- Traffic-actuated control definitions;

- Warrants for traffic-actuated control;

- Benefits and operating considerations for traffic-actuated control;

- Effects of coordination and phase-skipping for traffic-actuated control;

- Late-night, low-volume operation of coordinated actuated systems;

- Evaluation of traffic-actuated control by simulation;

- Prediction of phase times and cycle length for traffic-actuated control;

- Delay models for traffic-actuated control;

- Signalized intersection capacity models for traffic-actuated control; and

- Overview and evaluation of "Enhancement of the Value Iteration Program for Actuated Signals" (EVIPAS).

Traffic-actuated Control Definitions

Three basic forms of traffic control: pretimed, fully-actuated and semi-actuated were mentioned by Orcutt [11] in 1975. He indicated that pretimed control was used primarily in the Central Business District (CBD) area, especially where a network of signals must be coordinated. He defined actuated signals in terms of equipment that responds to actual traffic demand of one or more movements as registered by detectors. If all movements are detected, the operation is referred to as "fully-actuated." If detectors are installed for some, but not all, traffic movements, the term "semi-actuated" is applied. Orcutt suggested fully-actuated control should normally be used at isolated intersections.

Precise definitions of the basic controller types were described by the National Electrical Manufacturers Association (NEMA) standards [12] in 1976. According to the NEMA standards, the basic controllers include pretimed, semi-actuated, fully-actuated without volume-density features, and fully-actuated with volume-density features. In the remainder of this dissertation, fully-actuated without volume-density features will be just called fully-actuated control, and fully-actuated with volume-density features will be called volume-density control.

Warrants for Traffic-actuated Control

Warrants for selecting traffic control modes, which are very useful for practicing engineers, have been researched since the early 1960s. Studies of delay at actuated signals have been made for the purpose of evaluating warrants for this type of control on the basis of the information in the 1961 edition of the Manual on Uniform Traffic Control Devices (MUTCD). This information was expanded by the Texas Department of Highways and Public Transportation into a graphical format. The graphical relationships were studied in 1971 by Vodrazka, Lee and Haenel [13], who concluded that they provide good guidelines for selecting actuated equipment for locations where traffic volumes do not warrant pretimed signals. The current edition of the MUTCD stops short of numerical warrants for choosing between pretimed and traffic-actuated control, but it does suggest certain qualitative conditions under which traffic-actuated control should be implemented.

Benefits and Operating Considerations for Traffic-actuated Control

In 1967, Gerlough and Wagner [14] began to compare pretimed control effectiveness with volume-density control. They found that traffic-actuated control at higher traffic

volumes degraded performance. One of the problems cited for volume-density control was that the duration of green for each phase was dependent on the estimated queue length at the beginning of the phase. Difficulties with queue length estimation made this type of control less effective.

Long-loop presence detection operates by producing a vehicle call for the duration of time that the vehicle is over the detector. This is as opposed to the mode of small-area detector operation in which the detector outputs a pulse of less than 0.1 seconds when the vehicle is first detected. This latter mode of operation is known as passage, pulse or count detection. The long-loop presence detector with fully-actuated controllers in a mode known as lane-occupancy control or loop-occupancy control (LOC). LOC operation occurs when the controller is programmed for an initial green interval of zero. Extensions are set either to zero or to a very low value. There is no need for a non-zero initial interval or minimum green time because the long loops continuously register the presence of any vehicles that are waiting, causing the controller to extend the green until the entire queue is discharged. The result is a signal operation that responds rapidly to changes in traffic flow.

In 1970, Bang and Nilsson [15] compared LOC operation with small area detector (pulse detector) operation. They concluded that delay was reduced 10 percent and stops by 6 percent under the same traffic conditions with LOC. In 1975, Cribbins and Meyer [16] compared pulse and presence detectors. They concluded that the longer the length of the presence detector on the major approach to the intersection, the longer the delay. They also concluded that the highest intersection travel time values occurred when either long-loop presence or pulse detectors were used on both major and minor approaches. The intersection

travel time was defined here as the average time it takes a vehicle to pass through an intersection, whether it is stopped or slowed.

Numerous theoretical studies on traffic signal timing were conducted between 1958 and 1970. The theoretical work on pretimed control by Webster [17] in 1958 and Miller [18] in 1963 has been applied to the computation of optimum cycle lengths as a function of vehicle arrival rates. It has also been used for evaluating vehicle delay, intersection capacity, probability of stops and so on. These results were also well validated through the comparison of field data. In 1969, Newell [19] and Newell and Osuma [20] expanded the body of theory by developing relationships for mean vehicle delay with both pretimed and actuated control at intersections of one-way streets and intersections of two-way streets, respectively. Newell [19] demonstrated that the average delay per vehicle for an actuated signal is less than that of a pretimed signal by a factor of about three for intersections of one-way streets. Osuma [20] considered intersections of two-way streets without turning vehicles. For the particular traffic-actuated policy which holds the green until the queue has been discharged, the traffic-actuated control will not perform as well as pretimed control under the following two conditions: 1) flows are nearly equal on both approaches of a given phase and 2) the intersection is nearly saturated.

In 1976, Staunton [21] summarized the work of numerous signal control researchers. In his paper, the comparisons of delay produced by pretimed control and actuated control, as a function of vehicle volumes, were presented. Staunton demonstrated that fully-actuated control with 2.5-sec extensions will always be better than the best form of pretimed operation, given optimum settings for all volumes. Longer values for the extensions can easily degrade

actuated control performance. His conclusions were based on simulation, but the details of the detector configuration were not specified. In view of the 2.5-sec extension time, short or passage detectors were probably used in his study. The performance estimates from Staunton were supported by Bang [22].

In 1981, Tarnoff and Parsonson [23] compiled an extensive literature review on the selection of the most appropriate form of traffic control for an individual intersection. Three complementary approaches were used to evaluate controller effectiveness: 1) field data collection using observers to manually measure vehicle volumes, stops and delay; 2) simulation using the NETSIM model developed by the Federal Highway Administration (FHWA) to evaluate control system performance; and 3) analytical techniques developed by the research team and other agencies. The general conclusions from their extensive literature review were as follows:

1. Pretimed controllers operate most effectively when the shortest possible cycle length is used subject to the constraints of providing adequate intersection capacity and minimum green times for pedestrians and vehicle clearance intervals.

2. The delay produced by fully-actuated controllers is extremely sensitive to the value of the extension that is used. In general, shorter extensions reduce vehicle delay.

3. For small area detectors (motion or pulse detectors), at low and moderate volumes when extensions of two or three seconds are employed, the use of the fully-actuated controllers will reduce delays and stops over those which can be achieved using pretimed controllers. When high traffic volumes occur both on the main street and on the side street causing the controller to extend the green time to the

maximum on all phases, the fully-actuated controller will perform as a pretimed controller, producing comparable measures of vehicle flow.

4. The relative effectiveness of the various control alternatives depends on the quality of the signal timing employed. A poorly timed actuated controller will degrade traffic performance to as great an extent as a poorly timed pretimed controller.

Through the detailed evaluation of controller performance, the conclusions by Tarnoff and Parsonson [23] are described as follows: semi-actuated controllers produce a higher level of stops and delays for all traffic conditions than either the fully-actuated or pretimed controllers. However, for side street traffic volumes that are less than 20 percent of main street volumes, there is an insignificant difference between semi-actuated and fully-actuated controller effectiveness. Fully-actuated controllers produce significant benefits when used in an eight-phase and dual-ring configuration over that which would be possible with a four-phase pretimed controller.

From the simulation results on small area detectors for fully-actuated control, the location of 150 ft produced a level of performance far superior for a 3-sec vehicle interval to that of closer detectors for the approach speed of 35 mph. Tarnoff and Parsonson concluded that it is appropriate to locate the detector such that the travel time is equal to the extension time. It was also concluded that for volumes in excess of 450 vehicles per hour per lane, additional improvement can be realized through the use of the added initial feature of volume-density controller for an approach of 35 mph or higher.

They indicated that further modest gains in performance for fully-actuated control were possible with the use of long loops and short (or zero) initial and extension settings.

This application was found to produce a performance similar to a 2-sec extension time with a short loop. From the simulation results, they concluded that LOC was more effective than pulse detection over a wide range of traffic volumes. LOC offered the further advantage not reflected by the simulation results of screening out false calls caused by vehicles approaching but not traveling through the intersection.

Volume-density controllers provide the greatest benefit at intersections with high approach speeds where a detector setback in excess of 125 ft from the intersection requires a variable initial green time. Tarnoff and Parsonson found that the variable initial and gap reduction options of the volume-density control did not improve the controller's performance over that of a fully-actuated controller unless the option is used to reduce the vehicle extension to a value that is less than the one used for the fully-actuated controller. Thus, if the volume-density controller is timed to provide a 3-sec passage time and a 2-sec minimum allowable gap, its performance will be superior to that of a fully-actuated controller with a constant 3-sec allowable gap. Noted that the above simulation results given by Tarnoff and Parsonson do not properly account for the problem of premature termination of green due to the variation in queue discharge headways that occur under normal operating conditions.

In 1985, Lin [24] studied the optimal timing settings and detector lengths for fully-actuated signals operating in presence mode using the RAPID simulation model. He suggested the optimal maximum green for hourly flow patterns with a peaking hour factor of 1.0 was about 10 seconds longer than the corresponding optimal greens with a peaking hour factor of 0.85, and the optimal maximum green was approximately 80 percent longer than the corresponding optimal greens. This result was similar to the 1.5 times pretimed split

suggested by Kell and Fullerton [25]. Lin indicated that optimal vehicle intervals were a function of detector length and flow rate. For detectors 30 ,50 and 80 ft long, the use of 2-sec, 1-sec and 0-sec vehicle intervals can lead to the best signal performance over a wide range of operating conditions, respectively. The use of vehicle intervals greater than zero second for detectors 80 ft or longer is not desirable unless the combined critical flow at an intersection exceeds 1,400 vph.

In order to improve the VIPAS model, a new optimization algorithm and a new intersection simulation were designed and programmed. The original VIPAS traffic characteristics and vehicle generation routines were combined with these new models to create the enhanced version called EVIPAS. In 1987, Bullen, Hummon, Bryer and Nekmat [26] developed EVIPAS, a computer model for the optimal design of a traffic-actuated signal. The EVIPAS model was designed to analyze and optimize a wide range of intersection, phasing, and controller characteristics of an isolated, fully-actuated traffic signal. It can evaluate almost any phasing combination available in a two to eight-phase NEMA type controller and similar phasing structures for a Type 170 controller. The model has been field tested and validated.

In 1987, Messer and Chang [27] conducted field studies to evaluate four types of basic fully-actuated signal control systems operating at three diamond interchanges. Two signal phasing strategies were tested: a) three-phase and b) four-phase with two overlap. Two small-loop (point) detection patterns (single- and multi-point) were evaluated for each type of phasing. They concluded that 1) single-point detection was the most cost-effective three-phase design; and 2) multi-point detection was the more delay-effective four-phase

configuration. Four-phase control characteristically operates a longer cycle length than the three-phase for a given traffic volume. This feature may produce higher average delays unless the cycle increase is controlled to the extent that the internal progression features of four-phase control can overcome this deficiency.

In 1989, Courage and Luh [28] developed guidelines for determining the traffic-actuated signal control parameters which would produce the optimal operation identified by SOAP84. They also evaluated the existing signal control parameters on an individual traffic-actuated signal. The significant conclusions are summarized as follows:

Under low volumes, the maximum green settings have little or no effect on the performance of actuated signal controllers. Under moderate volumes, shorter maximum greens increase the average delay considerably. Longer maximum greens, however, have no significant effect on delay. Under high volumes, the maximum green settings become more important. There is a setting which minimizes average delay. Other settings with longer or shorter maximum greens will produce more average delays. The optimal maximum green setting can be achieved by running SOAP under actuated control with an optimal saturation level set in the BEGIN card. They indicated that the settings that are optimal at some time may not be appropriate in other times of day.

The value of 0.95, which is the default value used in SOAP actuated control, was suggested for multi-phase operation and a slightly higher saturation level may be desirable for two-phase operation. For approaches with a reasonably even distribution of traffic volume by lane, settings of 4.0, 2.0 and 1.4 seconds were recommended by the study for one, two and three lanes as the best values for unit extension, respectively.

In the same year, Bullen [29] used the EVIPAS simulation and optimization model to analyze traffic-actuated traffic signals. The variables studied were detector type, detector placement, minimum green time and vehicle interval. The evaluation criterion was minimum average vehicle delay. The study showed that the optimum design of a traffic-actuated signal was specific for some variables but relatively unaffected by others. The design was critical only for high traffic volumes. At low volumes, vehicle delay is relatively unaffected by the design parameters studied in his paper. The most critical variable Bullen found was vehicle interval, particularly for passage detectors, where it should be at least 4.0 seconds regardless of detector placement and approach speed. This conclusion somewhat contradicts previous study results. However, it should be noted that the EVIPAS model used by Bullen considered variable queue discharge headways.

Detector configuration is essential to the success of actuated control. Kell and Fullerton [30] in their second edition of the Manual of Traffic Signal Design in 1991 indicated the small area detector might ideally be located three or four seconds of travel time back from the intersection, with the allowable gap set accordingly. Similar principles were proposed in previous research by Tarnoff and Parsonson. Kell and Fullerton also indicated that, in some states, the detectors setback were determined on the safe stopping distance. The main purpose is to avoid the dilemma zone in which a vehicle can neither pass through the intersection nor stop before the stopline. For long loop detectors, they indicated the concept of loop occupancy can provide good operation when vehicle platoons are well formed. The use of several smaller loops instead of one long loop was suggested to solve the problem of random vehicles causing excessive green.

In 1993, Bonneson and McCoy [31] proposed a methodology for evaluating traffic detector designs. They indicated that the safety and efficiency of a traffic detector design can be determined by the probability of max-out and the amount of time spent waiting for gap-out and the subsequent phase change. The stopline detector and advance loop detector with presence and pulse mode were discussed, respectively. The methodology presented by Bonneson and McCoy determined the optimal combination of design elements in terms of safety (via infrequent max-out) and operations (via a short waiting time for phase change). The design elements included detector location, detector length, vehicle speed, passage time settings, and call extension setting). They concluded a large maximum allowable headway will have an adverse effect on performance by increasing the max-out probability and the length of wait for phase change.

Effects of Coordination and Phase Skipping for Traffic-actuated Control

In 1986, Jovanis and Gregor [32] studied the coordination of actuated arterial traffic signal systems. In the past, all optimization methods required that each actuated signal be converted to its nearest equivalent pretimed unit. Using bandwidth maximization as a starting point, a new procedure was developed by Jovanis and Gregor that specifically accounts for actuated timing flexibility. Yield points and force offs at non-critical signals are adjusted so they just touch the edges of the through-band while critical signals are unmodified. This method was applied to a data set describing midday traffic conditions on an urban arterial system of six signals in central Illinois. Simulation was used to evaluate these signal timings and compare them with corresponding pretimed alternatives. They were surprised to find out that pretimed, coordinated control appeared superior in general to actuated coordinated

control in this experiment. They also concluded that the level of service of side streets was much more important for pretimed than actuated strategies.

In 1989, Courage and Wallace [33] developed the guidelines for implementing computerized timing designs from computer programs such as PASSER II, TRANSYT-7F and AAP in arterial traffic control systems. The coordination of a group of traffic-actuated signals must be provided by some form of supervision which is synchronized to a background cycle length with splits and offsets superimposed. Both external and internal coordination of the local controllers were addressed.

This report focused on the external coordination of traffic signal controllers. Permissive periods were introduced to indicate the time interval following the yield point during which the controller is allowed to yield to cross street demand. If the computed splits are longer than the minimum phase times, it might be possible to establish a permissive period without further sacrifice or compromise on the rest of the sequence. The methodology of computing permissive periods was introduced. The effect of phase-skipping due to lack of traffic demand was also presented. The Timing Implementation Method for Actuated Coordinated Systems (TIMACS) program was developed to perform the computations of permissive periods.

Since most previous studies were more specific to certain geometric and phasing combinations, the qualitative and quantitative evaluation methodology for coordinated actuated control needed to be fully investigated. In 1994, Chang and Koothrappally [34] designed a field study to demonstrate the operational effectiveness of using coordinated, actuated control. They concluded 1) there was significant improvement, based on both delay

and number of stops, between the semi-actuated control, fully-actuated, and pretimed coordinated timing during the study; 2) there were no significant differences in performance among all the semi-actuated operations as long as the progression-based signal coordination timing was developed correctly; and 3) the use of longer background cycle lengths generally caused fewer arterial stops. However, it would generate much higher overall system delays.

Late-night, Low-volume Operation of Coordinated Actuated Systems

Coordinating the timing of adjacent signals to promote progressive traffic movement was recognized as one of the most effective means for reducing vehicular stops, delay, fuel consumption and exhaust emissions. Early efforts on the subject of signal control always indicated the need to interconnect signals into a single system and to work toward maximizing progressive movement during peak periods.

In 1990, Luh and Courage [35] evaluated the late-night traffic signal control strategies for arterial systems. They stated that late-night, low-volume arterial signal control involved a trade-off between the motorists on the artery and those on the cross street. The conventional measures of effectiveness such as stops, delay, and fuel consumption were not appropriate for evaluating this trade-off. Luh and Courage proposed a methodology to choose between coordination and free operation on arterial roadways controlled by semi-actuated signals when traffic is light. The choice was made on the basis of a disutility function that was a combination of the number of stops on the artery and the average cross-street waiting time. The results indicated that this method provides a promising tool for late-night arterial signal control.

Evaluation of Traffic-actuated Control by Simulation

Simulation modeling has become an extremely important approach to analyzing complex systems. After 1980, more and more simulation modeling was used in traffic operations. In 1984, Lin and Percy [36] investigated the interactions between queuing vehicles and detectors for actuated controls, which govern the initiation, extension, and termination of a green duration. They emphasized that a model used in the simulation analysis should be calibrated in terms of observed characteristics such as queue discharge headway, arrival headway, the relationship between the arrival time of a queuing vehicle and the departure time of its leading vehicle, the number of queuing vehicles in a defined area at the onset of a green duration, and the dwell time of a vehicle on the detection area. They also indicated, under a presence control, the chance for premature termination of a green duration increases when detector lengths are shortened and a detector length of longer than 80 ft can effectively eliminate the premature termination. Using long detectors, however, results in longer dwell times and may reduce control efficiency.

Lin and Shen [37] also indicated that the modeling of the vehicle-detector interactions should take into account the stochastic aspects of queuing in relation to detectors. The use of average characteristics of departure headway could result in underestimates or overestimates of the probabilities of premature termination of the green.

Later, Lin [38] evaluated the queue dissipation simulation models for analysis of presence-mode fully-actuated signal control. The queue dissipation models used in the NETSIM program and the VIPAS program were evaluated. He indicated that both models were capable of producing realistic departures of queuing vehicles from the detector area.

The models were rather weak, however, in representing other aspects of vehicle-detector interactions. A major weakness of the model in NETSIM was that the simulated movements of queuing vehicles have little to do with the discharge times generated separately from a probability distribution. The weakness of VIPAS was that the Pitt car-following model used in VIPAS did not provide a flexible model structure for calibration. Therefore, the outputs of the model could not be made to conform easily and simultaneously with observed departure, arrival and dwell characteristics of queuing vehicles.

In 1988, Chang and Williams [39] investigated the assumption that independent vehicle arrivals at traffic signals, such as in the Poisson distribution, have been widely used for modeling delay at urban intersections. The study introduced an effective yet economic approach to estimate the degree of correlation among arriving vehicles under given conditions and geometric characteristics. With the proposed technique, traffic professionals can easily determine if the existing delay formulas and other traffic simulation models based on the Poisson distribution are applicable.

The presence of high variability in traffic simulation results often leads to concern about their reliability, and consequently precludes a rigorous evaluation of the target traffic system's performance under various control strategies. In 1990, Chang and Kanaan [40] presented the variability assessment for NETSIM. The batch-means method, which allows the user to assess the variability of parameters, such as the average delay per vehicle, through a single relative long run, was introduced. This study provided a good contribution to traffic simulation users, given the large expenditures on computer simulation.

<u>Prediction of Phase Times and Cycle Length for Traffic-actuated Control</u>

Traffic-related phenomena at a signalized intersection, such as lane capacity, delay and queue length are influenced by the green times (or phase times) and cycle length. For traffic-actuated control, green split and cycle length fluctuate with respect to the traffic demand. Consequently, it becomes desirable to predict the average phases times and cycle length. The phase time is equal to the green time displayed plus intergreen time (clearance interval or duration of yellow plus all-red).

In 1982, Lin [7] began to develop a model to estimate the average phase duration for fully-actuated signals. The model was developed primarily on the basis of probabilistic interactions between traffic flows and the control. He assumed the arrival at the upstream side of an intersection would be at random, so the arrival pattern in each lane was represented by a Poisson distribution. Later, Lin and Mazdeyasna [8] developed delay models for semi-actuated and fully-actuated controls that employ motion detectors and sequential phasing. These models were based on a modified version of Webster's formula. The modifications included the use of average cycle length, average green time, and two coefficients of sensitivity reflecting the degree of delay sensitivity to a given combination of traffic and control conditions. In 1992, Lin [2] proposed an improved method for estimating average cycle lengths and green intervals for semi-actuated signal operations as mentioned before.

In 1994, Akçelik [9, 10] proposed an analytical methodology for the estimation of green times and cycle length for traffic-actuated signals based on the bunched exponential distribution of arrival headway. The discussions in his papers were limited to the operation of a basic actuated controller that used passage detectors and a fixed allowable gap setting.

Both fully-actuated and semi-actuated control cases were studied. A discussion of arrival headway distributions was presented since the estimation of arrival headways is fundamental to the modeling of actuated signal timings. The formulae were derived to estimate the green times and cycle length based on the bunched exponential distribution of arrival headway.

The bunched arrival model was proposed by Cowan [41] and used extensively by Troutbeck [42, 43, 44, 45, 46, 47] for estimating capacity and performance of roundabouts and other unsignalized intersections. The bunched arrival model considers that the bunched relationship between vehicles increases when the flow arrival rate increases. Since the bunched arrival model appears to be more representative of real-life arrival patterns in general, Akçelik used this arrival model for deriving various formulae for the analysis of traffic-actuated signal operations. The random arrival model which uses negative exponential or shift negative exponential distribution of arrival headway can be derived as a special case of the bunched arrival model through simplifying assumptions about bunching characteristics of the arrival stream. The methods given in his papers provide essential information (average green times and cycle length) for predicting the performance characteristics (capacity, degree of saturation, delay, queue length and stopped rate) of intersections.

Delay Models for Traffic-actuated Control

With the increase of computer software, the comparison of different traffic programs for pretimed and actuated controls became intuitively appealing. In 1974, Nemeth and Mekemson [48] compared the delay and fuel consumption between deterministic Signal Operations Analysis Package (SOAP79) and the microscope and stochastic NETSIM simulation for pretimed and actuated controls. They indicated that in terms of delay

prediction, SOAP79 and NETSIM were found to be entirely compatible except for the difference in delay definitions.

In 1988, Akçelik [49] evaluated the 1985 HCM [1] delay formula for signalized intersections. He stated that the HCM formula predicted higher delays for oversaturated conditions. An alternative equation to the HCM formula was proposed. This formula gave values close to the HCM formula for degrees of saturation less than 1.0, and at the same time, was similar to the Australian, Canadian and TRANSYT formulas in producing a delay curve asymptotic to the deterministic delay line for a degree of saturation greater than 1.0.

The signalized intersection methodology presented in the 1985 HCM [1] introduced a new delay model. Lin [3] evaluated the delay estimated by the HCM with field observed delay in 1989. Some inconsistency existed in the delay estimation between the HCM results and field observation. He suggested improving the progression adjustment in the HCM procedure and using a reliable method to estimate average cycle lengths and green durations for traffic-actuated signal operations.

In 1989, Hagen and Courage [50] compared the HCM [1] delay computations with those performed by the SOAP84 and TRANSYT-7F Release 5. The paper focused on the effect of the degree of saturation, the peak-hour factor, the period length on delay computations and the treatment of left turns opposed by oncoming traffic. They indicated that all of the models agreed closely at volume level below the saturation point. When conditions became oversaturated, the models diverged; however, they could be made to agree by the proper choice of parameters. The computed saturation flow rates for left turns opposed by oncoming traffic also agreed closely. However, the treatment of protected plus

permitted left turns produced substantial differences. It was concluded that neither SOAP nor HCM treats this case adequately.

A delay model was recommended in the HCM [1] for level-of-service analysis at signalized intersections. The use of this model for the evaluation of traffic-actuated signal operations required the knowledge of the average green times and cycle length associated with the signal operation being analyzed. Since the method suggested in the HCM to estimate delay of traffic-actuated signal operations was not reliable, Lin [2] proposed an improved method for estimating average green times and cycle length in 1990. The method was appropriate for semi-actuated signal operations. Lin stated that the method was sufficiently simple and reliable. Realistic examples were used to illustrate the application of the method.

In 1993, Li, Rouphail and Akçelik [4] presented an approach for estimating overflow delays for lane groups under traffic-actuated control using the 1985 HCM [1] delay model format. The signal timing used in the delay model was from a cycle-by-cycle simulation model. This study was limited, however, to two-phase single-lane conditions. The results indicated that the signal timings are much related to the controller settings, with longer extension times producing higher cycle length. It was found that overflow delay increases with longer extension times. Further, by applying the 1985 HCM delay formula to the simulated signal settings, the resultant delays were much higher. This implies the need for calibration of the second delay term to account for the actuated control effects.

Signalized Intersection Capacity Models for Traffic-actuated Control

Intersection capacity analysis is essential for measurements of most traffic control effectiveness. The first U.S. Highway Capacity Manual (HCM) in 1950 contained a chapter

for estimating the capacities of signalized intersections. Numerous studies were undertaken to evaluate the different aspects of signalized intersections, and many capacity methods were developed. In 1983, May, Gedizlioglu and Tai [51] began the evaluation of eight available methods for capacity and traffic-performance analysis at signalized intersections including pretimed and actuated controls. The eight methods included the U.S. Highway Capacity Manual method (1965), British method (1966), Swedish method (1977), Transportation Research Board (TRB) Circular 212 planning method (1980), TRB Circular 212 operations and design method (1980), Australian method (1981), National Cooperative Highway Research Program (NCHRP) planning method (1982), and NCHRP operations method (1982). They concluded that the NCHRP operations method and the Australian method were found to be the most cost-effective.

In 1991, Prevedouros [5] studied the traffic measurements and capacity analysis for actuated signal operations. He verified that the methodology in Chapter 9 of the 1985 HCM [1] was not appropriate to treat the pretimed and actuated controls identically, especially concerning the estimation of capacity and performance of existing intersections. The main sources of error and their potential impacts were presented. He developed a comprehensive data collection and analysis methodology to complement the procedure in the 1985 HCM.

Overview and Evaluation of EVIPAS

EVIPAS [52] is an optimization and simulation model for actuated, isolated intersections. It is capable of analyzing and determining the optimal settings of controller parameters for a wide range of geometric configurations, detector layouts, and almost any phasing pattern available in a single or dual-ring NEMA and Type 170 controllers. It will

generate the optimized timing settings for controllers ranging from pretimed to volume-density actuated controllers. The optimum settings of timing parameters include minimum green time, maximum green time, unit extension, minimum gap, time before reduction, time to reduce, variable (added) initial and maximum initial for each phase.

The value of optimal timing is defined as the timing setting which results in the minimum "total cost." The model allows the user to define "total cost: to include a variety of measures of effectiveness, such as delay, fuel consumption, depreciation, other vehicle costs and emissions. The EVIPAS model allows for two modes of operation. In its optimization mode, the model is used to obtain optimal timing settings by a multivariate gradient search optimization module and an event-based intersection microscopic simulation. In the simulation mode, EVIPAS allows the evaluation of a prespecified signal plan just by microscopic simulation.

For the capacity and level of service of traffic-actuated control, the performance outputs are primarily concerned, which includes the summary of delays and signal performance. The summary of delay table provides delay statistics for the intersection and for each approach and lane. The summary of signal performance table shows the average phase length and average cycle length. All above delay measures, average phase length, and average cycle length are based on the microscopic simulation results.

Since both EVIPAS and TRAF-NETSIM are microscopic simulation models, the phase time comparison between these two models becomes necessary. The phase times estimated from the EVIPAS simulation model will be compared with those from NETSIM simulation model later in this chapter.

Preliminary Model Development

The purpose of this study is to accurately predict the average phase times and corresponding cycle length for actuated operations. The preliminary model developed in this study is limited to through movements and left turns with "protected only" phasing from an exclusive lane. However, this preliminary model is very useful for later development of a complete and comprehensive model.

It is important to note that the proposed preliminary model is mainly based on the methodology proposed by Courage and Akçelik [6] for evaluating the operation of a traffic-actuated controller in their working paper NCHRP 3-48-1 for National Cooperative Highway Research Program (NCHRP) project 3-48, "Capacity Analysis of Traffic-actuated Signals."

The proposed analytical model for predicting average phase times and corresponding cycle length applies several traffic engineering concepts and theories. They include traffic-actuated operation logic, dual-ring control concept, average phase time prediction for traffic-actuated signals, queue accumulation polygon (QAP) concept, vehicle arrival headway distribution, circular dependency relationship and sequential process. These concepts and theories are used for both preliminary and comprehensive model development, and their model implementation.

In the discussion of the preliminary model, the method in the Appendix II to HCM Chapter 9 will initially be reviewed following the model development issues. Then, each concept and theory used in the model development will be presented. Finally, the computational framework proposed by Courage and Akçelik [6] for modeling traffic-actuated controller operations will be summarized.

<u>Review of the Appendix II Method to HCM Chapter 9</u>

In the HCM [1] Chapter 9 Appendix II methodology, an actuated signal is assumed to be extremely efficient in its use of the available green time. Thus, the average cycle length is estimated using a high critical volume over capacity ratio (v/c) which is approximately equal to 0.95. In other words, the controller can be effective in its objective of keeping the critical approach nearly saturated. The formula for the average cycle length may be stated as

$$C_{av} = L / (1-Y/X_c) \qquad (2-1)$$

where

C_{av} = the average cycle length;

L = the total lost time per cycle, i.e., the sum of the lost times associated with the starting and stopping of each critical lane group in the phase sequence;

Y = the critical flow ratio, determined as the sum of the flow ratios (v/s) for the individual lane groups that are critical in each phase. The flow ratio for each lane group is defined as the ratio of the traffic volume (v) to the saturation flow rate (s); and

X_c = the target degree of saturation (volume/capacity ratio or v/c ratio). A value of 0.95 is suggested in Appendix II for traffic-actuated control.

After the average cycle length has been computed, the average effective green time (g_i) for each lane group I can be determined by dividing the average cycle length (C_{av}) among lane groups in proportion to their individual flow ratios ($(v/s)_i$) over target degree of saturation (X_c). The formula of average effective green time for each lane group may be stated as

$$g_i = C_{av} [(v/s)_i / X_c] \tag{2-2}$$

The effective green time, rather than the signal displayed green time, is usually used in signal timing computation which is the signal displayed green time plus the intergreen time (change interval or yellow plus all-red clearance) minus the lost time in the phase.

As mentioned before, the Appendix II method for estimating the signal timing for actuated operation has been questioned in the literature. There are three major problems with the Appendix II methodology:

1. The assumption that a traffic-actuated controller will maintain 95% saturation on the critical approach to each phase has not well been accepted. Several studies have indicated that a somewhat lower degree of saturation often results.

2. The effects of actuated design parameters such as minimum green time, maximum green time, unit extension and detector configuration are not reflected in the formula for average cycle length, so it is not sensitive to the above parameters.

3. The simplistic nature of this model does not provide for real-world complications such as minimum or maximum green time setting, shared-lane permitted left turns, left turns that are allowed to proceed on both permitted and protected phases, phase skipping due to lack of demand, constraints imposed by coordination, etc.

In their working paper, Courage and Akçelik [6] indicated that the limitations of Appendix II technique can be overcome, but not without adding considerable complexity to the computational procedures. The HCM has traditionally dealt with "single pass" analytical models that may be described in manual worksheets. The updated version (1994) of HCM Chapter 9 worksheets are analytically much more complicated, however, they have retained,

with one minor exception, their "single pass" characteristics. Therefore, Courage and Akçelik proposed a model with a sequential process of multiple iterations to improve the model addressed in Appendix II with "single pass."

<u>Model Development Issues</u>

Since the entire Chapter 9 methodology has reached the limits of single-pass procedures, the limitations of Appendix II, as mentioned before, cannot be addressed without resorting to complex iterative procedures. Because the limitation of the Appendix II technique is a result of the primitive treatment of actuated control, it may only be overcome by improving the actuated control model. Thus, the model to be developed in this study must be able to perform effective comparisons between the pretimed and traffic-actuated control modes. The model must also be functionally capable of providing reasonable estimate of operating characteristics (timing and performance measures) of traffic-actuated controllers under the normal range of practical design configurations. It must be sensitive to common variations in design parameters. The design parameters include

- Actuated controller settings (minimum green time, maximum green time and allowable gap);

- Conventional actuated vs. volume-density control strategies;

- Detector configurations (length and setback);

- Pedestrian timings (Walk and Flashing Don't Walk, FDW);

- Left turn treatments (permitted, protected, permitted and protected, and not opposed); and

- Left turn phase positions (leading and lagging).

Additional input data are needed to improve the accuracy of the analysis methodology. The information that is already required by the Chapter 9 procedure will naturally be used to the fullest extent possible to avoid the need for new data. Most of the additional data items are related to the operation itself. The proposed model will be based on the standard eight-phase dual-ring control concept that is more or less universally applied in the U. S. A. In this study, a standard assignment of movements to phase is adopted. It can greatly simplify the development and illustration of all modeling procedures without affecting the generality of the capacity and level of service results.

It is difficult to analytically deal with the very low volume operation that typically occurs late at night. Under this condition, the repetitive cyclical operation upon which the analysis is based no longer applies. The effort required to develop a model for dealing accurately with delays of a few seconds per vehicle (i.e., level of service A) is difficult to justify. An approximation of the operating characteristics for very low volumes will generally be acceptable from a capacity and level of service perspective.

In the literature, many analytical studies on traffic-actuated operation assume that passage detectors are used, whereas in actual practice, presence detectors are much more common. Passage detectors transmit a short pulse to the controller upon the arrival of each vehicle. Presence detectors transmit a continuous signal to the controller as long as the vehicle remains in the detection zone. For purpose of this study, variable length presence detectors will be assumed. The operation of using passage detectors to detect vehicles may be approximated by using short length presence detectors.

<u>Traffic-actuated Operation Logic</u>

Actuated operation is one kind of traffic control which uses the information collected by detectors to determine the signal timing of an intersection. The detector type can be either passage or presence. The main advantage of traffic-actuated control is that the traffic signal can properly display the green times according to traffic demand. There are three types of actuated controllers. They are semi-actuated, fully-actuated and volume-density.

The operation of the semi-actuated signal is based on the ability of the controller to vary the length of the different phases to meet the demand on the minor approach. Maximum and minimum green times are set only for the minor street. Detectors are also placed only on the minor street. On the other hand, fully-actuated controllers are suitable for an intersection at which large fluctuations of traffic volumes exist on all approaches during the day. Maximum and minimum green times are set for each approach. Detectors are also installed on each approach. The volume-density control is one kind of actuated control with added features which 1) can keep track of the number of arrivals, and 2) reduce the allowable gap according to several rules. It is usually used at intersections with high speed approaches. For illustration purposes on actuated control logic, a passage detector will first be assumed because it is simple. Some basic term definitions are addressed as follows:

- Initial interval is the first portion of the green phase that an actuated controller has timed out for vehicles waiting between the detector and stopline during the green time to go through the intersection.

- Vehicle interval, also called "unit extension" or "allowable gap" is the time that the green time is extended for each detector actuation.

- Maximum green time is simply the total green time allowed to the phase.

- Minimum green time is the shortest green time that can be displayed.

To avoid vehicles being trapped between the detector and stopline, it is necessary that the vehicle interval be at least the "passage time" of a vehicle from the detector to the stopline.
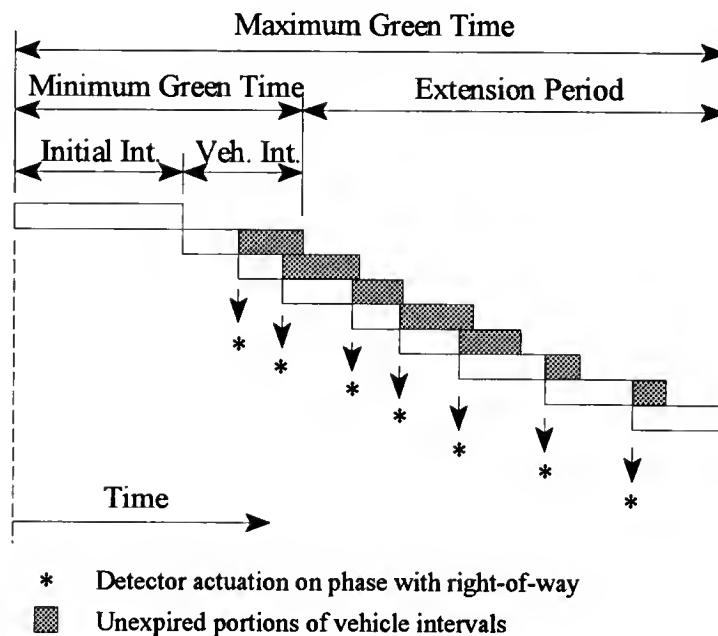
Figure 2-1. The operation of an actuated phase under significant demand.

Figure 2-1 shows the operation of an actuated phase under significant demand. Prior to the beginning of the figure, a "call" for green had been put in by the arrival on the studied approach. Then, the phase with right-of-way on this approach will first display the initial interval plus one unit extension for the arrival. The sum of initial interval and one unit extension is usually called minimum green time. During the minimum green time, if an

additional vehicle arrives, as shown in Figure 2-1, a new unit extension is begun from the time

of detector actuation. The unexpired portion of the old vehicle interval with the shaded area

shown in the figure is wiped out and superseded. If vehicle actuation continues, the green

time will also be extended with the same process until the maximum green time is reached.

The total extension time after the minimum green time is referred to as the extension period.

If the traffic volume is less intense, the extension period will not reach the maximum

green time. When a vehicle interval expires without an arrival of a new vehicle (indicated by

an asterisk [*]), the green time will be terminated and the signal light will turn to yellow plus

red clearance if there is a vehicle waiting for the next subsequent phase. Since in this

illustrated example significant demand is assumed, the maximum green time is reached.

Dual-ring Control Concept

In a pretimed controller, the controller operates under a single ring sequential timing

process. Each phase is taken as an interval of time in which specified traffic movements are

serviced. Of course, it is possible to have a given movement served on more than one phase

of the sequence, and it is expected that a combination of two non-conflicting movements (two

throughs, two left turns or a left turn plus through) will be serviced on any one phase.

However, the vast majority of modern traffic control systems use NEMA standard

traffic-actuated controllers which employ a dual-ring concurrent timing process. By keeping

the non-conflicting phases in separate rings, it is capable of displaying them simultaneously

to optimize the combinations of movements which are displayed on each cycle. Since the

standard eight-phase dual-ring operation is more or less universally applied in the U. S. A.,

and in this study a standard assignment of traffic movements is also based on the dual-ring

NEMA phase configuration, it is essential to be familiar with the dual-ring concurrent phasing scheme with assigned movements. The dual-ring phasing scheme and operation logic will be presented next.

The standard dual-ring concurrent phasing scheme using NEMA phase definition is shown in Figure 2-2. In Figure 2-2 phases 1, 2, 3 and 4 are belong to ring 1, while phases 5, 6, 7 and 8 are belong to ring 2. A specific traffic movement is assigned to each NEMA phase as shown at the corner of each phase box. For example, NEMA phase 2 is an eastbound through movement and NEMA phase 7 is the southbound left turn. In a standard dual-ring concurrent phasing scheme, east-west movements are assigned to the left side of barrier (phases 1, 2, 5, 6), whereas north-south movements are assigned to the right side of barrier (phases 3, 4, 7, 8). The barrier can be reversed to assign north-south movements to the left side and east-west movements to the right side if needed.

Traffic movements for phases 1 and 2 conflict with each other. It is also true for phases 3 & 4, 5 & 6, and 7 & 8. Since the conflicting phases on each ring are sequential, on the side of the barrier, none of the phases within ring 1 will conflict with any of the phases within ring 2. In such a way, non-conflicting phases can be displayed simultaneously to optimize the combinations of movements.

An example of the dual-ring concurrent phasing scheme based on the east-west movement in Figure 2-2 is presented as follows. The phase sequence begins with the non-conflicting combination of NEMA phases 1 and 5. The next phase sequence can be either the combination of NEMA phases 1 and 6 or NEMA phases 2 and 5 according to the traffic demand. If the demand for eastbound left turns is heavier than that of westbound left turns,

in general, the combination of phases 2 and 5 will display most of the time. Finally, NEMA phases 2 and 6 will display.

It is a standard convention to assign the odd number to the left turn in any phase pair (1-2, 3-4, 5-6, 7-8), and the even number to the through movement. This reflects the popularity of leading left turn protection. When the lagging left turn protection is to be implemented, the phase assignment may be reversed (i.e., even number to the left turn). Although any phase may be theoretically designated as the coordinated phase in each ring, it is common to designate the phase with through movement on the left side of the barrier as the coordinated phase. It is necessary to note that the above phasing assignments conform to those used by the PASSER II arterial signal timing. It has also been adopted by the WHICH program for mapping data into NETSIM.
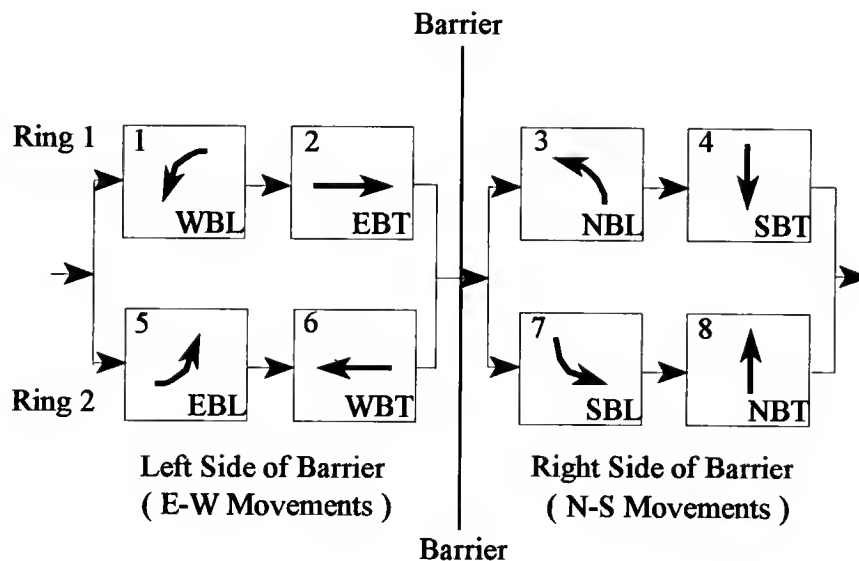
Figure 2-2. Dual-ring concurrent phasing scheme with assigned movements.

Average Phase Time Prediction for Traffic-actuated Signals

The main objective of this study is to accurately predict the average phase times for traffic-actuated signals. The average phase time includes two major portions of timing. One is the queue service (clearance) time and the other is the extension time after queue service. Therefore, accurate phase time predictions are mainly dependent on the accurate predictions of both queue service times and extension times after queue service.

Before the illustration of the methodology to predict average phase times and cycle length, some key term definitions need to be addressed first. The phase time is the signal displayed green time (controller green time) plus the intergreen time. In the signal timing analysis, the effective green time and the effective red time are frequently used. Therefore, appropriate conversion of the displayed green time to an effective value is required before the signal timing analysis.
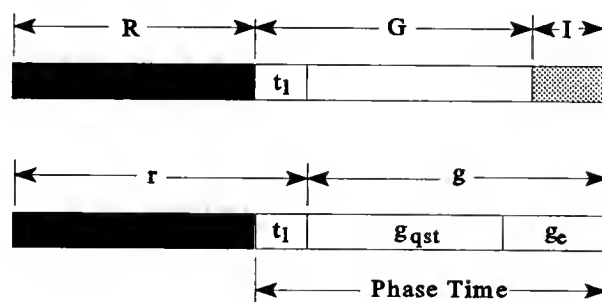
Figure 2-3. The relationships among the components in the phase time.

The relationship among phase time (PT), displayed green time (G) and effective green time (g) shown in Figure 2-3 is expressed as follows:

$$PT \;=\; G + I \;=\; t_l + g \;=\; t_l + g_{qst} + g_e \tag{2-3}$$

$$\text{subject to} \qquad PT_{min} < PT < PT_{max}$$

In more detail, Equation 2-3 can be expressed as follows:

$$PT \;=\; t_{sl} + G_{qst} + E_g + I \;=\; t_{sl} + g_{qst} + e_g + I \;=\; t_{sl} + g_{qst} + g_e + t_{sl} \tag{2-4}$$

$$\text{subject to} \qquad PT_{min} < PT < PT_{max}$$

where

I = intergreen time (yellow plus all-red);

t_l = lost time, which is the sum of start-up lost time, t_{sl}, and end lost time, t_{el};

g_{qst}, G_{qst} = the queue service time (saturated portion of green), where $g_{qst} = G_{qst}$;

e_g, E_g = the green extension time by gap change after queue service, where $e_g = E_g$, and the total extension time, EXT, is defined as (e_g+I) or (E_g+I);

g_e = the effective extension time by gap change after the queue service period,

        where $g_e = e_g + I - t_{el}$;   (2-5)

PT_{min} = the minimum phase time, $PT_{min} = G_{min} + I$, where G_{min} is minimum green time; and

PT_{max} = the maximum phase time, $PT_{max} = G_{max} + I$, where G_{max} is maximum green time.

Queue Accumulation Polygon (QAP) Concept

The analysis of queue accumulation polygon (QAP) is an effective way to predict the queue service time, g_{qst} (= G_{qst}). The QAP is a plot of the number of vehicles queued at the

stopline over the cycle. For a single protected phase which could be the through phase or the protected left turn phase, when traffic volume does not exceed its capacity, QAP is just a single triangle as shown in Figure 2-4. In Figure 2-4, g_s stands for actual queue service time (in this case, $g_{qst} = g_s$), while g_e is the effective extension time after queue service. More complex polygons occur when a movement proceeds on more than one phase.

Based on the vehicle arrival rate q_r during effective red time, the accumulated queue (Q_r) before the effective green time can be estimated. The time taken to discharge the accumulated queue can be computed simply by dividing the accumulated queue of Q_r with the net departure rate ($s - q_g$) which is equal to the departure rate (s) minus the vehicle arrival rate (q_g) during the effective green time. For this simple protected phase, the departure rate s is equal to the saturation flow rate. The target v/c ratio may be considered in the peak hour analysis. However, it must be set to 1.0 to determine the actual queue service time. In order to determine the critical queue service time (g_{qst}) of different lane groups within the same phase, a lane utilization factor is considered in the computation of actual queue service time (g_s). In general, g_s can be estimated from the following formula:

$$g_s = f_q \ f_u \ \frac{q_r r / X_T}{s - (q_g / X_T)} \tag{2-6}$$

where

f_q = a queue length calibration factor [7] proposed by Akçelik to allow for variations in queue service time, where

$$f_q = 1.08 - 0.1 \ (G / G_{max})^2 \tag{2-7}$$

f_u = a lane utilization factor for unbalance lane usage based on the HCM Table

        9-4;

q_r, q_g = q_r is red arrival rate and q_g (veh/sec) is green arrival rate (veh/sec);

X_T = a specified target volume/capacity (v/c) ratio; and

r, s   = r is red time (sec) and s is saturation flow (veh/sec).

In multi-lane cases, the saturated portion of green time should represent the time to clear the queue in the critical lane (i.e. the longest queue for any lane) considering all lanes of an approach in the signal phase. More complex polygons occur when a movement proceeds on more than one phase. The computation for queue service time is mainly based on the QAP concept.
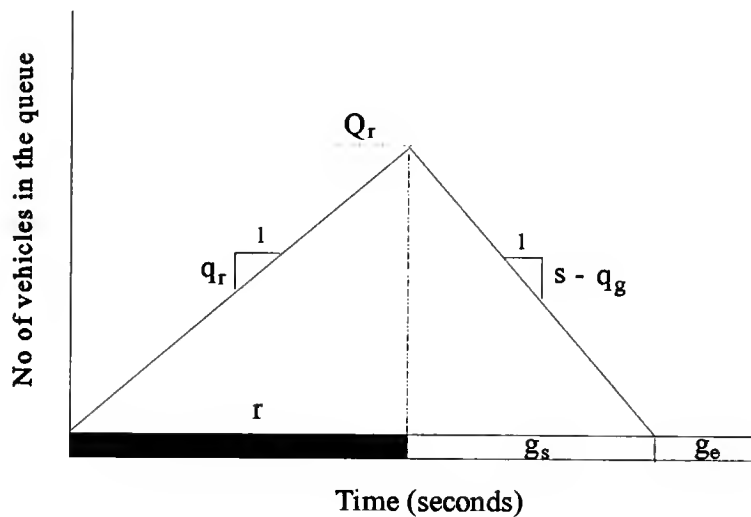
Figure 2-4. Queue accumulation polygon for a single protected phase.

Vehicle Arrival Headway Distributions

Arrival headway distributions play a fundamental role in the estimation of green extension time, e_g (or E_g), at actuated signals. The bunched exponential distribution of arrival headways was proposed by Cowan [36], which considers that the bunched relationship increases among the arriving vehicles when the traffic volume increases. The free (unbunched) vehicles are those with headways greater than the minimum headway (Δ), and the proportion of free vehicles (φ) represents the unbunched vehicles with randomly distributed headways. Thus, the measurement of the proportion of free vehicles (φ) depends on the choice of minimum headway (Δ). The proportion of bunched vehicles in the arrival stream is ($1-\varphi$). In this arrival model, all bunched vehicles are assumed to have the same intra-bunched headway (Δ). The cumulative distribution function, $F(t)$, for this bunched negative exponential distribution of arrival headways, representing the probability of a headway less than t seconds, is

$$F(t) = 1 - \varphi e^{-\lambda(t - \Delta)} \qquad \text{for } t \geq \Delta \qquad (2\text{-}8)$$

$$= 0 \qquad\qquad \text{for } t < \Delta$$

where

Δ = minimum arrival (intra-bunch) headway (seconds);

φ = proportion of free (unbunched) vehicles; and

λ = a parameter calculated as

$$\lambda = \frac{\varphi q}{1 - \Delta q} \qquad (2-9)$$

subject to $q \leq 0.98/\Delta$

where

q = total equivalent through arrival flow (vehicles/second) for all

lane groups that actuate the phase under consideration.

A detailed discussion of the application of this model on actuated control and the results of its calibration using real-life data for single-lane and multi-lane cases are given in Akçelik and Chung [53]. The more commonly used simple negative exponential and shifted negative exponential models of arrival headways are special cases of the bunched exponential model. Therefore, in this study, the bunched arrival model is used to estimate the extension time after queue clearance.

The method for estimating the green extension time, e_g, for an actuated controller that uses a passage detector and a fixed gap time (unit extension) setting (e_o) was described by Akçelik [34]. In this study, presence detectors are assumed. The headway (h) between two consecutive vehicles is equal to the sum of the gap time (e) and the detector occupancy time (t_o). Therefore, the headway, h_o, that corresponds to the allowable gap time setting, e_o, is

$$h_o = e_o + t_o \qquad (2-10)$$

where t_o is the detector occupancy time given by

$$t_o = (L_d + L_v) / v \qquad (2-11)$$

where

L_d = effective detector length (ft);

L_v = vehicle length (ft); and

v = vehicle speed (ft/sec).

There is no need for the estimation of an extension time if the actual queue service time, g_s, is less than the minimum effective green time, g_{min}, or g_s is greater than the maximum effective green time, g_{max}. If $g_s < g_{min}$ then g will be set to g_{min} and if $g_s > g_{max}$ then g is equal to g_{max}. Detection of each additional vehicle between g_{min} and g_{max}, in general, extends the green period by an amount that is, in effect, equal to the headway time, h_o. The green period terminates when the following two conditions are satisfied.

1. the headway between two successive vehicle actuations exceeds the headway that corresponds to the gap time setting, $h > h_o$ (gap change); or

2. the total green extension time after the expiration of minimum green time equals the maximum extension setting. It is equivalent that g is equal to g_{max}.

During a gap change, the green period terminates after the expiration of the gap time. Assuming that the termination time at gap change is the headway corresponding to the gap time setting ($h_o = e_o + t_o$), the green extension time, e_g, by gap change can be estimated from the following formula [6, 9, 10] based on the bunched exponential headway distribution.

$$e_g = \frac{e^{\lambda(e_o + t_o - \Delta)}}{\varphi q} - \frac{1}{\lambda} \qquad (2\text{-}12)$$

Once the green extension time, e_g, is obtained, the effective extension time, g_e, is just equal to the sum of e_g and the intergreen, I, minus the end lost time, t_{el}, as shown in Equation 2-5.

As mentioned before, the more commonly used simple negative exponential and shifted negative exponential models of arrival headways are special cases of the bunched exponential model. For simple negative exponential model, use

$$\Delta = 0 \quad \text{and} \quad \varphi = 1 \qquad \text{(therefore } \lambda = q) \qquad (2\text{-}13)$$

and for the shifted negative exponential model (normally used for single-lane traffic only), use

$$\varphi = 1 \qquad \text{(therefore } \lambda = q / (1 - \Delta q)) \qquad (2\text{-}14)$$

These two models unrealistically assume no bunching ($\varphi = 1$) for all levels of arrival flows. The bunched model can be used either with a known (measured) value of φ, or more generally, with a value of φ estimated as a function of the arrival flow rate. The following relationship suggested by Akçelik and Chung [53] can be used for estimating the proportion of unbunched vehicles in the traffic stream (φ)

$$\varphi = e^{-b \, \Delta \, q} \qquad (2\text{-}15)$$

The recommended parameter values based on the calibration of the bunched exponential model by Akçelik and Chung [53] are:

Single-lane case: $\Delta = 1.5$ seconds and $b = 0.6$ (2-16a)

Multi-lane case (number of lanes =2): $\Delta = 0.5$ seconds and $b = 0.5$ (2-16b)

Multi-lane case (number of lanes > 2): $\Delta = 0.5$ seconds and $b = 0.8$ (2-16c)

Effect of Phase Skip

The minimum phase time requires more attention when the phase may be skipped due to low traffic volume. The minimum phase time would only be valid if the controller was set to recall each phase to the minimum time regardless of demand. On the other hand, the real significance of the minimum phase time in an actuated controller is that a phase must be displayed for the minimum time unless it is skipped due to lack of demand. This situation may be addressed analytically by determining the probability of zero arrivals on the previous red phase. Assuming a bunched arrival headway distribution, this may be computed by using the following equation:

$$P_{0V} = \varphi \ e^{-\lambda \ (R \ - \ \Delta)} \qquad (2\text{-}17)$$

where

P_{0V} = probability of zero arrivals during the previous red phase; and

R = previous red phase time.

So, assuming that the phase will be displayed for the minimum time, except when no vehicles have arrived on the red, the adjusted vehicle minimum time then becomes

$$AVM = MnV \ (1 - P_{0v}) \qquad (2\text{-}18)$$

where

AVM = the adjusted vehicle minimum time; and

MnV = the nominal minimum vehicle time.

The similar concept for adjusted vehicle minimum time may also be applied to compute an adjusted pedestrian minimum time.

If the phase may be skipped due to lack of demand, the adjusted minimum phase time is the maximum of adjusted vehicle minimum time and adjusted pedestrian minimum time. It will be used as lower bound of the predicted phase time. When the P_{0v} for a phase is not zero, the estimated phase time must also be modified by multiplying the $(1-P_{0v})$ factor to the original total extension time. Therefore, the predicted phase time becomes

$$PT = t_{sl} + G_{qst} + (1 - P_{0v})(E_g + I) \qquad (2\text{-}19)$$

Circular Dependency Relationship and Sequential Process

The determination of required green time using the Appendix II method is relatively straight forward when the cycle length is given. However, traffic-actuated controllers do not work on this principle. Instead, they determine, by a mechanical analogy, the required green time or phase time given only the length of the previous red interval. The green time or phase time required for each phase is dependent on the green time or phase time required by the other phases. Thus, a circular dependency relationship exists between actuated phase times.

There are two way to resolve this type of circular dependency. The first one is simultaneous solutions of multiple equations. The second one is a sequential process involving repeated iterations that converge toward a unique solution. Either method could be applied to solve this dependency problem. Since the simultaneous solution will not lend itself to the complications that must be introduced to solve the more general problem, Courage and Akçelik [6] proposed and set up an iterative procedure that will apply to the general problem. This iterative procedure is adopted in this study to predict the average phase time for general cases, not just limited to the protected phases.

An initial set of values for all phase times must be established before the iterative procedure may begin. With each iteration, the phase time required by each phase, given all of the other phase times, may be determined. If the minimum phase times turn out to be adequate for all phases, the cycle length will simply be the sum of the minimum phase times of the critical phases. If a particular phase demands more than its minimum time, then a longer red time will be imposed on all the other phases. This, in turn, will increase the phase time required for the subject phase. Through a series of repeated iterations, the circular dependency will come to an equilibrium and converge to a unique solution. When the convergence of cycle length is reached, the final cycle length and phase times are determined.

This convergence may be demonstrated easily by using an simple example. Consider the intersection shown in Figure 2-5. This is a trivial intersection with four identical single-lane approaches carrying the through volume of 400 vph. A saturation flow rate of 1900 vphgpl is assumed. Each phase has assigned the following constant parameters:

Detector:	30 feet long, placed at the stopline
Intergreen time (I):	4 seconds
Lost time (t_l)	3 seconds per phase
Start-up lost time (t_{sl}):	2 seconds per phase
Minimum phase time:	15 seconds
Allowable gap:	3 seconds
Maximum phase time:	50 seconds

No pedestrian timing features.

No volume-density features.
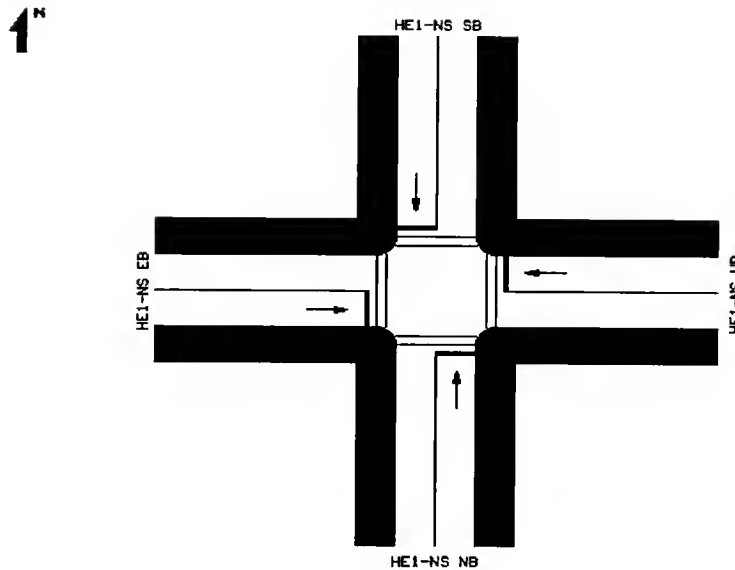
Figure 2-5. The intersection used as an example for circular dependency illustration.

The QAP for the first iteration in this example is shown in Figure 2-6. Initially, the "trial time" is the nominal minimum vehicle time (15 seconds in this case) for each phase. Although this operation has four through phases, it can actually be treated as a two-phase operation because the northbound through phase is identical to the southbound through phase and the eastbound through phase is the same as the westbound through phase.

Hence, the trial cycle length is equal to 15 x 2 = 30 seconds. This initial timing would result in an effective red time of 18 seconds for each phase. The traffic volume for each approach is 400 vehicles per hour. In other words, the arrival rate is equal to 400/3600 = 0.11 vehicles per second. Therefore, during the effective red time, the accumulated queue can be computed as the product of arrival rate and effective red time, which is equal to 0.11 x 18 = 2 vehicles.
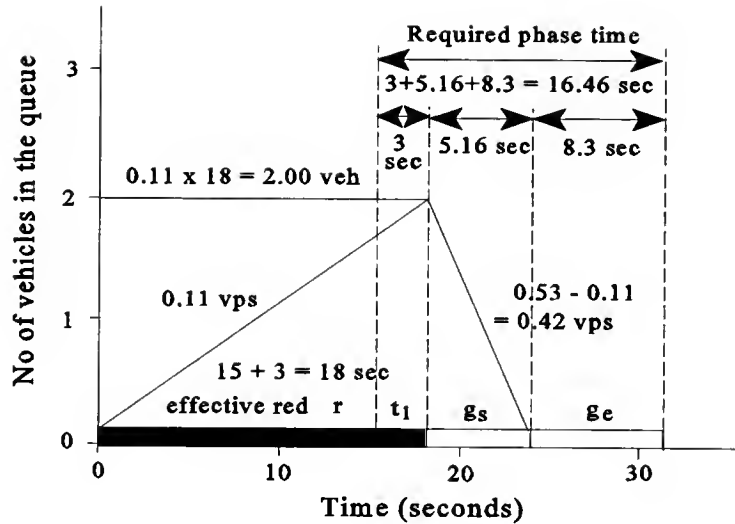
Figure 2-6. Queue accumulation polygon in the first iteration of the illustrated example.

The departure rate is the saturation flow rate (1900 vehicles per hour), so the phase can discharge $(1900/3600) = 0.53$ vehicles per second. Therefore, the net service rate is equal to $(0.53 - 0.11) = 0.42$ vehicle per second. Since f_q is about 1.07 and f_u equals 1.0, the actual queue service time, g_s, taken to discharge the queue will be $(1.07 * 2) / 0.42 = 5.16$ seconds. The extended green time, e_g, is 5.3 seconds and intergreen time, I, is 4 seconds. Thus, the total extension time, EXT $(= e_g + I)$, is 9.3 seconds $(= 5.3 + 4)$ and the effective extension time, g_e, equals 8.3 seconds $(= 5.3 + 4 - 1)$. By using Equation 2-3, the phase time, PT, equals the sum of the lost time, t_l, the queue service time, g_{qst}, $(= g_s$ in this example) and the effective extension time, g_e, which is about 16.46 seconds $(= 3 + 5.16 + 8.3)$. By using Equation 2-4, PT is equal to the sum of t_{sl}, g_{qst} $(= g_s$ in this example) and EXT which is also about 16.46 seconds $(= 2 + 5.16 + 9.3)$. The new phase times produce a new cycle length

of (16.46 x 2) = 32.92 seconds. This will generate another version of Figure 2-6 with different dimensions. By repeating these calculations with a new cycle length each time, the computed cycle length will converge to within 0.1 second. Convergence for this example is especially rapid. The process is very reliable. Table 2-1 shows the iteration result and convergence for this trivial example.

Table 2-1. The iteration results and its convergence for the illustrated example.

Iteration	Cycle (sec)	Old phase time (sec)	Acc. queue	Total service time (= $t_{sl} + g_s$) (sec)	Total ext. time (= $e_g + I$) (sec)	New phase time (sec)	New cycle (sec)	Difference (sec)
1	30.0	15.0	2.00	7.16	9.3	16.5	32.9	2.9
2	32.9	16.5	2.16	7.57	9.3	16.9	33.7	0.8
3	33.7	16.9	2.21	7.68	9.3	17.0	33.9	0.2
4	33.9	17.0	2.22	7.71	9.3	17.0	34.0	0.1

Computational Process

The computation framework with five worksheets proposed by Courage and Akçelik [6] for modeling traffic-actuated controller operations for simple through and protected left turn phases is adopted by this study as the basis for more complicated and general model development. This computation process will be introduced here. The worksheets play a very important part in overcoming the "black box" image of a complex model such as the one in this study. They provide a structure for presenting the results of intermediate computations in a common form that is compatible with their proposed techniques.

Worksheet 1 is "Traffic-actuated Control Data Input". "Lane Group Data" is shown

in Worksheet 2. Worksheet 3 is "Traffic-actuated Timing Computation" and Worksheet 4

is "Required Phase Times". The last worksheet, worksheet 5, is "Extension Times Based on

Allowed Gaps". The worksheet format offered a clear and concise way to document the

information. This format is also consistent with the current HCM. While the worksheets

themselves are quite simple, the overall procedure contains iterative loops. In this research,

the worksheets proposed by Courage and Akçelik will be modified and enhanced for the

computation of more general and complicated scenarios, not just limited to simple protected

scenarios. The complete procedure involving the five worksheets is illustrated in Figure 2-7.

This figure shows the five worksheets, the main information flow path and two iterative

loops indicated as "Loop A" and "Loop B".
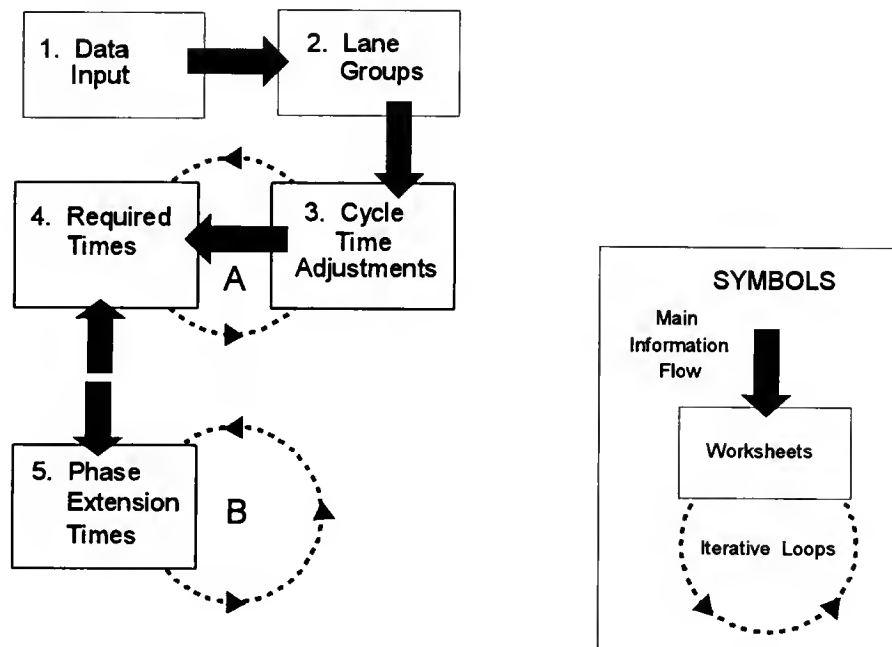
Figure 2-7. Iterative loops in the phase time and cycle time computation procedure.

- Loop A. Required Time - Cycle Time Adjustment: This is an external iteration between Worksheets 3 and 4. It is required to make the phase times converge to a stable cycle length. Worksheet 4 must also refer to Worksheet 5 if phase time extensions are required to compute the required phase times.

- Loop B. Phase Extension Time: This is an internal iteration within Worksheet 5. It is only required when gap reduction is employed. When the allowable gap is a function of the phase time, the phase time cannot be computed without iteration.

<u>Simulation Models</u>

Simulation is one of the most powerful analysis tools available to those responsible for the design and operation of complex process and systems. Simulation might have more credibility because its behavior has been compared to that of a real system, or because it has required fewer simplifying assumptions and thereby has captured more of the true characteristics of the real system.

NETSIM, a popular and powerful microscopic traffic simulation model, has been continually developed by the Federal Highway Administration (FHWA) for many years. NETSIM is able to model an eight-phase, dual-ring controller explicitly, recognizing all of the phase-specific parameters. EVIPAS is an optimization and simulation model for actuated controlled, isolated intersections. In the simulation mode, it is also capable of providing simulated phase times for a wide range of actuated parameter settings. Thus, both the NETSIM and EVIPAS simulation models could be used as tools to verify the phase time estimation from the proposed analytical model.

<u>Comparison between NETSIM and EVIPAS Simulation Results</u>

Since both NETSIM and EVIPAS are simulation-based models, it becomes necessary to compare the simulation results between EVIPAS and NETSIM. The current version of NETSIM (β version 5.0) produces very detailed tables of several performance measures. It does not, however, provide sufficient information on the operation of the controller itself in the standard output tables. To obtain this information, it was necessary to develop a postprocessor to extract the operational data from special files used to support the animated graphics features of NETSIM.

The actuated-controller data for each second of operation are recorded and stored in a text file that is given a file name with extension of ".F45" by NETSIM. The format of ".F45" files is hard to read. After it is properly converted, a readable text file can be produced with extension of ".X45". Then, a postprocessor was developed to read the .X45 file and produce a summary of the operation. Both conversion and postprocessor were combined into a program called "NETCOP" for "NETSIM Controller Operation Postprocessor." It provides phase-specific information such as percent skipped, percent gapout, percent maxout, average cycle length, average phase time, adjusted cycle length and adjusted average phase time. The "adjusted cycle length" is computed by subtracting the number of seconds of dwell (i.e., the time during which no demand was registered on any phase) from the total number of seconds simulated before dividing by the number of cycles. The adjusted phase time is computed according to the adjusted cycle length. Since the adjusted phase time from NETSIM can represent the effective use of phase time, it is adopted for later phase time comparison.

Although the simulation techniques used in EVIPAS and NETSIM may differ in some degree, theoretically, the phase time estimates for the same traffic conditions, geometric configurations and actuated timing settings should be close. Thus, an evaluation has been made by comparing the simulated phase times from both NETSIM and EVIPAS based on 9 hypothetical examples with traffic-actuated operations. These examples cover both two-phase and multi-phase actuated operations. The comparison result is shown in the Figure 2-8.

In a simple regression analysis between the above two simulated phase times, a 0.96 coefficient of determination, R^2, was achieved. As expected, the simulated phase times from EVIPAS are very close to those from NETSIM simulation, which demonstrates that the EVIPAS model has the similar effectiveness on phase time estimation as NETSIM.
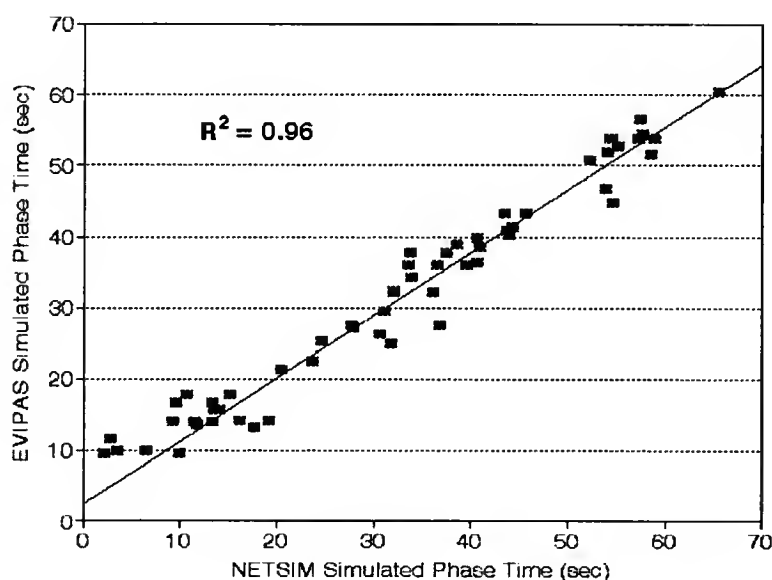
Figure 2-8. Phase time comparison between EVIPAS and NETSIM.

Arterial Considerations

As urban roadways become more congested, and resources available for building new facilities become more limited, transportation professionals are exploring all possible alternatives to improve the existing transportation systems. Fully-actuated traffic signals are powerful for isolated intersections, but not proper for coordinated intersections. One major area that holds great potential in reducing urban congestion is the implementation of coordinated semi-actuated traffic signals on arterial streets. Unlike pretimed signals, semi-actuated signals are intrinsically more intelligent and complex to implement and they provide a better coordination than pretimed signals [34].

In semi-actuated operation, detectors are placed only on the minor street and exclusive left turn lanes on the major street. No detectors are installed for the through movements on the major street. Under this operation, once there is no detection on the minor movements, the green will always come back to the through (coordinated) movements on the major street. Therefore, the major benefit of using semi-actuated control is to assign unused minor street green to the major street. This concept is fundamental to the signal timing prediction for coordinated semi-actuated operation.

In pretimed control, the phase time of each movement is fixed, so the effective green over cycle length ratio (g/C) for each movement is a constant. Unlike pretimed signals, the phase time of each lane group for actuated signals does not stay constant but fluctuates from cycle to cycle, so the g/C ratio for each movement fluctuates. Therefore, the major difference between pretimed and traffic-actuated intersections lies in the g/C. The g/C ratio is important because it is required for the capacity and delay computation. It is necessary to note that the

coordination for actuated signals must be provided by some form of supervision which is synchronized to a background cycle length. Since coordinated semi-actuated control is frequently used at intersections along an artery, the g/C ratio of the critical through-lane group on the major street is especially important.

The true g/C ratio of each movement is difficult to access in current practice directly from a traffic controller. Therefore, an alternative for obtaining the g/C ratio is needed. It is found, in general, that the g/C ratio on a major street is high when the demand on minor streets is low, and vice versa. This observation suggests the potential for using minor street traffic demand measures to predict the major street g/C ratio. To verify the concept of the assignment of unused minor street green to the major street, attempts have been made to quantify the relationship between the major street g/C ratio and minor street traffic demand.
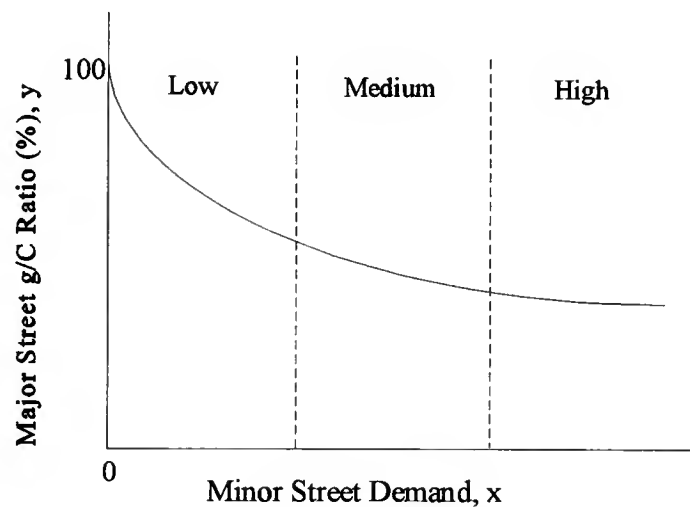
Figure 2-9. Conceptual relationship between major street g/C and minor street demand.

Since traffic volume and detector occupancy are easy to measure with reasonable accuracy for minor street demand, a conceptual model focusing on these two variables was developed to predict the major street g/C ratio. As the minor street demand, x, increases from zero, the major street g/C ratio, y, should start as a sharply decreasing function. The rate of decrease should attenuate as x increases. The conceptual relationship between y and x is shown in Figure 2-9.

Data Acquisition

Data from a closed loop signal system were used for the calibration of the candidate models. The data set includes 98 intersection records generated from four coordinated semi-actuated intersections during seven time periods along SW 34th St. in Gainesville, Florida. A layout of the arterial system is shown in Figure 2-10. The SW 34th St. artery is a major street, and Radio Rd., Hull Rd., SW 20th Ave. and Windmeadows are four minor streets. Protected left turn signals exist on the major street at all four intersections.
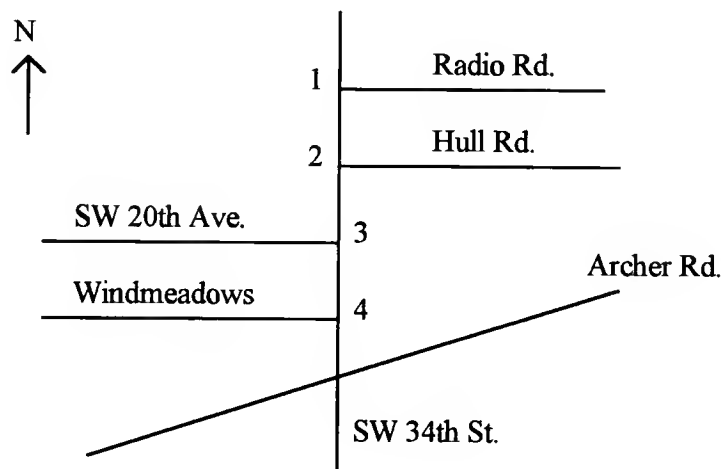
Figure 2-10. The location of four studied intersection.

The Traffic Actuated Controller Monitor/Analyzer (TACMAN) computer package [54] uses information collected by a microcomputer-based control system, the Signalized Intersection Monitor (SIMON) [54], to produce hourly phase-specific descriptive information and performance measures. The descriptive information includes traffic volume, detector occupancy, etc., and performance measures include stops, delay and fuel consumption. The measures used in the study pertain to the critical movements.

<u>Model Calibration</u>

Statistical Analysis System (SAS) [55] programs were applied to perform correlation and regression analyses. Regression techniques were used to calibrate the parameters of the conceptual models. Regression results show that either the minor street volume or detector occupancy can explain most of the variation in the major street g/C. Furthermore, the F and t values indicate that both candidate models are overall significant and the coefficients in each model are also individually statistically significant. The power model (volume model) produced the highest adjusted R^2 using the traffic volume data, while the logarithmic model (occupancy model) was better for detector occupancy data. These two models can be expressed as follows:

$$MAJG = 100(1 + 0.01 \ VOLUME)^{-0.3045} \qquad Adj. \ R^2 = 0.88 \qquad (2\text{-}20)$$

$$MAJG = 100 - 12.0954 \ LN(1 + OCCUPANCY) \qquad Adj. \ R^2 = 0.91 \qquad (2\text{-}21)$$

where

MAJG = g/C ratio (%) for the major street critical through movement;

VOLUME = hourly volume for the minor street critical movement; and

OCCUPANCY = hourly detector occupancy for the minor street critical movement.

The curves for these two minor street demand measures are shown in Figures 2-11 and 2-12, respectively. As expected, the shape of both curves conforms to the described conceptual model. Although the occupancy model might be slightly better than the volume model, the volume model may frequently be used because minor street volumes are often known, estimated or forecast when no information is available about detector occupancy.

Based on the concept that the unused minor street green time is assigned to the major street in coordinated semi-actuated operation, the relationship between the g/C ratio of the critical through-lane group on a major street (major street g/C ratio) and the traffic demand of the critical movement on minor streets (minor street demand) was quantified by the above volume model and occupancy model. In the further study, this concept will continue to be implemented in the phase time estimation for coordinated semi-actuated operation.
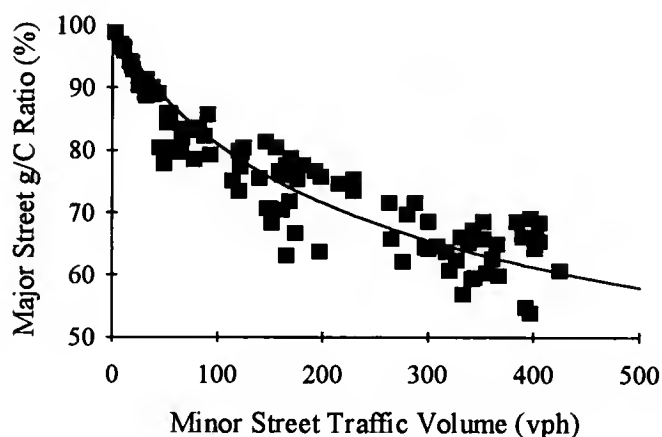
Figure 2-11. Prediction of the major street g/C ratio based on a power model for minor street traffic volume.
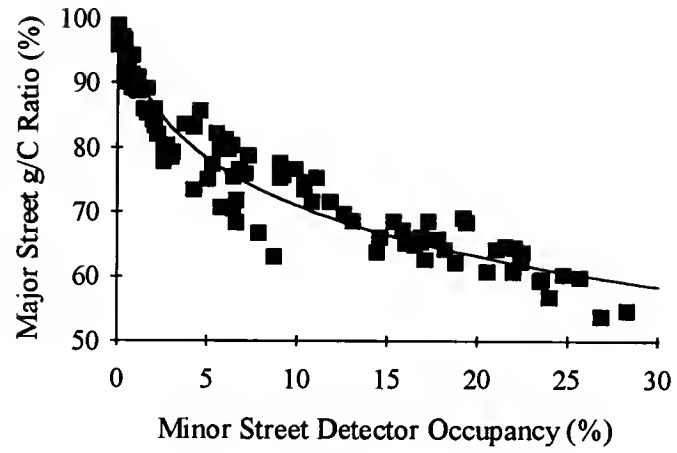
Figure 2-12.   Prediction of the major street g/C ratio based on a logarithmic model for minor street detector occupancy.

CHAPTER 3
MODEL DEVELOPMENT

Introduction

The scope of the preliminary model development presented in chapter 2 was limited to basic through movements and protected left turn movements from an exclusive lane. This chapter continually explores the analytical basis for extensions of the preliminary methodology to cover permitted left turns in both shared and exclusive lanes and the complicated compound left turn protection (i.e., protected plus permitted phasing or permitted plus protected phasing).

Determination of Arrival Rates

In the previous analytical work, the arrival and departure rates were constant parameters determined externally. The arrival rates were determined by the specified traffic volumes and the departure rates were determined by the saturation flow rates. Neither depended on the signal timing. In fully-actuated operation which is very often used at an isolated intersection, the progression effect is not considered, therefore, the arrival type 3 (green arrival rate = red arrival rate) is appropriate. For coordinated semi-actuated operation, since the progression effect is an important consideration, the use of different arrival types to represent progression quality is required. The derivation of arrival rate is presented first in this chapter for later application on coordinated semi-actuated intersections.

63

With arrival type 3, the arrival rate is constant over the whole cycle at q veh/sec. With other arrival types, two different arrival rates must be computed. q_g is the arrival rate on the green phase, and q_r is the arrival rate on the red phase. For a given average arrival rate, the values of q_g and q_r will depend on the platoon ratio, R_p, associated with the arrival type, and the green ratio, g/C, which is a part of the timing plan. The HCM defines the platoon ratio as follows:

$$R_p = P C / g \tag{3-1}$$

where

P = the probability of arrival on the green;

g = the green time for the phase; and

C = the cycle length.

Basic Continuity Relationship: $q_r r + q_g g = q(r+g)$
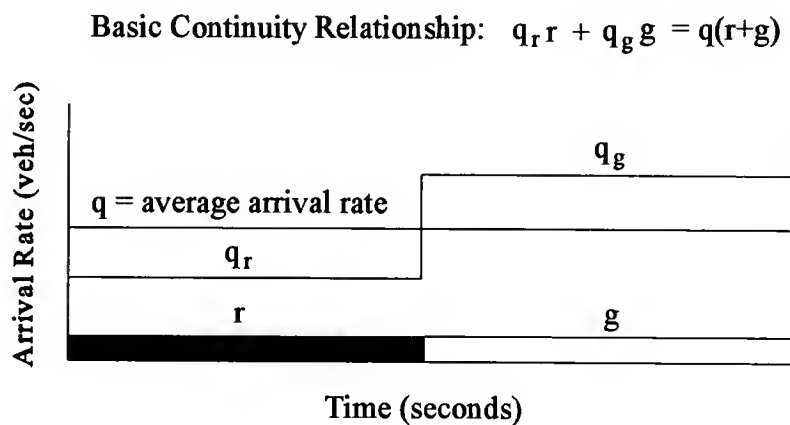
Figure 3-1. Arrival rate over a full cycle with coordinated operation.

From Equation 3-1,

$$P = R_p \, g/C$$

Now, with arrival type 3, $R_p = 1$, so $P = g/C$, and $q = q_g = q_r$. On the other hand, if $R_p \neq 1$,

then the arrival rates will be different on the red and green phases, as illustrated in Figure 3-1.

The problem is to determine q_r and q_g given q, R_p, g and C.

From Equation 3-1:

$$R_p = \frac{P(r+g)}{g}$$

But, by definition,

$$P = \frac{gq_g}{q(r+g)}$$

So,

$$R_p = \frac{gq_g(r+g)}{q(r+g)g}$$

or,

$$R_p = \frac{q_g}{q}$$

Therefore,

$$q_g = qR_p \qquad\qquad (3\text{-}2)$$

As an extension of this derivation, the red arrival rate may be determined from the continuity

relationship shown on Figure 3-1.

$$q_r r \; + \; q_g g \; = \; q(r+g)$$

From which,

$$q_r r \; = \; q(r+g) \; - \; (q R_p) g$$

Therefore,

$$q_r \; = \; \frac{q(r+g) \; - \; (q R_p) g}{r} \qquad\qquad (3\text{-}3)$$

Permitted Left Turn Phasing

Before beginning the discussion of permitted left turn (LT) phasing, the concept of green time determination for a protected phase is briefly reviewed first. This concept is based on the queue accumulation polygon (QAP) shown in Figure 3-2 which was presented earlier. It is convenient to be shown here again for the illustration. The QAP shows the number of vehicles accumulated in a queue on a signalized approach over one cycle of operation. Each cycle is assumed to repeat the same pattern indefinitely. The number of vehicles accumulated at any time in the cycle may be determined as the difference between the cumulative arrivals and departures since the start of the cycle.

The queue accumulation increases throughout the red phase at the rate of q_r veh/sec. The maximum accumulated queue occurs at the end of the red phase, and is indicated on Figure 3-2 as Q_r. During the green phase, the queue decreases at the net departure rate, (s - q_g), until it has been fully serviced. The time required to service the actual queue is indicated on Figure 3-2 is g_s. The green phase will continue until the occurrence of a gap in the arriving

traffic of sufficient length to cause the controller to terminate the phase. The effective extension time is indicated on Figure 3-2 as g_e. Of course, this whole process is subject to a specified maximum phase time. An analytical model for predicting g_s, g_e and average phase time, PT, was presented in the preliminary methodology. In this simple case, the queue accumulation polygon is just a triangle. In the remainder of the cases to be discussed in this dissertation, the QAP will assume a more complex shape.
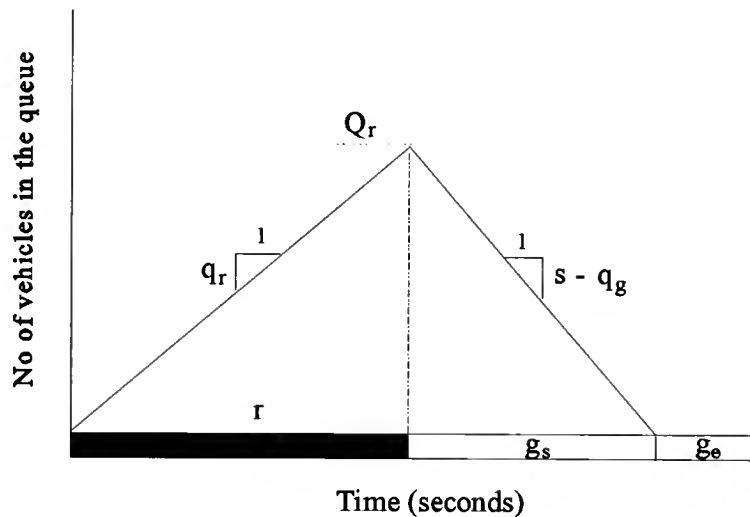
Figure 3-2. Queue accumulation polygon for a single protected phase.

Permitted Left Turns from Exclusive Lanes

The basic QAP concept may be extended to cover a slightly difficult case in which a permitted left turn is from an exclusive lane, yielding to oncoming traffic, instead of a protected movement. This introduces a couple of important changes in the QAP. Since the number of opposing lanes, n_{opp}, may influence the net arrival rate during the period when the opposing queue is being serviced, it will be considered for the permitted left turns form

exclusive lanes. Based on the number of opposing lanes, the QAPs for condition 1 ($n_{opp} > 1$) and condition 2 ($n_{opp} = 1$) shown in Figures 3-3 and 3-4 are discussed, respectively.

If the number of opposing lanes is greater than one (see Figure 3-3), the queue continues to accumulate throughout the first part of the green with the arrival rate of q_g while the opposing queue is being serviced. The time required to service the opposing queue is indicated on Figure 3-3 as g_q. There is no chance for a permitted left turner to make a maneuver during the period of g_q. The maximum queue, indicated on Figure 3-3 as Q_q, can be computes as follows:

$$Q_q = Q_r + q_g * g_q \qquad (3-4)$$

If the number of opposing lane is equal to one (see Figure 3-4), the left turns from the opposing lane do create the chance for the left turns from the exclusive left turn lane to make maneuvers. According to the HCM Chapter 9, the adjusted saturation flow rate, s_q, during the period of g_q can be computed using the following formula:

$$s_q = s / E_{L2} \qquad (3-5)$$

where

s_q = the permitted saturation flow rate during the period of g_q;

s = the protected saturation flow rate; and

E_{L2} = the left turn equivalence as determined from Equation 9-22 in the HCM.

the queue continues to accumulate throughout the period of g_q with the net green arrival rate of $(q_g - s_q)$ while the opposing queue is being serviced. The maximum queue, indicated on Figure 3-4 as Q_q, can be computes as follows:

$$Q_q = Q_r + (q_g - s_q) * g_q \qquad (3-6)$$

Thereafter, the LT vehicles will filter through the opposing traffic at a rate determined by the opposing volume. This is indicated on Figures 3-3 and 3-4 as the permitted saturation flow rate, s_p. The net departure rate is shown as the difference between the permitted saturation flow rate and the green arrival rate, which is equal to $(s_p - q_g)$. Fortunately, the HCM Chapter 9 worksheets already provide the means to compute these values. The value of g_q is determined explicitly on the supplemental worksheet for permitted left turns. The value of permitted saturation flow rate, s_p, may be determined as

$$s_p = s / E_{L1} \qquad (3-7)$$

where

s_p = the permitted saturation flow rate;

s = the protected saturation flow rate; and

E_{L1} = the left turn equivalence as determined from Figure 9-7 in the HCM.
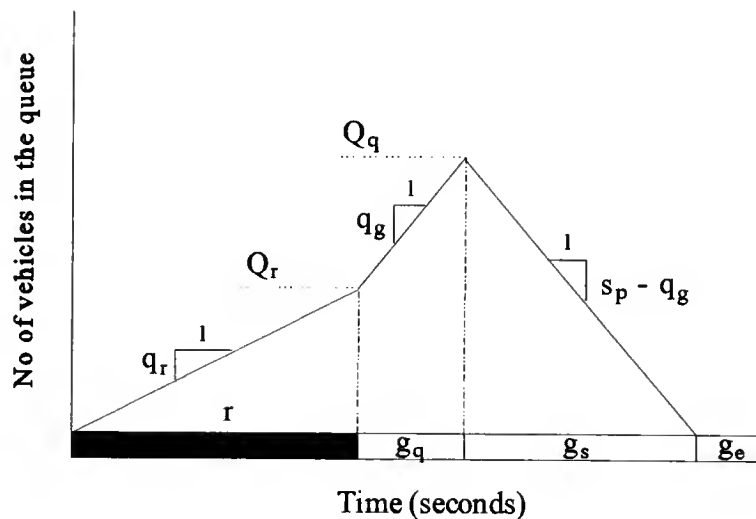
Figure 3-3. Queue accumulation polygon for a permitted left turn from an exclusive lane with opposing lane number greater than one.
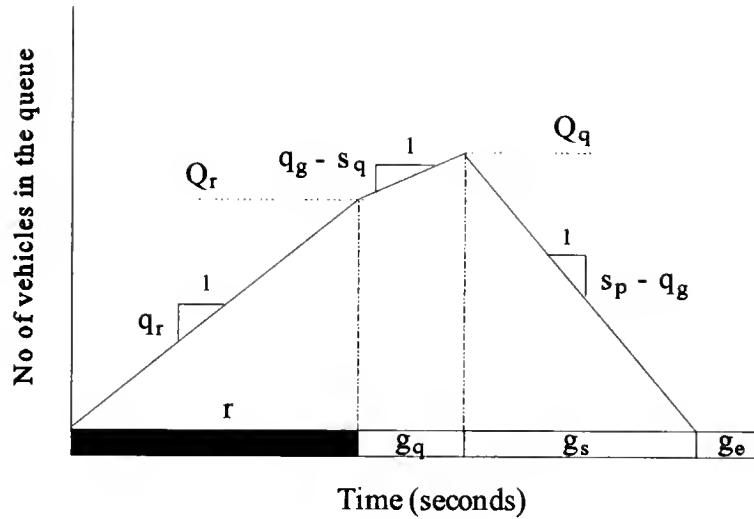
Figure 3-4. Queue accumulation polygon for a permitted left turn from an exclusive lane with opposing lane number equal to one.

Green Time Extension for Permitted Movements

The model for estimating the effective green time extension, g_e, assumes that the arrivals after the queue has been serviced will be free-flowing as they cross the detector. This will not be the case for permitted left turns. A complex stochastic model would be required to treat this situation in detail.

It should, however, be possible to use the left turn equivalence, E_{L1}, described above as an approximation in this situation. In other words, the equivalent through volume, $V_L E_{L1}$, would be used in place of the actual left turn volume, V_L. The green extension time must be determined using an equivalent through volume of $(V_T + V_L E_{L1})$ in place of the actual volume of $(V_T + V_L)$.

<u>Effect of Sneakers</u>

Sneakers are permitted LT vehicles that exit the intersection at the end of the green phase, usually during the intergreen interval. It is common to assume that a maximum of two vehicles per cycle may be released from the queue. Sneakers are treated implicitly in the Chapter 9 worksheets by imposing a lower limit of two vehicles per cycle on the capacity of each exclusive LT lane with permitted movements. For purposes of this analysis, sneakers must be recognized explicitly in the QAP. This requires the definition of some new terms:

- Maximum Sneakers, S_m: The maximum number of LT vehicles released at the end of the green phase assuming that the LT queue has not already been serviced.

- Permitted phase terminal queue, Q_p: The number of vehicles accumulated at the end of the permitted phase before sneakers have been released.

- Adjusted permitted phase terminal queue, Q_p': The number of vehicles accumulated at the end of the permitted phase after sneakers have been released.

- Actual Sneakers, S_a: The actual number of sneakers released at the end of the green phase. This is determined as Min (S_m, Q_p).

For the purpose of illustration, the effect of sneakers on the QAP for the condition, $n_{opp} > 1$, is shown in Figure 3-5. This illustrates the case in which the phase is terminated by the maximum green time before the queue of LT vehicles is completely serviced. If Q_p is greater than zero, then the maximum phase length will be displayed as a pretimed equivalent. The adjusted permitted phase terminal queue, Q_p', is equal to Q_p minus S_a. If Q_p' is greater than zero, then the v/c ratio for the approach will be exceeded. These parameters will be involved in a more complex way in the analysis of compound left turn protection.
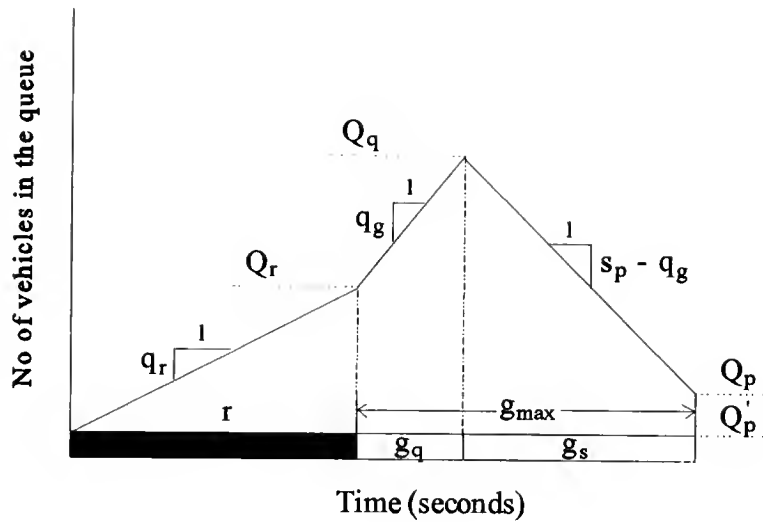
Figure 3-5. Queue accumulation polygon for a permitted left turn from an exclusive lane with sneakers.

Multi-Lane Approaches

If LT vehicles are accommodated in an exclusive lane, it is reasonable to assume that there will be additional lanes available to handle the through traffic. It is also expected that the detectors installed in both the through and left turn lanes will activate and extend the same phase. Under these conditions, the queue service time, g_{qst}, for the through and LT lanes will be different. The required phase time (RPT) is the sum of lost time (t_l), effective extension time ($g_e = e_g + I - t_{cl}$) and the maximum value of through queue service time, g_{qst} ($= g_s$), and left turn queue service time, g_{qst} ($= g_q + g_s$):

$$RPT = \text{Max (Through } g_{qst}, \text{ Left turn } g_{qst}) + t_l + g_e \qquad (3\text{-}8)$$

and e_g must be determined using an equivalent through volume of $(V_T + V_L E_{L1})$ in place of the actual volume of $(V_T + V_L)$.

Shared Lane Permitted Left Turns

The shared lane permitted left turn case is only slightly more complicated than the exclusive lane permitted left turn case. The additional complication may be seen in the QAPs shown in Figures 3-6 and 3-7. The concept of free green, g_f, must be introduced here. In an exclusive left turn lane, the first vehicle in the queue will always be an LT vehicle. However, in a shared lane, the first vehicle could be either a through or LT vehicle. The portion of effective green blocked by the clearance of an opposing queue is designated as g_q. During the time, an LT vehicle may be stopped by the opposing traffic, but a through vehicle will not. Until the first left-turning vehicle arrives, however, the shared lane is unaffected by left turners. The free green represents the average green time from the beginning of green that will be available to move through vehicles in the shared lane. The Chapter 9 supplemental left turn worksheets provide a method for computing g_q and g_f. As indicated on Figures 3-6 and 3-7, there will be a net discharge rate of $(s - q_g)$ during the free green interval, and the queue remaining at the end of the interval is represented as Q_f.

The computation for queue service time, g_{qst}, is more complicated for a shared lane than that for an exclusive left turn lane or through lane. Basically, the g_{qst} for a shared lane can be divided into two parts. One is the green time before the beginning of the actual queue service time (g_s), and the other one is g_s itself.

In Figure 3-6, since g_q is greater or equal to g_f, the g_{qst} is just equal to the sum of g_q and g_s. Note that according to the HCM Chapter 9, Q_q can be computed based on the number of the opposing lanes. The detail description for the computation of Q_q is in the HCM Chapter 9. Figure 3-7 represents the scenario that g_q is less than g_f. The accumulated queue,

Q_r, which belongs to through vehicles, will be served at a net service rate of $(s - q_g)$. Assume the time to clean all of these accumulated through vehicles is designated as g_t. If g_f is less than g_t, then g_{qst} will equal the sum of g_f and g_s. On the other hand, if g_f is greater or equal to g_t, then g_{qst} just equals g_t because g_s is zero for this condition. The time to clear all accumulated through vehicles, g_t, may be represented by Equation 2-6. The computation for g_{qst} may be summarized as the following equations. If g_q is greater than or equal to g_f, the queue service time, g_{qst}, can be computed as

$$g_{qst} = g_q + g_s \tag{3-9}$$

If g_q is less than g_f, the formula for the computation of the queue service time, g_{qst}, becomes

$$g_{qst} = g_f + g_s \qquad \text{when} \quad g_f < g_t \tag{3-10}$$

$$g_{qst} = g_t \qquad \text{when} \quad g_f \geq g_t \tag{3-11}$$

The remainder of Figures 3-6 and 3-7 follows the same process as the exclusive lane cases shown in Figure 3-3 and 3-4. The permitted movement saturation flow rate for the shared lane must, however, be computed somewhat differently. In an exclusive LT lane, the left turn equivalence, E_{L1}, was applied to all of the vehicles in the LT lane. In a shared lane, it is only appropriate to apply this factor to the LT vehicles. So, s_p should be computed as

$$s_p = \frac{s}{1 + P_L(E_{L1} - 1)} \tag{3-12}$$

where

$P_L =$ the proportion of left turns in the shared lane, as computed by the supplemental

worksheet for permitted left turns, and all other terms are as defined previously.

e_g should be computed in the same manner as described for the exclusive LT lane case and using an equivalent through volume of $(V_T + V_L E_{L1})$ instead of the actual volume.
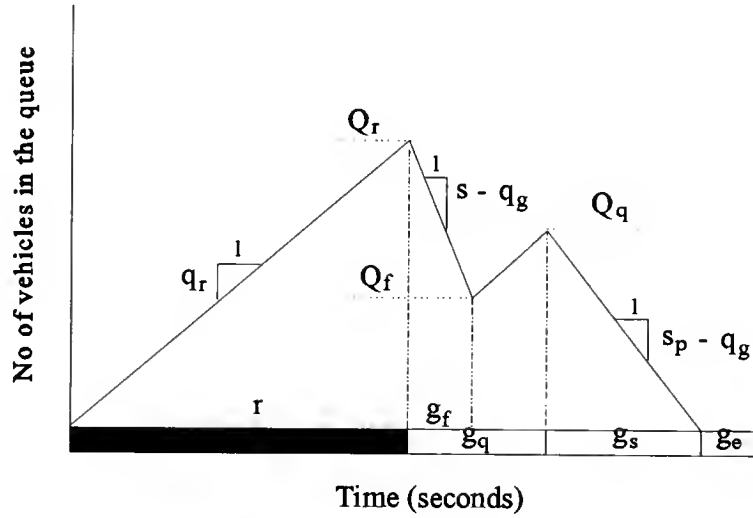
Figure 3-6. Queue accumulation polygon for a permitted left turn from a shared lane $(g_q \geq g_f)$.
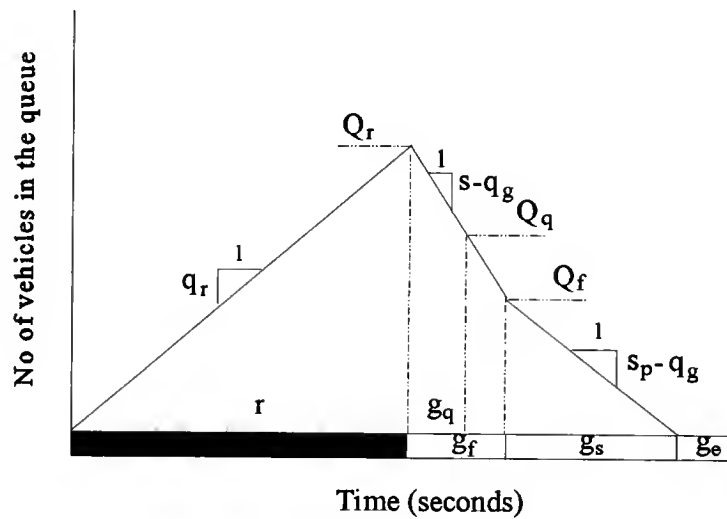
Figure 3-7. Queue accumulation polygon for a permitted left turn from a shared lane $(g_q < g_f)$.

Compound Left Turn Protection

The QAP concept may be extended to cover the case in which an LT movement

proceeds on both permitted and protected phases from an exclusive lane. One important

difference between the simple permitted LT phasing and the compound protected LT phasing

is the assignment of detectors to phases. It is assumed that detectors will be installed in all

LT lanes to ensure that LT vehicles will not face a permanent red signal. The discussion of

simple permitted LT phasing assumes that the detector in the LT lane (either shared or

exclusive) will actuate the same phase as the concurrent through traffic. On the other hand,

it is logical to assume that a protected left turn will have a detector that actuates the protected

left turn phase. This has very important implications for the analysis of compound left turn

protection. It means that LT vehicles will not extend the permitted phase. When they occupy

the detector during the permitted phase, they will simply be placing a call for their own

protected phase. In the analysis of compound left turn protection, it is necessary to make a

strong distinction between protected plus permitted (leading), and permitted plus protected

(lagging) left turn phasings. Each of these cases will be analyzed separately.

Protected Plus Permitted Phasing

The QAP for protected plus permitted phasing is presented in Figure 3-8. In Figure

3-8, it is necessary to note that if the number of opposing lanes, n_{opp}, is greater than one, s_q

will be equal to zero. Keep in mind that the QAP is used for the purpose of determining the

length of the protected phase only. The length of the permitted phase will be determined by

the simple process of its corresponding through phase because there are no permitted left

turns that actuate the detector. The The most important piece of information provided by

the QAP in this case is the size of the queue accumulated at the beginning of the green arrow, Q_{ga}. With protected plus permitted phasing, this is equal to the queue at the end of effective red time, Q_r. Given Q_{ga}, the determination of green time follows the simple procedure for protected movements.
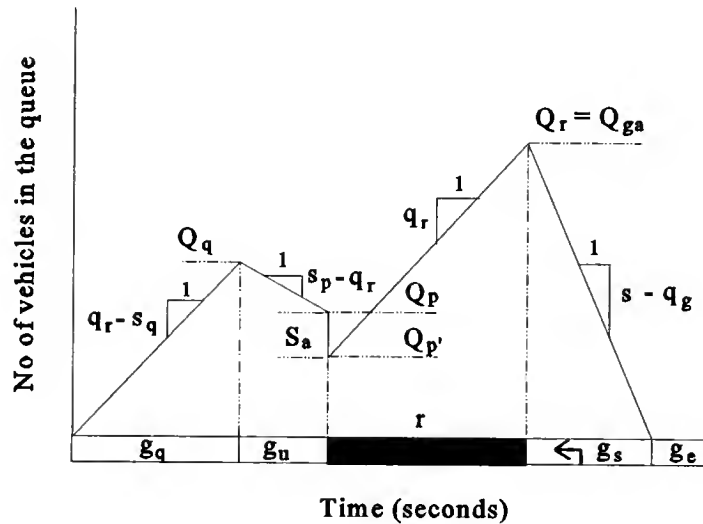
Figure 3-8. Queue accumulation polygon for protected plus permitted LT phasing with an exclusive LT lane.

Permitted Plus Protected Phasing

This case is illustrated in Figure 3-9, which is essentially the same as Figure 3-8, except that the order of the phases has been reversed. It is very important to note that the protected (green arrow) phase must be presented last in both cases, because this is the phase whose length we are trying to determine.

Again, it is needed to know the number of vehicles accumulated at the beginning of the green arrow phase, Q_{ga}, which is equal to Q_p' in this case. This will raise an interesting

question. Suppose that the value of Q_p' is zero. This could happen if the permitted phase was able to accommodate all of the left turns. Theoretically, the protected phase should never be called under these conditions. However, there is a stochastic element which dictates that all of the phases will be called occasionally. In this scenario, the adjusted minimum phase time will be used to estimate the phase time for this protected phase.
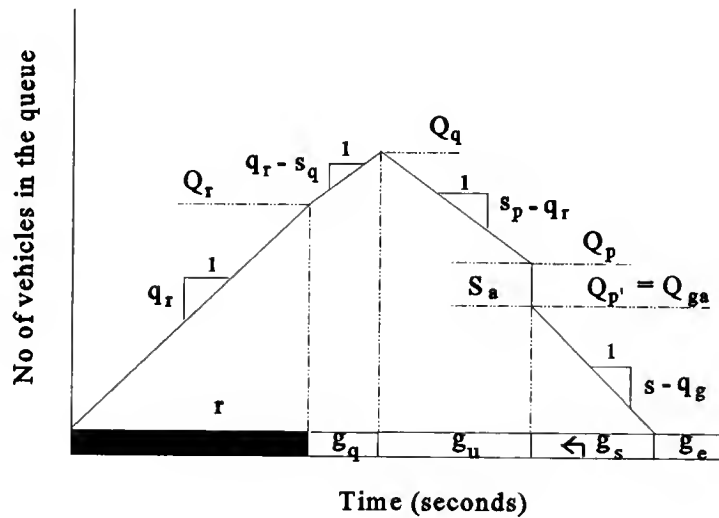
Figure 3-9. Queue accumulation polygon for permitted plus protected LT phasing with an exclusive LT lane.

Applications

The analysis presented in this chapter fills the gaps left in the preliminary methodology. The complete analytical basis for a practical computational method to predict traffic actuated signal timing are conducted. This method should be sensitive to a wide range of actuated controller parameters. The QAP concept is especially attractive because it can provide a clear picture for estimating the signal timing. Another essential benefit is that it can

also provide a direct estimate of the uniform delay that is compatible with the current HCM

Chapter 9 delay model. The methodology presented in this chapter will be incorporated into

the computational framework described in the preliminary model structure to develop a

complete model implementation for predicting the signal timing at a traffic-actuated signalized

intersection. The model implementation and model evaluation will be presented in the next

two chapters, respectively.

CHAPTER 4
MODEL IMPLEMENTATION

Introduction

A specific analysis program, ACT3-48, was developed by Courage and Lin in this study as a tool to implement the developed analytical model and procedure to predict the traffic-actuated signal timing. The original worksheets have also been modified in accordance to the analytical model to cover all possible movements described in Chapter 3. The ACT3-48 program can produce intermediate outputs in a format identical to the modified worksheets. The computer program is required because the iterative nature of the procedure makes it totally impractical for manual implementation. The program is able to evaluate the proposed analytical models using a variety of data. In this chapter, the computer program structure and logic are presented.

The analytical model developed in this study is for isolated mode of actuated operation. An effective method to predict the phase times for coordinated mode of actuated operation is to apply the analytical model for isolated mode to predict the phase times of actuated phases and then properly assign the unused phase times to the non-actuated phases (arterial through movements). By appropriate implementation of the analytical model for isolated mode, a procedure has been built to predict the phase times for coordinated mode, which will also be addressed in this chapter.

Structure and Logic of the ACT3-48 Program

The major structure of the ACT3-48 program is shown in Figure 4-1. It is not difficult to recognize an iterative loop inside the flow chart. The iterative loop is required to make the cycle time converge to a stable value. The program structure is divided into six major parts: 1) Data Input, 2) Lane Group Specification, 3) Accumulated Queue Computation, 4) Extension Time Computation, 5) Required Phase Time Computation, and 6) Cycle Time Adjustments. These six parts will be addressed separately.

Data Input

The data input for the ACT3-48 program is from the WHICH program, which not only has a user-friendly input scheme, but also provides sufficient information for actuated operations. After the data is input, the ACT3-48 program can be executed from WHICH to process these data and compute phase times.

In the "control specification" shown in Figure 4-1, control treatments are determined first according to the input data. These treatments include left turn types (protected, permitted or compound protection), phase swaps and overlaps. In addition, a left turn equivalence, E_{L1}, is computed. Finally, the phase sequence pattern is recorded.

The phase sequence pattern needs to get more attention because in each iteration, it is required for the accumulated queue computation and phase time prediction. The computation of most time elements such as g, r, g_f and g_q in the QAP are also based on the phase sequence pattern. The initial phase pattern is from the input of WHICH. Due to the dual-ring control logic, the phase sequence pattern may change during the iterative process. Therefore, possible phase sequence patterns are required to be considered in the program.

Start

↓

Data Input
from
WHICH

↓

Control
Specification

↓

Worksheet 1 ← Actuated
Parameter
Specification

↓

Worksheet 2 ← Lane Group
Specification

↓

Queue
Length
Computation → Green Model → Worksheet 3

Green Model → Worksheet 4
and
Worksheet 5

Green Model ↓↑ Extension
Time
Computation

Dual-ring
Operation

Red Arrival
Rate
Computation

Yes ← Opposing
Lane > 1? → No

Multi-lane
Scenario ← Opposing Lane > 1? → Single Lane
Scenario

Shared Lane
Group
Specification ← g_f, g_q and P_L
Computations ← No — Done
or I > 40 ? — Yes → Final Cycle
Length and
Phase Times

↓

End

Figure 4-1. Major structure of the ACT3-48 program.

There are eight possible cases of phase sequence patterns in all. For the purpose of illustration, only the phase sequence patterns in the north-south direction are shown in figures. Case 1 is a standard case for permitted turns which is shown in Figure 4-2. Case 2 is the phase sequence for leading green which is shown in Figure 4-3. In contrast to Case 2, Case 3 is the phase sequence for lagging green which is presented in Figure 4-4. Case 4 shown in Figure 4-5 is the phase sequence for leading and lagging green. Case 5 is a left turn phase with leading green which is shown in Figure 4-6. Case 6 is leading dual left turns, and Case 7 is lagging dual left turns. Cases 6 and 7 are shown in Figures 4-7 and 4-8, respectively. In Cases 6 and 7, the phases for dual left turns will terminate simultaneously. Finally, Case 8 shown in Figure 4-9 is leading and lagging with dual left turns. Case 4 and Case 8 are interchangeable. For example, when the volume of northbound left turn volumes are heavy and through traffic is light, Case 4 may become Case 8.
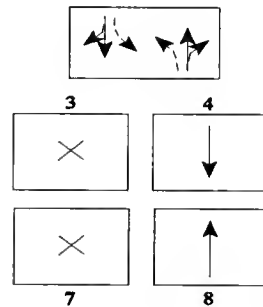
Figure 4-2. Case 1: Phase sequence for simple permitted turns.
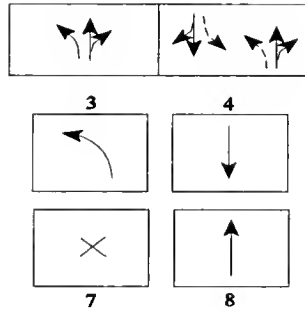
Figure 4-3. Case 2: Phase sequence for leading green.
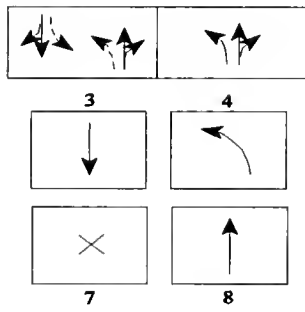
Figure 4-4. Case 3: Phase sequence for lagging green.
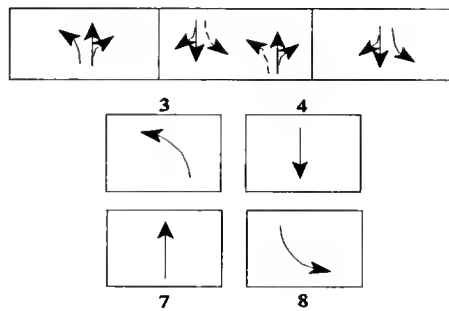
Figure 4-5. Case 4: Phase sequence for leading and lagging green.
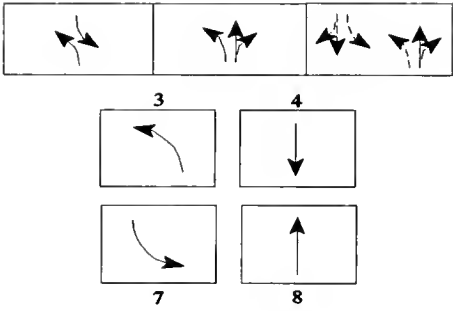
Figure 4-6. Case 5: Phase sequence for LT phase with leading green.
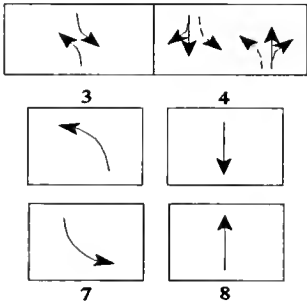
Figure 4-7. Case 6: Phase sequence for leading dual left turns.
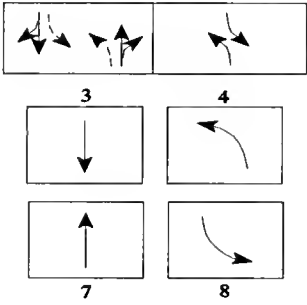
Figure 4-8. Case 7: Phase sequence for lagging dual left turns.
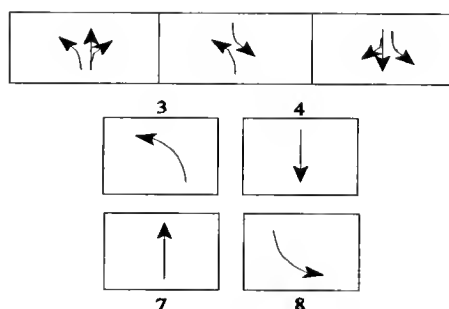
Figure 4-9. Case 8: Phase sequence for leading and lagging with dual left turns.

In "actuated parameter specification", the actuated parameters are specified based on each NEMA phase which was defined in Chapter 2. The actuated parameters consist of minimum initial, maximum initial, minimum phase time, maximum green time, allowable gap recall, detector configuration and so on. Based on the control specification and the actuated parameter specification, Worksheet 1: Traffic-actuated Control Input Data can be produced by the ACT3-48 program.

Lane Group Specification

In "lane group specification", the ACT3-48 program will determine the phase movements for each NEMA phase and the lane group movement within each NEMA phase. For example, if a NEMA phase includes all left turns, through traffic and right turns, the phase movement of this NEMA phase will be specified as "LTR". If a lane group within the NEMA phase is just for through and right turns, it should be presented as "TR". The purpose for this specification is to associate each of the lane group with its NEMA phase.

The lane group specification is convenient and necessary for later computation. For example, the phase time computation for permitted left turn movement from an exclusive lane ("L") will be different from that for through and right turn movements ("TR"). In addition, the ACT3-48 program will also determine the traffic volume (veh/hr), arrival rate (veh/sec), saturation flow (veh/hr) and departure rate (veh/sec) for each lane group based on the input data from WHICH. Worksheet 2: Lane Group Data is then generated.

Accumulated Queue Computation

In a new iteration, the most important step is to create a new queue accumulation polygon (QAP). With the phase sequence pattern, phase times and other information from the last iteration, the new QAP can be produced easily for simple through or protected phases. It becomes more difficult in computation for permitted left turns from either an exclusive or a shared LT lane and compound left turn protection because more information is required before accumulated queues can be computed.

In the analytical model for permitted left turns from an exclusive lane, the opposing queue service time, g_{qp} is needed for QAP. For the permitted left turns from a shared LT lane, both g_q and free green, g_f are required. In the compound LT protection, an exclusive LT lane is assumed, so g_q must be obtained. Fortunately, the method for estimating g_q and g_f has been presented in HCM Chapter 9, which is used in this study to compute g_q and g_f. In the ACT3-48 program, the computation of g_q is based on 1994 version of HCM Chapter 9. Since the computation of g_f is based on the length of green time in the latest HCM version which may cause unreliable convergence of cycle length, the method presented in 1985 HCM Chapter 9 is used instead. Based on the number of opposing lanes, there are two scenarios described

in the HCM Chapter 9 for the computation of g_q and g_f. If the number of opposing lanes is one, the single lane scenario is applied. Otherwise, the multi-lane scenario is used.

For the shared lane condition, the P_L factor must be considered, which is the proportion of left turns in the shared lane. The value of P_L is influenced by many factors such as proportion of left turns, number of lanes, left turn saturation factor, effective green in the lane group and so on. In each iteration, the value of P_L will be computed by the ACT3-48 program using the method described in HCM Chapter 9. The value of P_L will influence the volumes on the shared LT lane and other existing through lanes in the next iteration. Thus, the arrival rate of each lane group will be slightly changed.

Since the behavior of left turns from a shared lane is more complicated than that from an exclusive lane, the treatment for the shared lane should be different. A shared lane group specification is necessary and will be made by the ACT3-48 program. The movement of the first lane group for the phase with a shared lane will be specified as "LT". However, if there is only one lane total, it will be specified as "LTR". The method of specification for other lane groups is the same as before. Based on the value of P_L, the arrival rates for the shared lane condition will be modified. Note that according to the HCM Chapter 9, the saturation flow rate for the other through lanes in the same approach with the shared lane will be reduced to 91 percent of its original value due to the shared lane effect. The departure rates for the through lanes also need to be modified.

Next, based on the derivation in the model development, green arrival and red arrival rates are then computed based the arrival type of the movements. For fully-actuated operation, progression effects are not important, so arrival type 3 is adopted for fully-actuated

operation. Therefore, the red arrival rate is the same as the green arrival rate. For coordinated semi-actuated operation, the arrival types other than type 3 can be specified for the coordinated phases on the artery.

Now, it is ready to compute the accumulated queues in the QAP. Basically, there are different kinds of queues required to be computed by the ACT3-48 program for the phases with permitted left turns. The first kind of queue is called Q_r, which is the queue at the beginning of the effective green time. This queue is mainly accumulated during the red period. The second one is called Q_f, which is the queue accumulated at the end of free green g_f. The third kind of queue is called Q_q, which is the queue accumulated at the end of e_g. For the through movements or simple protected LT movements (not compound left turn protection), $Q_q = Q_f = Q_f$.

For the compound protection, according to the analytical model, the Q_q of LT movements in the permitted portion of protected plus permitted phasing is the only the accumulated queue during g_q period. The queue of LT movement at the beginning of protected portion of permitted plus protected phasing is the residual queue of the permitted phase minus the sneakers.

Extension Time Computation

In the extension time computation, the parameters such as the minimum headway (Δ) and the proportion of free vehicles (φ) and λ are calculated first. Next, the equivalent through volume described in Chapter 3 is computed to accommodate the effect of permitted left turns. The equivalent through volume is used in place of the actual volume in the

extension time computation. The extension time will be computed based on the method specified (bunched arrival model or random arrival model) by the program user. If the HCM Chapter 9 Appendix II method is specified, no extension time computation will be performed.

Required Phase Time Computation

In the "green model", the required phase times of an iteration are computed. The required phase times include two major parts. One is the queue service time and the other one is the extension time after queue service. Based on the accumulated queue length and net vehicle departure rate (net service rate), the queue service time, g_{qst}, can be obtained. The effective extension time, g_e, can also be computed based on the extension model. The lost time per phase, t_l, is an input value. Thus, the phase time, PT, is just the sum of g_{qst}, g_e and t_l. However, it cannot exceed the maximum phase time or fall below the adjusted minimum phase time. Worksheets 3, 4, and 5 will then be produced by the ACT3-48 program.

Cycle Time Adjustments

In each iteration, the new estimated phase times must be processed through the dual-ring operation according to the phase swap specification and termination type (independent or simultaneous). After the dual-ring operation, the phase times and their corresponding cycle length are obtained. This cycle length will be compared with the previous cycle length. If the convergence of cycle length is reached or the number of iterations exceeds 40, the ACT3-48 program will terminate and produce the final cycle length and phase times. If not, the program will proceed with the associated adjustment related to the phase time and continue next iteration. It is necessary to note that the phase sequence pattern will be checked here to keep the later computation on the right track.

Extension of the Development of Coordinated Operations

Pretimed coordination often performs very well under high volumes and predictable conditions. However, it is unable to provide the flexibility for a low volume scenario or variable demand. On the other hand, actuated controllers have the capability to improve the shortcoming of pretimed control and handle variable demand. Semi-actuated operation has been successfully adopted at isolated intersections and coordinated systems [34].

The phase times of an isolated semi-actuated operation can be easily estimated by setting the maximum recall to the arterial in the previous developed analytical model for fully-actuated operation. Although the analytical model in the isolated mode is not valid for the coordinated one, it is possible to apply the analytical model iteratively to converge to a solution that satisfies all of the requirements of coordination. The analytical model and procedure for predicting the signal timing for fully-actuated operation have already been implemented in the ACT3-48 program. A separate procedure that makes iterative use of ACT3-48 as an external module to predict the signal timing for coordinated semi-actuated operations will be demonstrated in this section.

Description of the Procedure

In the isolated mode of actuated operation, the phase times and cycle length are mainly dependent on the traffic demands indicated by vehicle detectors. In a coordinated mode, the controller is constrained to operate on a specified background cycle length with the constraints placed on the length of all of the phases. Some of the benefits of traffic-actuated operation are eliminated. However, the coordinated mode produces the benefits of improved progression and reduced delay of the arterial traffic.

Due to the constraint of the specified background cycle length, the signal timing for a coordinated intersection is based on a pretimed equivalent. The actuated controller must operate within the constraint but any green time not used by the actuated phases may be reassigned to the through movements on the arterial street which generally carries heavier traffic volumes. Therefore, an effective method to estimate the phase times for coordinated node is to apply the proposed analytical model for isolated mode to predict the phase times of actuated phases and then properly reassign the difference between the computed cycle length from the model and the specified background cycle length to the non-actuated phases (arterial through movements).

The procedure [56] for adopting the ACT3-48 program to coordinated operation involves the following steps:

1. Set up the controller timing parameters for the ACT3-48 initial run. The coordinated arterial phases (usually 2 and 6) should be set for *recall to maximum*. The maximum green times for all phases should be determined by their respective splits in the pretimed signal timing. No recall modes should be specified for any of the actuated phases.

2. Perform the timing computations with ACT3-48 to determine the resulting cycle length. If the maximum green times have been specified correctly in step 1, then the computed cycle length will not exceed the specified cycle length.

3. If the computed cycle length is equal to the specified cycle length, then there is no green time available for reassignment. In this case the procedure will be complete and the final signal timing will be produced.

4. If the computed cycle length is lower than the specified cycle length, then some time should be reassigned to the arterial phases. This is accomplished by increasing the maximum green times for phases 2 and 6. In the procedure, one half of the difference between the computed cycle and the specified cycle is assigned to the arterial phases. This provides a reasonable speed of convergence without overshooting the specified cycle length.

5. Repeat steps 2 through 4 until the computed and specified cycle lengths converge.

This procedure has also been implemented in software. A program called NONACT was developed in cooperation with the ACT3-48 program to predict the phase times for coordinated semi-actuated operation. The computational procedure is simple and an iterative procedure is also involved. The NONACT program can set up the input data, execute ACT3-48 as an external program and read results. Since the ACT3-48 program obtains its data from WHICH data file, the NONACT program must make changes to that file to implement steps 2 through 4 as described above. The NONACT program will run ACT3-48 iteratively until the computed cycle length converges to the specified background cycle length.

CHAPTER 5
MODEL TESTING AND EVALUATION

Introduction

The structure and details of the proposed analytical model and procedure for traffic-actuated operation in both isolated and coordinated modes have been described. The model and procedure which are implemented in the ACT3-48 program may be used to predict the average phase times and cycle length which are generated by a traffic-actuated controller with specified traffic data and operating parameters. In this chapter, testing is performed first to evaluate the developed analytical models by NETSIM simulation and field data for fully-actuated operation. Then, other testings are performed to examine the performance of the NONACT program which implements the proposed procedure to predict the phase times of coordinated semi-actuated operation. Finally, an intensive evaluation is conducted to explore the headway distributions of vehicular arrivals at the stopline (due to the use of presence detectors) produced by the analytical model and the NETSIM simulation model which may cause the difference on the phase time prediction for fully-actuated operation.

Fully-actuated Operation

Three major tasks were performed to evaluate the analytical models for fully-actuated operation. The first task is to compare the predicted cycle length between the analytical model and NETSIM with a very simple example with a two-phase traffic-actuated operation.

The second task is to compare the phase time estimates between the analytical model and NETSIM with different hypothetical examples including four HCM Chapter 9 sample calculations and five hypothetical examples. The last task is to compare the predicted phase times between the analytical model and NETSIM with those from real field data.

Cycle Length Comparison with a Two-phase Traffic-actuated Example

The objective of this testing focuses on the comparison of estimated cycle lengths among the HCM Appendix II method, proposed analytical model and NETSIM simulation. The cycle lengths were determined as a function of the traffic volume level by four methods: 1) the HCM Appendix II method given in Equation 2-1 assuming the recommended 95% v/c ratio; 2) the HCM Appendix II method based on the iterative procedure with adjusted vehicle minimum; 3) the proposed analytical model with bunched exponential arrivals; and 4) simulation by NETSIM, using the traffic-actuated control option. Note that methods 2 and 3 were performed by the ACT3-48 program and the results of each NETSIM run were summarized by the NETCOP postprocessor.

Consider the intersection shown in Figure 2-5. This is a trivial intersection with four single-lane approaches carrying the same through traffic. All approaches are configured identically. For simplicity, a saturation flow rate of 1800 vphgpl, corresponding to a headway of 2 seconds per vehicle, will be assumed. A 30-ft long detector is placed at the stopline for each approach. Each phase has been assigned the same constant parameters as follows. Intergreen time is 4 seconds. Lost time is 3 seconds per phase. Minimum phase time and maximum phase time are set at 20 and 70 seconds, respectively. Assuming there are no pedestrian timing features and no volume-density features.

Relatively long maximum phase times have been selected to ensure that the timing is not constrained artificially. This will give a better insight into the cycle computation procedure. The traffic volumes and the allowable gap setting were both varied to examine the sensitivity of the analytical model and the NETSIM simulation model to these parameters. The volume was varied throughout the range of 100 to 800 vehicles per hour, per approach. Three allowable gap settings of 1.5, 3.0 and 4.5 seconds were used to represent low, medium and high values respectively. The results are presented on four figures:

Figure 5-1: representing a 1.5-sec allowable gap setting.

Figure 5-2: representing a 3.0-sec allowable gap setting.

Figure 5-3: representing a 4.5-sec allowable gap setting.

Figure 5-4: representing a composite of Figures 5-1, 5-2, and 5-3 for comparison.
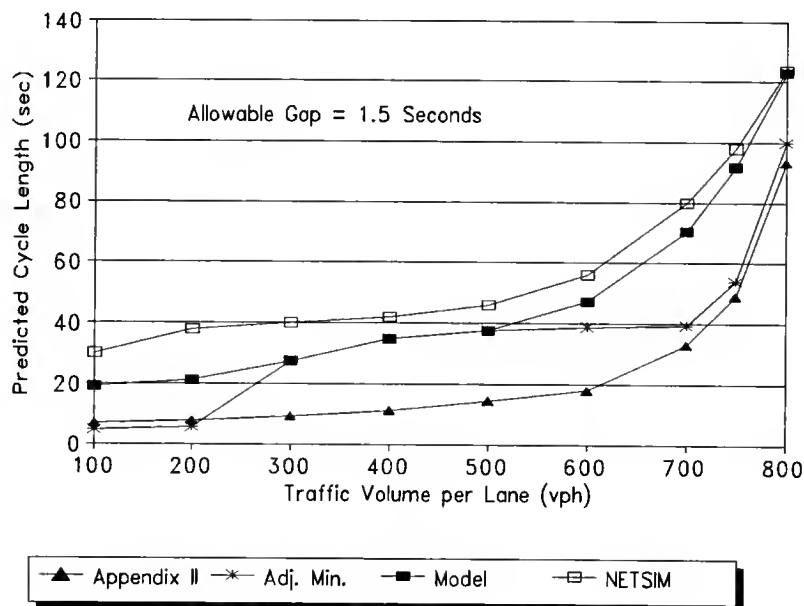
Figure 5-1. Cycle length computation for a 1.5-sec allowable gap setting.
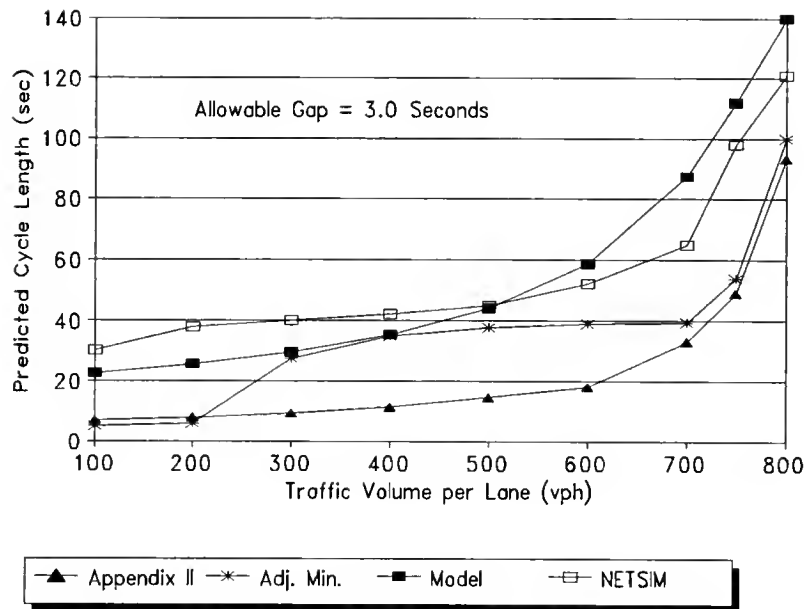
Figure 5-2. Cycle length computation for a 3.0-sec allowable gap setting.
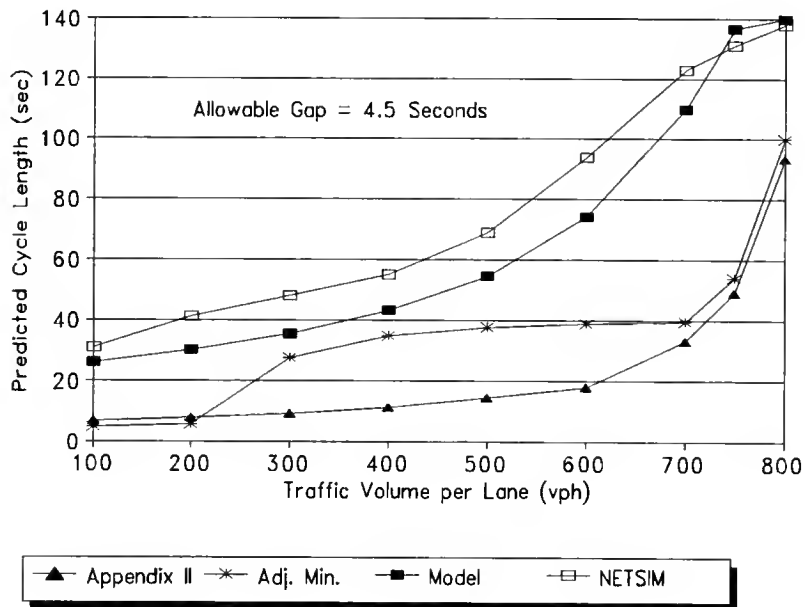
Figure 5-3. Cycle length computation for a 4.5-sec allowable gap setting.
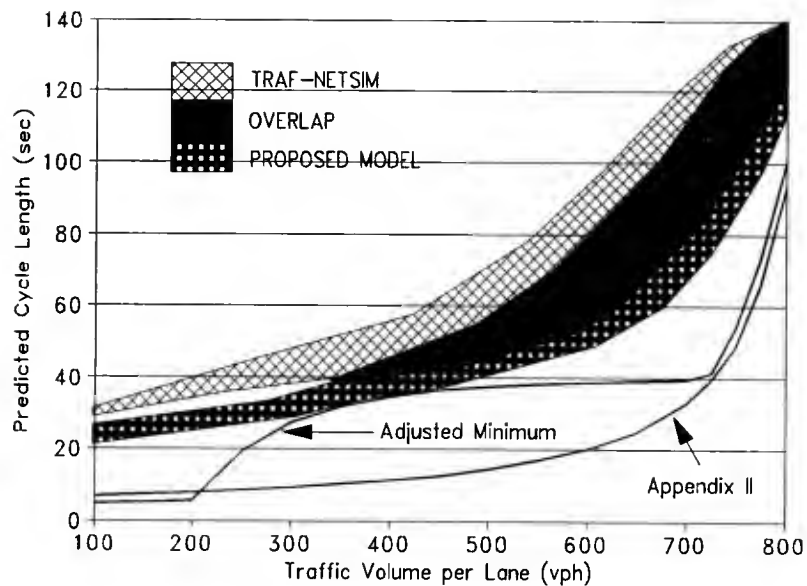
Figure 5-4. Composite cycle length computations with all gap settings.

Some interesting observations may be made from these figures:

1. It is quite clear that all of the computational techniques yield longer cycle length estimates than the current Appendix II method.

2. All of the models tested showed a credible sensitivity to the allowable gap setting. As the gap setting increased, the cycle length increased. The specified maximum cycle length of 140 seconds was reached for the proposed model and NETSIM simulation at volume levels ranging from 750 to 800 vph on each approach.

3. All of the techniques produce a more gradual increase in cycle length throughout the volume range than the Appendix II method. Note that the Appendix II cycle length remains below the 40-sec minimum value until the volume exceeds 700 vph, and then rises very rapidly to an value of about 100 seconds. The other

methods all predict much longer cycle lengths than those form the Appendix II method at much low volumes.

4. The bunched exponential gap extension model predicts cycle lengths that are very close to those predicted by the gap extension model that assumes random arrivals. The results of both models were plotted as a single curve in the figures.

5. NETSIM's cycle length estimates tend to be somewhat longer than the corresponding estimates from the proposed analytical model. The reasons for these differences will be explained in more detail later in this chapter.
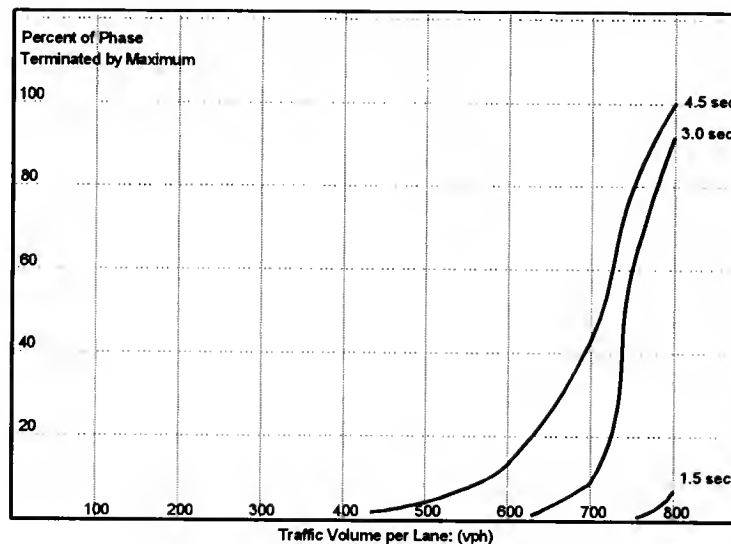
Figure 5-5. Percent of phases terminated by maximum green time for each gap setting.

The stochastic nature of the NETSIM model provides a more detailed picture of the variability of the operation from cycle to cycle. Based on the same traffic volume scale as the

previous figures, Figure 5-5 shows the percent of phases terminated on the maximum for the three specified gap extension settings. This information was produced from the NETSIM results by the NETCOP postprocessor. In Figure 5-5, the percent of phases terminated by the maximum is almost negligible with the 1.5-sec gap setting, even at the highest traffic volume. On the other hand, all of the phases will terminate on the maximum time at higher volumes for the longer gap settings.

Phase Time Comparison with Hypothetical Examples

To provide a general comparison between the HCM Chapter 9 Appendix II method and the proposed analytical model, several example data sets, including four HCM Chapter 9 sample calculations and five hypothetical examples, were subjected to phase time estimates by both models. Some of the traffic and operational data were modified slightly to increase the range of conditions included in this analysis. NETSIM was used as the evaluation tool. The results are plotted graphically in Figures 5-6 and 5-7. Both figures plot NETSIM phase time estimates against the corresponding estimates from the analytical model.

Figure 5-6 shows a phase time comparison between the Appendix II method and NETSIM. A considerable dispersion of the data points is evident in this figure. By inspection, the slope of the linear regression line indicates that the simulated phases times are much longer than those estimated by the Appendix II method. The correlation is low, as evident in the R squared value of only 0.70. Figure 5-7 shows a phase time comparison between the proposed model and NETSIM. The dispersion of the data points is much smaller, indicating a much better agreement between the two techniques. This is confirmed by a high R square value of 0.93. The regression line is also close to 1:1 slope.
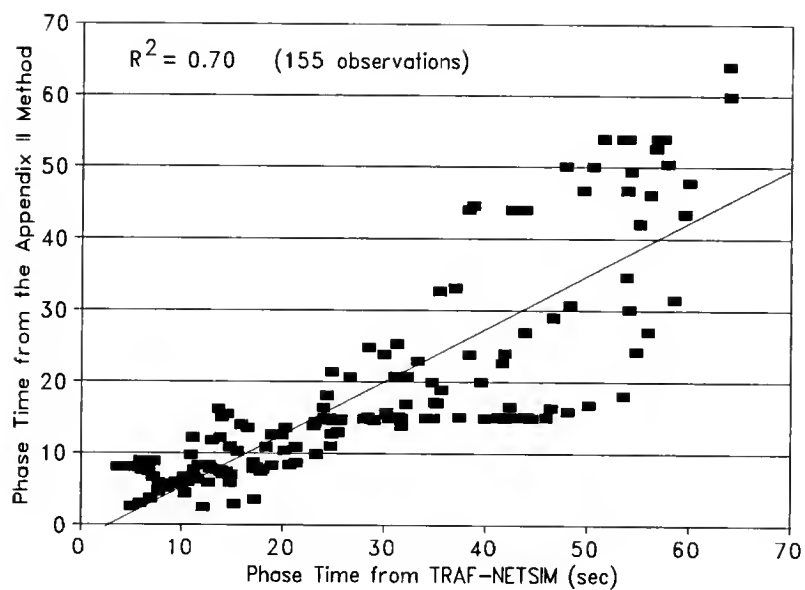
Figure 5-6. Phase time comparison between the Appendix II method and NETSIM.
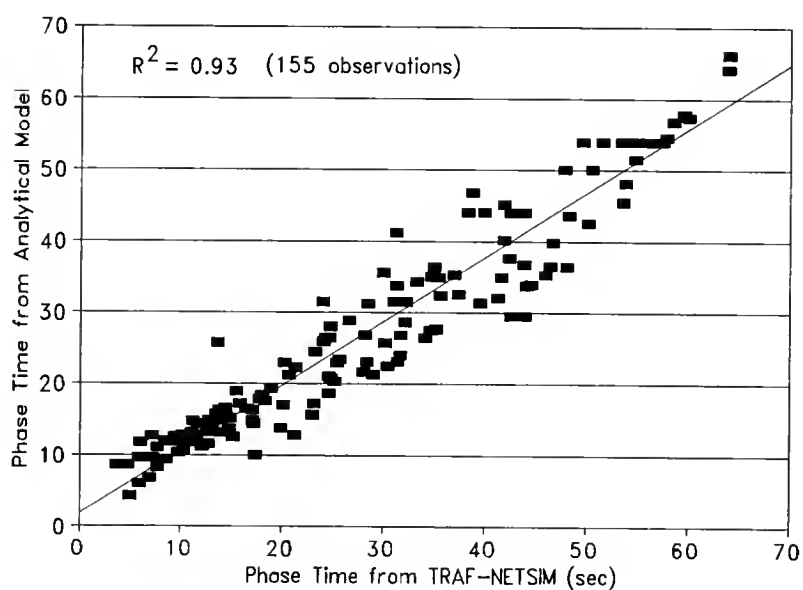
Figure 5-7. Phase time comparison between the proposed model and NETSIM.

Phase Time Comparison with Field Data

To further verify the analytical model, a field study was conducted at the intersection of Museum Road and North-south Drive on the campus of the University of Florida in Gainesville, Florida. In total, 32 hours of data were used in this evaluation which included the morning peak, mid-day and the afternoon peak of three weekdays. The site is a four-legged intersection with one through lane and one exclusive left turn bay about 250 feet in length on each approach. The configuration of the studied intersection for the field data evaluation is shown in Figure 5-8.
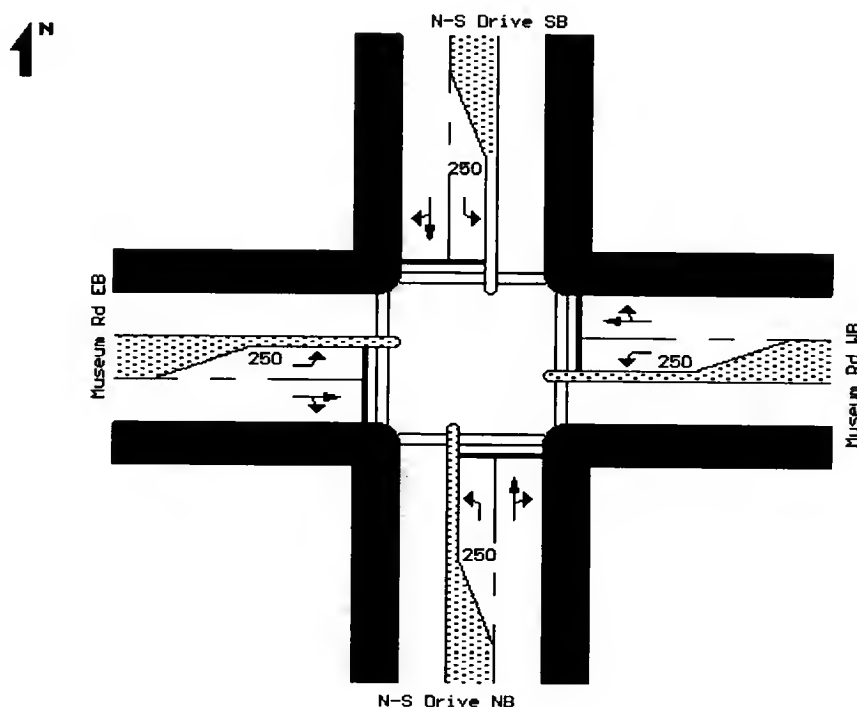
Figure 5-8. Intersection configuration of Museum Road and North-south Drive on the campus of the University of Florida.

Standard dual-ring phasing applies with protected plus permitted left turns. The ideal saturation flow rate is 1900 vehicles/hour. Pedestrian recall was set in the controller and the duration for WALK plus Flashing DON'T WALK was 22 seconds. The intergreen time was 5 seconds. The allowable gap setting was 3.5 seconds for through movements and 2.5 seconds for left turns. All detectors were 25 feet in length placed at the stopline. The minimum green time was set at 16.5 seconds for through phases and 10 seconds for left turns. The maximum green time was set at 45 seconds for through phases and 15 seconds for left turns on the heavier street. The corresponding maximum green time settings for the minor street were 30 and 10 seconds, respectively.

Figure 5-9 shows a phase time comparison between the estimates from the analytical model and field data. Two groups of data points are shown in the figure because the through traffic phases tended to be longer than the left turn phases. Although the phase time estimates from the model are slightly higher than the measured field data for left turn phases (low volume), the regression line is close to 1:1 slope. The dispersion of the data points is small, indicating that the phase time estimates from the model are close to the field data. This is confirmed by a very high R squared value of 0.95.

Figure 5-10 shows a phase time comparison between NETSIM and field data. Two groups of data points are also shown in the figure because the through traffic phases tended to be longer than the left turn phases. The phase times estimated by NETSIM are close to the field data indicated by a very high R square value of 0.96. By inspection, the regression line is close to 1:1 slope but slightly above it. NETSIM slightly overestimated the phase times at this intersection.
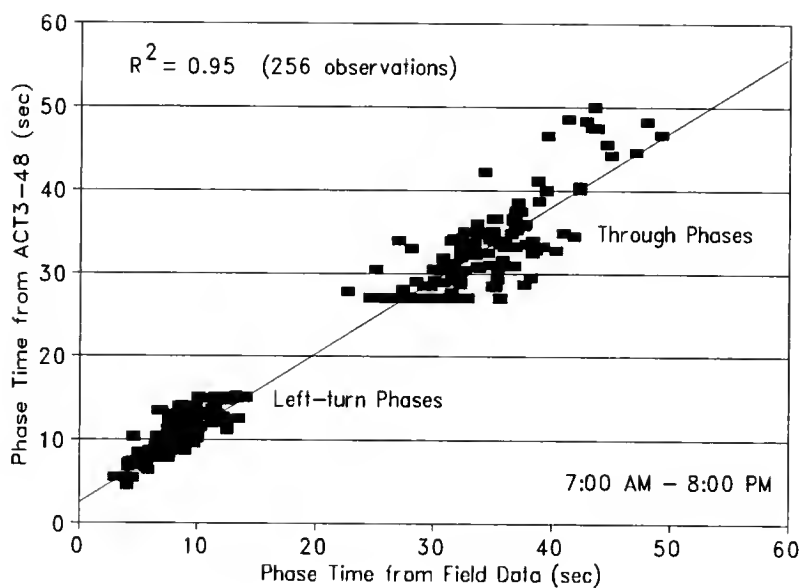
Figure 5-9. Phase time comparison between the analytical model and field data.
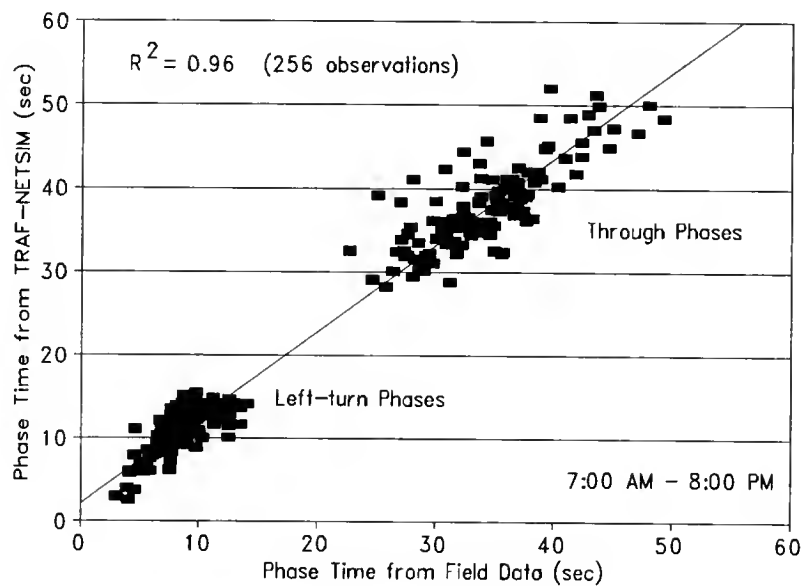
Figure 5-10. Phase time comparison between NETSIM and field data.

<u>Coordinated Actuated Operation</u>

In order to examine the capability of the NONACT program which implements the proposed procedure to predict the phase time of coordinated operation. NETSIM is also used as the evaluation tool. The estimated phase times from NONACT were compared with those estimated by NETSIM simulation with ten different scenarios based on possible intersection configuration, left turn treatments and traffic conditions.

<u>Phase Time Relationship between a Cross Street and an Artery</u>

A simple data set was used to examine how the timing of phases change as the cross street volume increases. The hypothetical intersection has four single-lane approaches carrying only the through traffic. It is a two-phase coordinated semi-actuated operation. The minimum and maximum phase times for the minor street are 15 and 30 seconds, respectively. The allowable gap for the minor street is 3 seconds. The detectors are 30 feet long placed at the stopline of minor street approaches. The traffic volume on the arterial street is fixed at 800 vph, while it varies from 100 to 800 vph on the cross street. The common background cycle length is specified as 60 seconds, and the initial split is 30 seconds for both phases. Figure 5-11 is the phase time comparison for arterial and cross streets between NONACT and NETSIM under the simplest scenario of coordinated operation.

Figure 5-11 shows a reasonable relationship of phase times between the arterial street and cross street for both NONACT and NETSIM's results. When the cross street volume increases, the phase times required by the cross street increase. Relatively, the phase times assigned to the arterial street decrease, which is equal to the background cycle length minus the minor street phase times. When the minor street volume is about 800 vph, the maximum

phase time, 30 seconds, on the cross street is reached. Since the background cycle length is

60 seconds, 30 seconds of phase time are also assigned to the arterial street.

Therefore, the curves of phase times for both the arterial and cross streets converge

at 30 seconds. It is easy to observe that the phase times estimated by the NONACT program

are very close to those estimated by the NETSIM simulation, which demonstrates that the

proposed procedure in the NONACT program is capable of predicting similar phase times for

coordinated semi-actuated operation to those by NETSIM simulation in the simplest scenario.
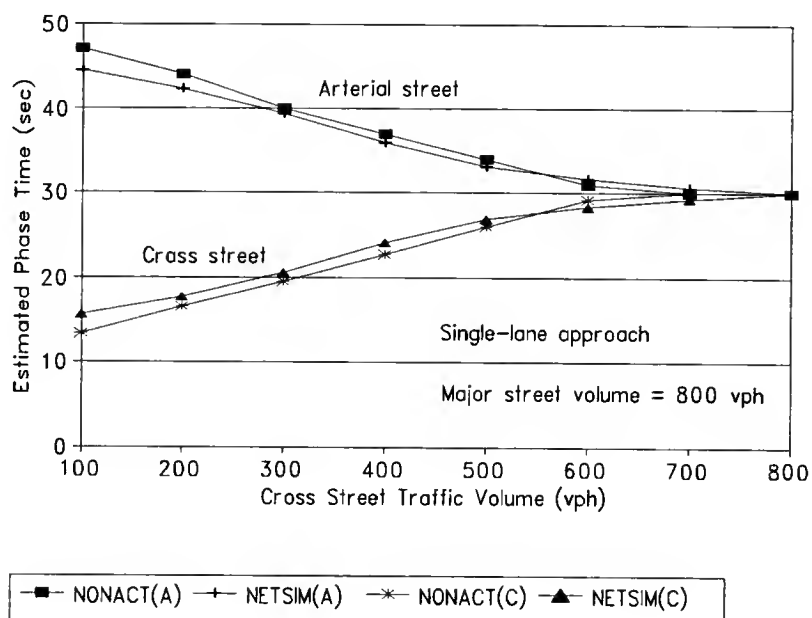
Figure 5-11. Phase time comparison between arterial street and cross street.

Phase Time Comparison with Hypothetical Scenarios

The objective of this test is to examine the performance of the NONACT program

which implements the proposed procedure to predict the phase time of coordinated actuated

operation. The hypothetical data sets fall into 10 categories based on intersection configuration, left turn treatment and number of lanes. These scenarios represent a wide variety of conditions. The reason for using so many data sets is to generally test the prediction capability of the proposed procedure for coordinated actuated operation. The parameters are fixed for these 10 scenarios as follows:

Background cycle length: 120 seconds

Unit extension (all phases):   3 seconds

Intergreen (all phases):   4 seconds

Saturation flow rate: 1800 vehicles/hour

Minimum green time: 11 seconds (through movements)

                        6 seconds (left turns)

Maximum green time: 56 seconds (approaches without left turn protection)

                        46 seconds (through phases)

                        26 seconds (protected left turn phases)

Figure 5-12 shows the phase time comparison between NONACT and NETSIM. Note that in this comparison, all phase time estimates belong to the actuated phases. The predicted phase times from the NONACT program are very close to those estimated by NETSIM. A very high R squared value of 0.97 is achieved which indicates the proposed procedure can accurately predict the phase times for coordinated actuated operation in the chosen examples. The NONACT program is able to provide credible estimates of phase times for coordinated operation of a traffic-actuated controller.
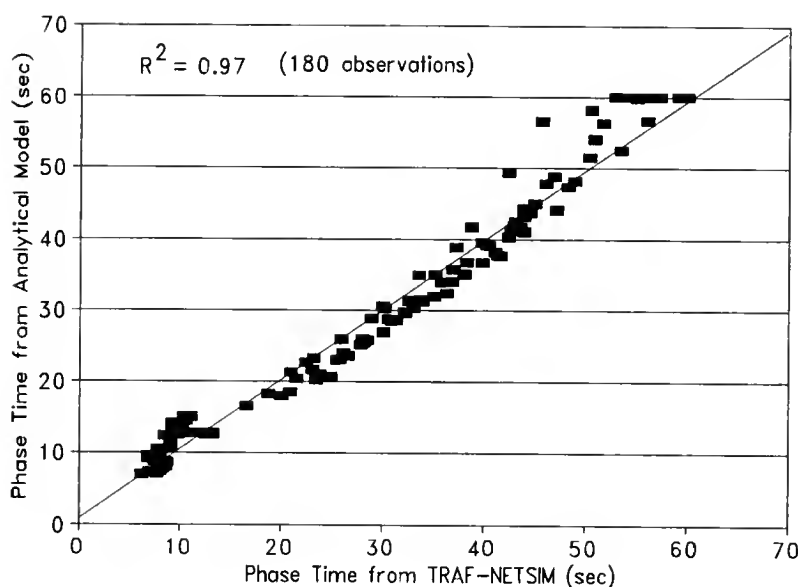
Figure 5-12.   Relationship of estimated phase times between NONACT and NETSIM.

Further Evaluation of the Analytical Model

In general, NETSIM simulation produces longer phase times than those from the

analytical model for most simulated phase times and shorter phase times when the simulated

phase times are short. A traffic-actuated controller terminates a given phase whenever a gap

appears at the detector that exceeds the allowable gap specified for that phase. Therefore,

the length of a phase will depend heavily upon the probability of a gap extended in the traffic

flow after the queue has been serviced. For example, a vehicular arrival distribution with a

higher accumulated probability to actuate a detector to extend the allowable gap after the

queue clearance will, in general, produce a longer phase time. If the analytical and simulation

models do not have the same vehicular arrival headway distributions at the stopline (due to

the use of presence detectors), then systematic differences will be built into any phase time

comparison that will cause the results to diverge. Hence, an effective approach to explore these systematic differences is to examine the headway distribution of vehicular arrivals at the stopline produced by NETSIM and the proposed analytical model.

Distribution of Arrivals by Bunched Model and NETSIM

The arrival headway distribution for the proposed analytical model is the bunched negative exponential model which was described in Chapter 2. For the convenience of explanation, its cumulative distribution function F(t) is expressed as follows:

$$F(t) = 1 - \varphi e^{-\lambda(t - \Delta)} \qquad \text{for } t \geq \Delta \qquad (5\text{-}1)$$
$$= 0 \qquad \text{for } t < \Delta$$

The definitions of φ, λ, and Δ are the same as those in chapter 2. Based on the input values of the parameters needed in Equation 5-1, its accumulative probability of the bunched arrival model can be computed. Equation 2-12 may be used to predict the expected extension time e_g before a gap of a specific length occurs to terminate the green time.

In the current version of NETSIM, it is impossible to specify the characteristics of the arrival distribution. Vehicles are released into each external link from a mythical entry node with constant headways that form a uniform distribution. NETSIM's queue propagation algorithm causes some bunching of vehicles to occur as they proceed though the link. The actual shape of the arrival distribution at any point downstream may depends variability of speeds of vehicle types and the length of the link. It is very difficult to predict analytically. To demonstrate NETSIM's arrival headway distribution mechanisms, several runs were made

in which traffic streams with different flow rates were introduced into single-lane links with different link lengths. Link lengths of 100, 1000, 2000 and 3000 feet are represented in Figures 5-13 to 5-16, respectively. Traffic volumes of 100, 300, 500, 700 and 900 vph are shown in each of the figures as separate curves. In these figures, the arrival headway is on the horizontal axis, and the accumulated probability is on the vertical axis.

Figure 5-13 illustrates the uniform distribution of entering vehicles which travel only 100 feet after they are introduced into the link. The shape of the arrival distribution 100 feet downstream is very similar to that at the entering node because little propagation occurs in such short distance. Note that the accumulated probability proceeds almost vertically between zero and 100 percent at a headway value that is very close to the average headway. For example a volume of 300 vph reflects an average headway of 12 (=3600/300) seconds per vehicle. The transition takes place very close to this headway value.

Figures 5-14 through 5-16 demonstrate the effect of increasing the distance between the point of entry and the point at which the distribution is observed. As this distance is increased, the abrupt transition of Figure 5-13 gives way to a smoother transition with the characteristic shape of a bunched exponential distribution. It is found for the same traffic volume that when the link length increases, the effect of bunching increases. For the same link length, when the traffic volume increases, the effect of bunching also increases. From these observations it may be seen that NETSIM is indeed capable of producing arrival distributions that agree qualitatively with our expectations. However, the parameters of the distributions vary with link length. This factor is not considered in the bunched exponential distribution used in the analytical model.
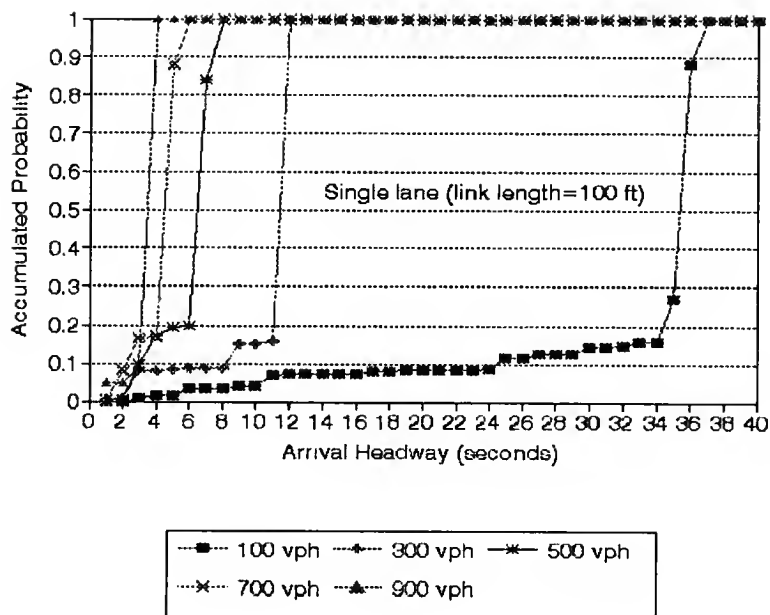
Figure 5-13. NETSIM arrival distributions for a single-lane link of 100-ft length.
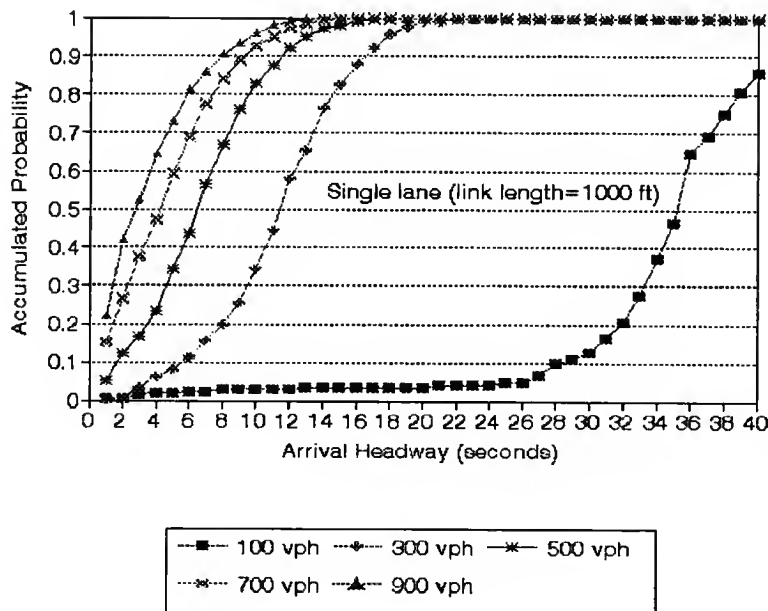
Figure 5-14. NETSIM arrival distributions for a single-lane link of 1000-ft length.
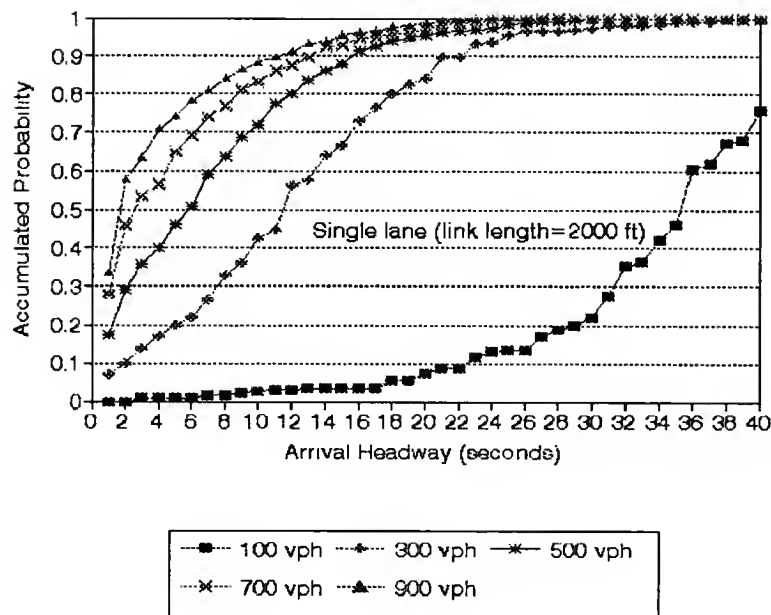
Figure 5-15. NETSIM arrival distributions for a single-lane link of 2000-ft length.
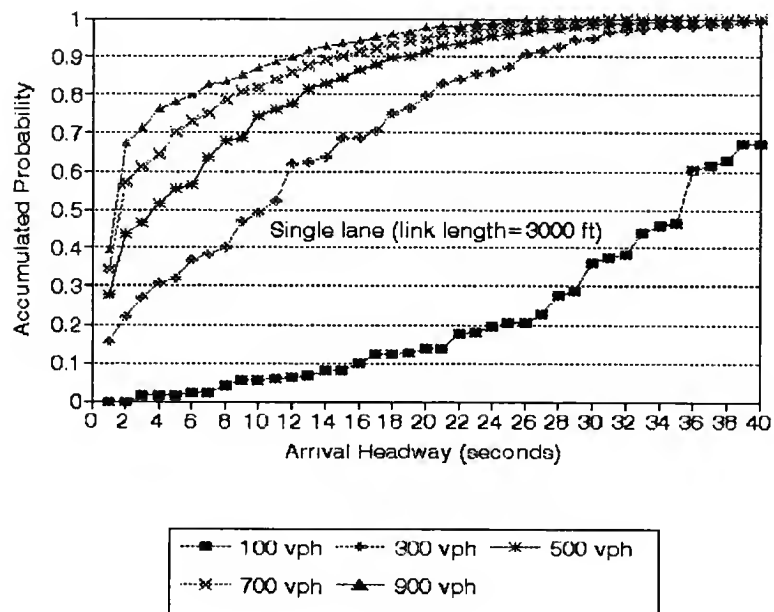
Figure 5-16. NETSIM arrival distributions for a single-lane link of 3000-ft length.

Comparison of Analytical and Simulated Arrival Distributions

The analytical distributions are independent of link length, but they naturally depend heavily on the traffic flow rate. Figures 5-17 through 5-21 represent the comparison of arrival distributions between the analytical model and NETSIM simulation on a single lane for low of 100, 300, 500, 700 and 900 vph, respectively. Separate curves are plotted on each figure for the analytical model and for the NETSIM distributions with different link lengths.

The results show a noticeable difference between the analytical and simulated distributions with low traffic volumes as shown in Figure 5-17. When traffic volume increases, the two methods tend to converge. However, even for the 900 vph level represented in Figure 5-21, there is a visible difference between them, especially at headways in the general range of typical unit extension times (i.e., less than 5 seconds) for traffic-actuated controllers. This suggests that, at least for single lane operation, there will continue to be a disparity between the signal timings estimated by NETSIM and the proposed model.

If two models suggest a different probability of a gap equal to or less than the specified vehicle interval for a given phase, then the model suggesting a higher probability will also estimate a longer green time for that phase. Now, inspection of Figures 5-17 through 5-21 indicates that the proposed analytical model suggests a higher value of phase time with low traffic volumes and a lower value with high traffic volumes. For mid-range volumes, say 500 vph, comparison could go either way, depending on the link length. This result may explain that in the previous phase time comparison, the proposed analytical model produces longer phase times for low traffic volumes and longer phase times for medium and high volumes than those from the NETSIM simulation model.

Figure 5-17. Comparison of analytical and simulation model arrival distributions for single-lane, 100-vph flow.

Figure 5-18. Comparison of analytical and simulation model arrival distributions for single-lane, 300-vph flow.

Figure 5-19.   Comparison of analytical and simulation model arrival distributions for single-lane, 500-vph flow.

Figure 5-20.   Comparison of analytical and simulation model arrival distributions for single-lane, 700-vph flow.
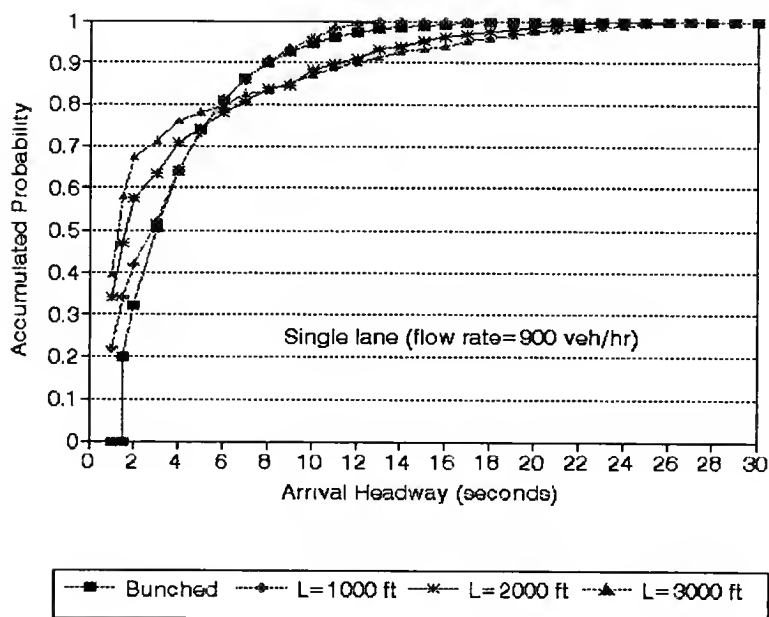
Figure 5-21.   Comparison of analytical and simulation model arrival distributions for single-lane, 900-vph flow.
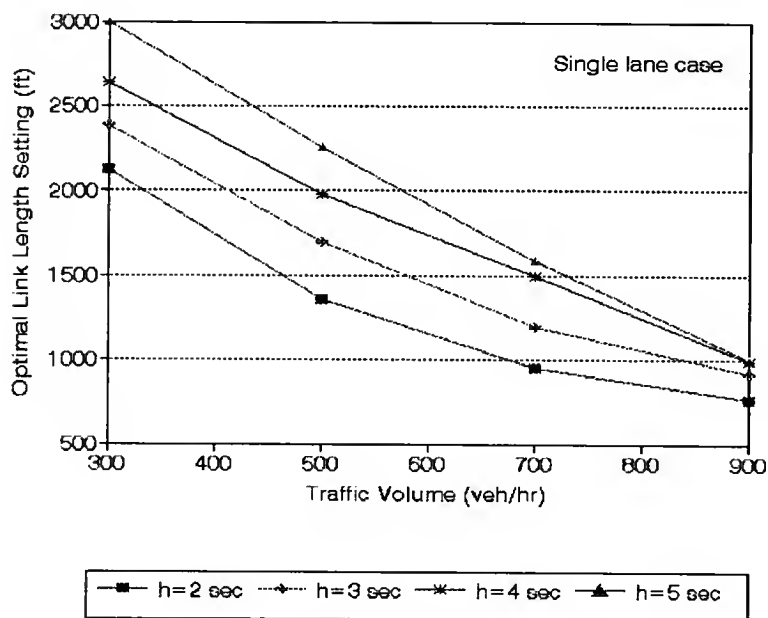
Figure 5-22.   Optimal NETSIM single-lane link length for various phase termination headway settings.

It is possible to carry this analysis one step further and determine the link length at which an equal probability of a gap of any specified length or shorter would be produced by both models. The results are shown in Figure 5-22, which shows the "optimal" link length for different traffic volumes and phase termination headways. The optimal link length is defined here as the link length that would produce an equal probability of a headway of the specified phase termination headway or shorter. The headway for phase termination must be used here directly, as opposed to the gap, because the actual gap value for a given headway will depend on the vehicle and detector lengths as well as the traffic speed. Note that the optimal link lengths vary between 1000 and 3000 feet and decrease as traffic volumes increase. The link lengths used in all of the sample problems were 2640 feet (one half mile).

Multiple Lane Arrival Headways

The preceding discussions and the results presented in Figures 5-17 through 5-22 assume a single lane operation. A similar comparison of arrival headway distributions for a two-lane operation with volumes of 200, 600, 1000 and 1800 vph is presented in Figures 5-23 through 5-26, respectively. Traffic volumes were increased because of the higher capacity of two-lane facilities. The same link lengths of 1000, 2000 and 3000 feet were used.

Examination of these figures shows a tendency that is similar to the single lane case at low volumes (see Figure 5-23). The proposed analytical model produces higher probabilities of headway in the range of the phase termination headways. However, differences in these estimates disappear quickly as traffic volumes increase. At high volumes (see Figure 5-26) they are barely discernable. This suggests that the proposed analytical model should show better agreement with NETSIM with respect to the controller operation.
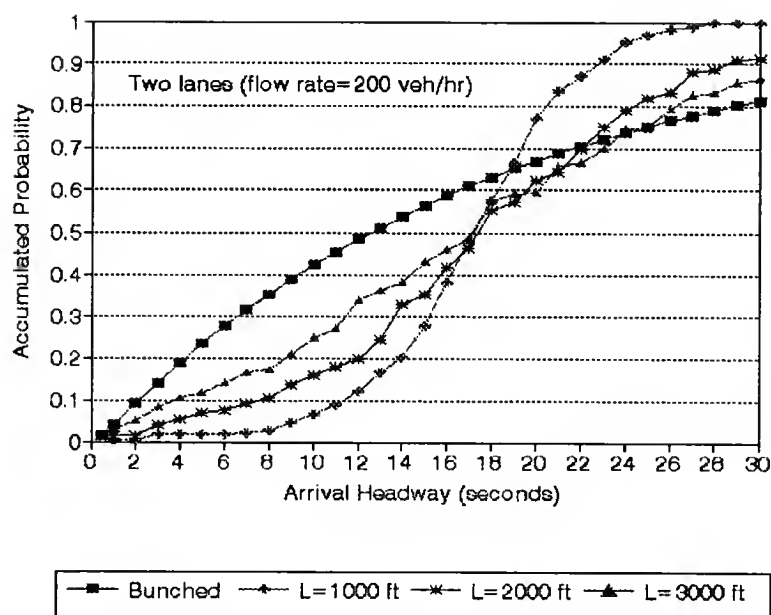
Figure 5-23. Comparison of analytical and simulation model arrival distributions for two-lane, 200-vph flow.
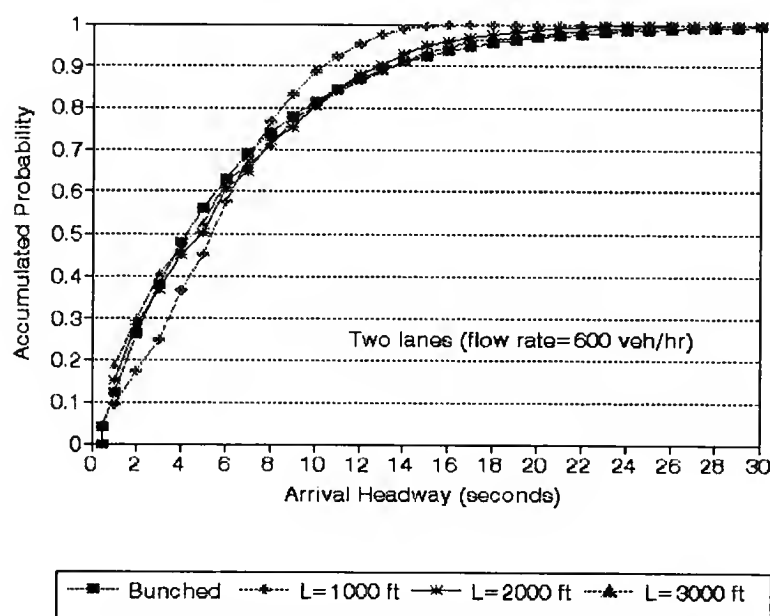
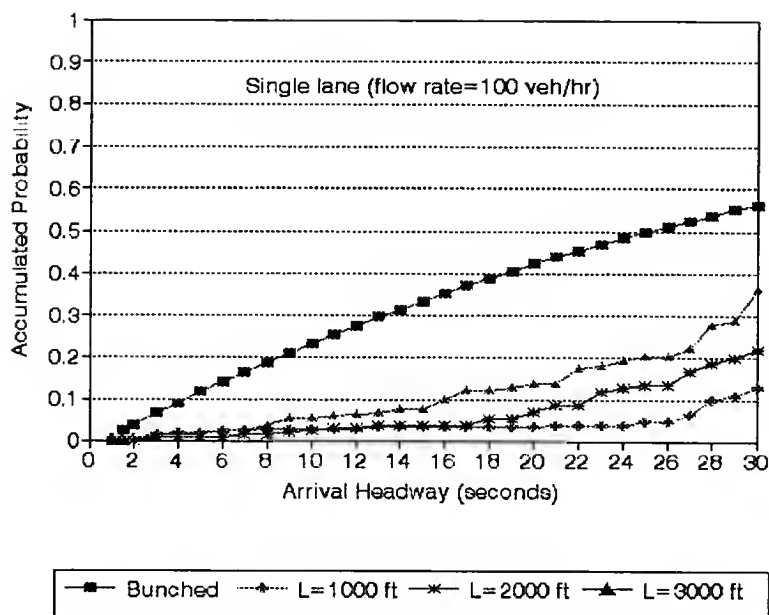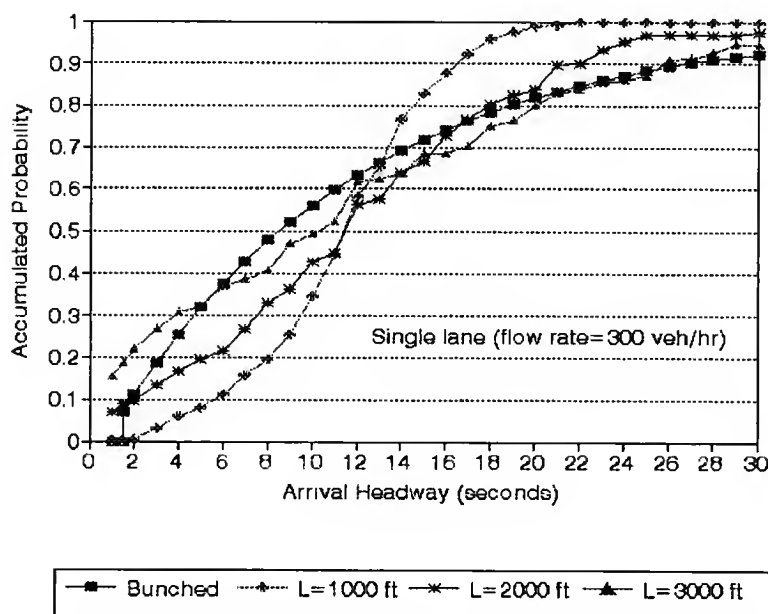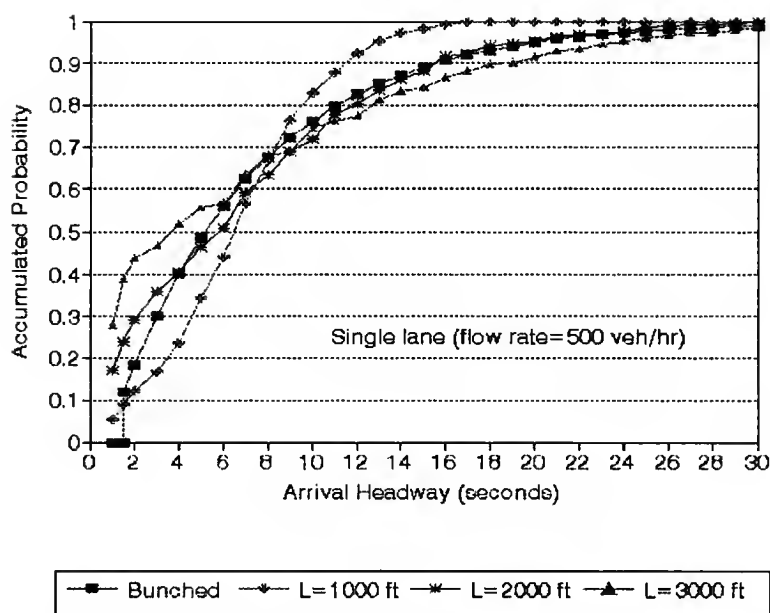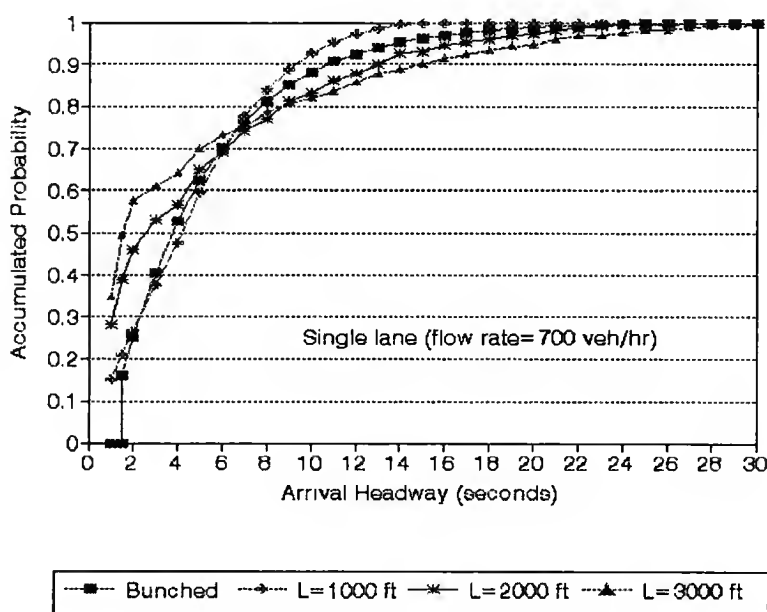Figure 5-24. Comparison of analytical and simulation model arrival distributions for two-lane, 600-vph flow.
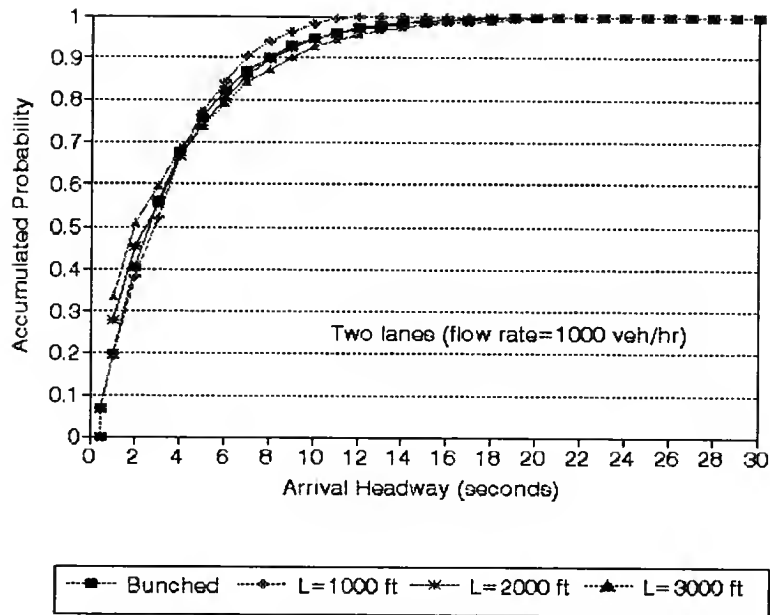
Figure 5-25. Comparison of analytical and simulation model arrival distributions for two-lane, 1000-vph flow.
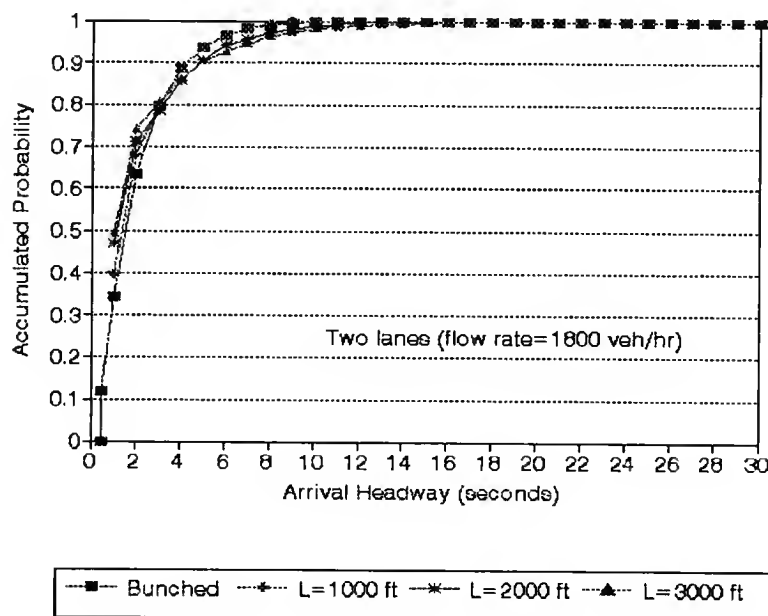
Figure 5-26. Comparison of analytical and simulation model arrival distributions for two-lane, 1800-vph flow.

Other Modeling Differences

The differences in arrival headway distributions are an important source of disparity between NETSIM and the proposed analytical model. They are also the easiest to explain. They are not however, the only differences between the two techniques. There are some stochastic aspects of the operation that do not lend themselves well to deterministic approximations. There is a significant divergence in the manner in which NETSIM and the HCM treat traffic complexities such as permitted left turns from shared lanes. The proposed analytical model has adopted the HCM approach as closely as possible in the treatment of traffic. This is essential if the results of this work are to be incorporated into the HCM.

The simulation runs presented in this dissertation were performed with the latest available version of NETSIM, a beta-test release of Version 5. This version has overcome several deficiencies which are evident in its predecessors, however, it is anticipated that additional enhancements to NETSIM will appear in the near future. For example, the changes in the vehicle generation algorithms will be forthcoming to allow user specified arrival headway distributions.

One of the most serious limitations of NETSIM at this point is the resolution of the input data for the average departure headway. This is currently 0.1 seconds, or about 5 percent of a typical departure headway. The HCM provides a method for estimating the saturation flow rate to a level of precision that definitely exceeds its accuracy. This is a currently insurmountable source of divergence between the two methods. For example, departure headways of 1.9, 2.0 and 2.1 seconds conform to saturation flow rates of 1895, 1800 and 1714 vphgpl, respectively. Saturation flow rates between these values are not

recognized by NETSIM. This problem was avoided in the most examples described in this dissertation by setting the saturation flow rates to 1800 vphgpl. It is suggested that, when a signalized intersection is operating at capacity, that 5 percent capacity increments are too coarse for an accurate analysis.

CHAPTER 6
EXTENDED REFINEMENT OF THE ANALYTICAL MODEL

Introduction

The previous chapters described a fully functional computation model to compute the average phase times and cycle length given the intersection configuration, traffic volumes, phasing and controller parameters. The model recognized all types of standard left turn treatments including permitted, protected and compound left turn protection (protected plus permitted or permitted plus protected). Permitted left turns could be made from either shared or exclusive lanes. The model was implemented in a program called ACT3-48, with data obtained directly from a data set created and edited by the WHICH program, which eliminates the need for a separate input data editor and facilitates the comparison of the ACT3-48 results with the corresponding results from other methods such as NETSIM. The results of the model evaluation in the last chapter are very encouraging. The model is analytically sound and the computational framework in which it has been implemented is robust. At this point, the model is ready for further refinement. In order to enhance the model to achieve a stronger capability to predict phase times and cycle length for actuated operation, some additional refinements of the analytical model are presented in this chapter. These refinements and enhancements include

122

1. Refinement of the analytical model for volume-density operation;

2. Refinement of the analytical model to incorporate free queue parameter; and

3. Incorporation of the analytical model into the HCM Chapter 9 procedure.

Refinement of the Analytical Model for Volume-density Operation

Volume-density operation is one version of traffic-actuated control which is best suited for an intersection with heavy volume on all approaches and a high approach speed (>35mph). In this operation, the controller employs a more complex set of criteria for allocating time and terminating the phase. In addition to actuated design parameters in fully-actuated operation, volume-density controllers have variable initial and gap reduction features, and detectors are usually placed at a distance from the stopline.

Volume-density Control Description

In volume-density control, the minimum initial interval (MnI) is the minimum assured green that is displayed. It must be long enough to allow vehicles stopped between the detector on the approach and the stopline to get started and move into the intersection. On some controllers the minimum green includes a minimum initial time plus a passage time. The minimum initial interval should be small to clear a minimum of vehicles expected during light volume. Another timed interval called variable initial interval (or added initial interval) will be added to the minimum initial interval. The length of the variable initial interval shown in Figure 6-1 is equal to the product of the number of vehicle arrivals on red and clearance intervals and the specified time interval for each vehicle actuation. This feature increases the minimum assured green so it will be long enough to serve the actual number of vehicles waiting for the green between the detector and the stopline.
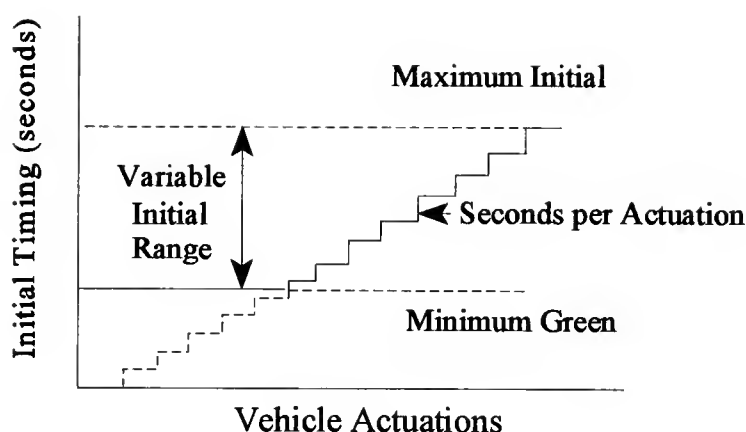
Figure 6-1. Variable initial feature for volume-density operation.

Another feature is gap reduction. The purposes of gap reduction are to reduce the probability of "maxout" and to prevent phase termination with vehicles in the "dilemma zone". The gap reduction feature shown in Figure 6-2 is accomplished by the following functional settings: time before reduction, passage time, minimum gap and time to reduce. These terms need to be defined.

The *time before reduction* period begins when the phase is green and there is a serviceable conflicting call (e.g. at time t in Figure 6-2). The *passage time* is the time required for a vehicle moving at average approach speed to travel from the detector to the stopline. The normal approach speed is assumed to be the 85th percentile speed. Upon completion of the *time before reduction* period, the linear reduction of the allowable gap

begins from the *passage time* to the *minimum gap*. The specified time for gap reduction is called *time to reduce*. Thus, the gap reduction rate is equal to the difference between the *passage time* and *minimum gap* settings divided by the setting of *time to reduce*. The purpose of gap reduction from the *passage time* to the *minimum gap* is to reduce the probability of maxout. In volume-density control, the last vehicle that actuates the detector before the allowable gap expires can extend the phase by one *passage time*. Therefore, this vehicle can safely pass the intersection and avoid the dilemma zone.
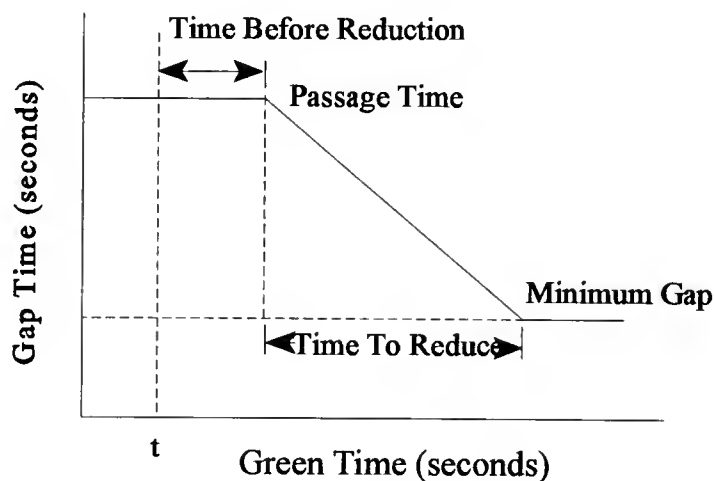
Figure 6-2. Gap reduction feature for volume-density operation.

Modeling of Volume-density Control

The previously developed analytical model is used to predict the phase time of any movement in a fully-actuated operation. However, it can also be applied to estimate the

phase duration for through vehicles and protected left turns for volume-density control if proper refinements of the analytical model are done. In this study, the time before reduction is assumed to be zero for simplicity and the gap reduction begins at the green phase. The proposed refinements to the model will be introduced next and a simple example application will follow.

Refinement of the Analytical Model

The main differences between the volume-density and basic fully-actuated operations are the minimum green time settings, the detector configuration, the gap reduction feature and the passage time setting for the last vehicle actuation. The refinement of the analytical model for volume-density operation focused on these areas.

The initial interval (II) (adjusted minimum green time) for volume-density operation is equal to the specified minimum green time (Smn) plus variable initial (added initial) subjected to the constraint of specified maximum initial setting, where the specified minimum green time here is equal to the minimum initial interval (MnI) plus starting gap (SG). It is common to choose a value for the starting gap which is equal to the passage time from the detector to the stopline. The variable initial interval is the product of the number of vehicles arrival on red the phase and the specified time for each vehicle actuation. The value of variable initial interval can be computed as follows:

$$\text{Variable Initial Interval (VII)} = Q_r * t_{act} \qquad (6\text{-}1)$$

where

Q_r = number of arrivals during previous red and clearance intervals; and

t_{act} = specified time per actuation.

Then, the initial interval (II) is equal to the sum of the specified minimum green (Smn) and variable initial interval (VII). However, this value cannot exceed the specified maximum initial interval (Smx). Therefore,

$$\text{Initial Interval (II)} \ = \ \text{Min. (Smn + VII, Smx)} \tag{6-2}$$

where

Smn = specified minimum green time; and

Smx = specified maximum initial interval.

The analytical model applies the queue accumulation polygon to compute the queue service time and the bunched arrival model to estimate the vehicle extension time after queue clearance. Based on the computation of total queue service time, QST ($= t_{sl} + g_{qst}$), and total vehicle extension time, EXT ($= e_g + I$), the final phase time, PT, can be obtained which is equal to the sum of QST and EXT. To estimate the phase times for the volume-density operation, the computation of the total queue service time, QST, needs to be modified because the location of presence detector is not necessarily at the stopline.

In the analytical model for fully-actuated operation, the detector is assumed to be placed at the stopline. However, It is common with volume-density control that the detector setback is greater than zero. In the queue discharge process when the signal turns green, the length of moving queue will decrease gradually if the volume to capacity ratio (v/c) is less than 1.0.

The last moving queue will pass through the upstream detector first and then the stopline. The queue service time is defined as the time required to serve the queue beyond the detector. Therefore, the queue service time for volume-density control, in general, is

shorter than that for fully-actuated operation. The proposed refined model will use the total queue service time of the fully-actuated operation minus a passage time to estimate the queue service time for the volume-density operation. This will be called *computed queue service time* (CQST).

The initial interval (adjusted minimum green) is the assured green that will be displayed. If, at the end of the initial interval, the length of the farthest backup queue (FBQ) from the stopline does not reach the upstream detector, the final queue service time should be equal to the minimum value of the initial interval and computed queue service time. For example, if the initial interval is less than the computed queue service time, the final queue service time is the initial interval because for the upstream detector the queue has been cleared at the end of initial interval. If the FBQ exceeds the upstream detector, the final queue service time is just equal to the computed queue service time.

An easy way to determine whether or not the FBQ reaches the upstream detector is to compare the FBQ and the maximum storage of vehicles (MSV) between the upstream detector and stopline. A vehicle is assumed to occupy 25 ft, so MSV is equal to the distance between the upstream detector and the stopline divided by 25. The length of the FBQ may be estimated from the average vehicle arrivals during the red and initial interval using the following formula:

$$FBQ = q_r * (R + II) \tag{6-3}$$

The computation for QST may be summarized as follows:

$$QST = Min. (CQST, II) \quad if \quad FBQ < MSV \tag{6-4}$$

$$QST = CQST \quad if \quad FBQ \geq MSV \tag{6-5}$$

Example Problem

With the above refinements, the model is able to predict the phase times of protected movements for volume-density operation. A simple scenario with a two-phase volume-density operation was examined as a basic evaluation. Each approach has just one lane and carries the same through traffic. The traffic volume is varied from 100 to 800 vph per approach to examine the sensitivity of the proposed method. The minimum and maximum green times are 6 and 60 seconds, respectively. The maximum initial is 16 seconds. The minimum allowable gap setting is set to 2 seconds. The detector is 30 feet in length. Each vehicle actuation during the red phase can add 2 seconds to the minimum green time. Three specific values of detector setbacks were used to represent short, medium and long values, respectively. The estimated phase times from the model were compared with those from NETSIM simulation runs.

The results for 0-ft, 150-ft and 300-ft detector setbacks are shown in Figures 6-1, 6-2 and 6-3, respectively. Both the proposed analytical model and the NETSIM simulation model show a credible sensitivity to the detector setback. As the detector setback increases, the predicted phase times from both model computation and NETSIM simulation decrease because the probability of accumulated queue beyond the detector decreases when the detector setback increases.

Generally speaking, the phase times estimated from the model are close to those from NETSIM simulation. Therefore, within the limits of this simple example, it appears that the proposed analytical model is able to provide reasonable estimates of phase times for volume-density operation.
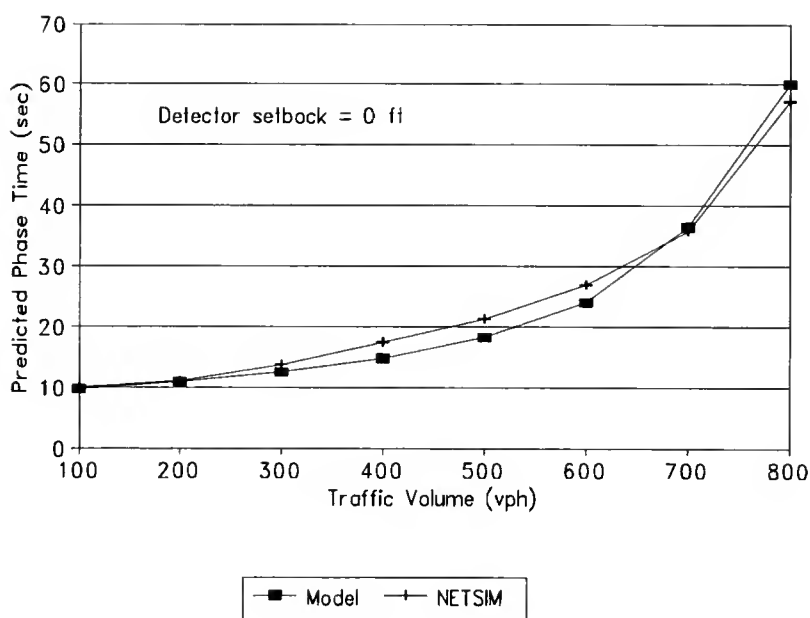
Figure 6-3.   Phase time comparison for volume-density operation with a zero detector setback.
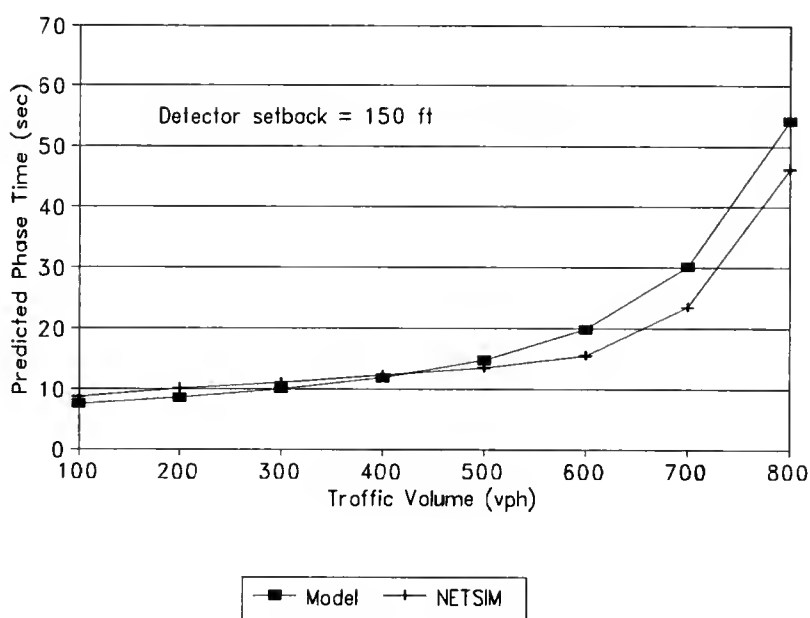
Figure 6-4.   Phase time comparison for volume-density operation with a 150-ft detector setback.
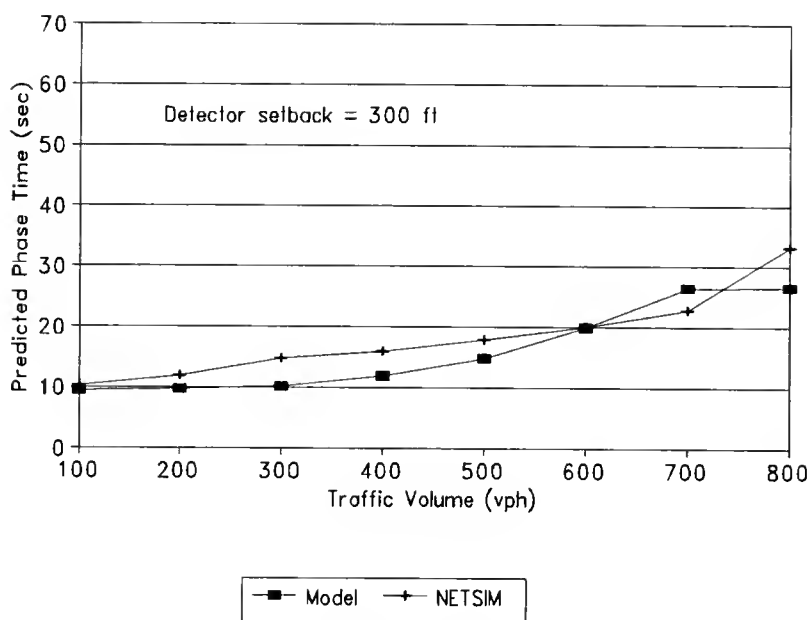
Figure 6-5.   Phase time comparison for volume-density operation with a 300-ft detector setback.

Refinement of the Analytical Model to Incorporate "Free Queue" Parameter

The free queue parameter indicates the number of left-turning vehicles that may be stored in a shared lane waiting for gaps in the opposing traffic without blocking the passage of the following vehicles. Therefore, both the left turn equivalence, E_{L1}, and the shared lane saturation flow rate are affected by the free queue parameter. The current HCM procedure assumes that the first waiting left turn will block all of the following vehicles in the shared lane. This produces pessimistic results in some cases.

At this point, only the SIDRA model considers the free queue explicitly which adopted the use of an average saturation flow to count for the effect of free queue. Because of its importance to traffic-actuated control, it is essential that the proposed analytical model

recognizes this phenomenon. The analytical basis of the model for free queue is described in this dissertation. A set of curves is developed to illustrate the effect of free queue on the estimated phase times as a function of the approach volume. Because NETSIM does not recognize the free queue explicitly, it was not possible to test this model by simulation.

Computation of New Through-car Equivalents

Left-turning vehicles will select gaps through the opposing flow after the opposing queue clears. During this unsaturated period, the HCM Chapter 9 assigns E_{L1} through-car equivalents for each left-turning vehicle. Normally, the permitted saturation flow rate of a shared lane can be computed based on the assigned value of E_{L1} and the proportion of left turns, P_L, in the shared lane. However, if a free queue exists, the block effect of left-turning vehicles may be reduced. Therefore, the value of E_{L1} needs to be modified to account for the effect of the free queues. The permitted saturation flow rate may become large because of reduced block effect.

The new E_{L1} for a left-turning vehicle on a shared lane with free queues can be computed based on 1) the value of E_{L1} for each combination of vehicles affected by the left-turning vehicle during its maneuver time; and 2) the probability of each combination. The proposed theory and method for computing the new E_{L1} are described below.

If old E_{L1} is equal to n, the original maneuver time required for the left-turning vehicle is equal to the maneuver time required for n through vehicles. That means this left-turning vehicle may block (n-1) following vehicles which can be left turns or through vehicles including right turns. Thus, these (n-1) vehicles following the left-turning vehicle need to be considered if a free queue exists because they are affected by the left-turning vehicle.

If no free queue exists, the individual E_{L1} for any vehicle combination is always the same because during the original maneuver time of the left-turning vehicle, only this left-turning vehicle can departure. The following (n-1) vehicles have no chance to leave due to the block by the left-turning vehicle. Therefore, the through-car equivalents for this left-turning vehicle is still equal to n.

If a free queue exists, the individual E_{L1} for a vehicle combination will be different if the combination of the following (n-1) vehicles is different. For example, assuming there exists one free queue, if the following (n-1) vehicles are all left turns, the new left turn equivalence for this combination is still equal to n because only this left-turning vehicle can departure during its original maneuver time. However, if the following (n-1) vehicles are all through vehicles, the new left turn equivalence for this combination is equal to one because all n vehicle can departure during the original maneuver time of the left-turning vehicle. No block effect occurs. Due to the existence of one free queue, this left-turning vehicle is equivalent to one through vehicle. Hence, the new value of E_{L1} may be computed as an weight average of the individual E_{L1} based on its probability of vehicle combination.

The proportion of left turns in a shared lane, P_L, is a very important factor for the computation of the probability for each combination of the following (n-1) vehicles. Because the following vehicles are belong to either left turn category (L) or through category (T), there are a total of $2^{(n-1)}$ combinations. For each combination, the individual left turn equivalence and its probability can be computed. By taking the weight average of individual E_{L1}, the new value of E_{L1} for the left-turning vehicle can be obtained. A simple example for the computation of new left turn equivalence is illustrated below.

Example: The through-car equivalents of a left-turning vehicle, $E_{L1} = 3$; and

The proportion of left turns in a shared lane, $P_L = 0.2$

The computation of the new through-car equivalents is as follows:

Total combinations = $2^{(n-1)} = 2^{(3-1)} = 4$

The probability of a left-turning vehicle in a shared lane = 0.2

The probability of a through vehicle in a shared lane = 1 - 0.2 = 0.8

Combination:	<u>1</u>	<u>2</u>	<u>3</u>	<u>4</u>
Left turn:	L	L	L	L
Following vehicles:	L	L	T	T
	L	T	L	T
Probability:	0.04	0.16	0.16	0.64
Individual E_{L1}:	3	3	2	1

Therefore,

New E_{L1} = (0.04 x 3) + (0.16 x 3) + (0.16 x 2) + (0.64 x 1) = 1.56

The range of original (old) E_{L1} vales presented in the HCM Chapter 9 is from 1.05 to 16.0 for permitted left turns in a shared lane and the range for P_L is from 0 to 1.0. The reasonable maximum value of the free queue considered in this study is 2.0 vehicles. Based on the proposed method, the new E_{L1} values for one and two free queues are shown in the Tables 6-1 and 6-2, respectively. If the old E_{L1} value, P_L value or the number of free queues is not a specified value in the tables, the new E_{L1} can be estimated by interpolation.

Table 6-1. Through-car equivalents, E_{L1}, for permitted left turns in a shared lane with one free queue.

Old E_{L1}	The Proportion of Left Turns in the Shared Lane, P_L										
	0	0.1	0.2	0.3	0.4	0.5	0.6	0.7	0.8	0.9	1
1.05	1.05	1.05	1.05	1.05	1.05	1.05	1.05	1.05	1.05	1.05	1.05
2	1.05	1.10	1.20	1.30	1.40	1.50	1.60	1.70	1.80	1.90	2.00
3	1.05	1.29	1.56	1.81	2.04	2.25	2.44	2.61	2.76	2.89	3.00
4	1.05	1.56	2.05	2.47	2.82	3.13	3.38	3.58	3.75	3.89	4.00
5	1.05	1.90	2.64	3.23	3.69	4.06	4.35	4.57	4.75	4.89	5.00
6	1.05	2.31	3.31	4.06	4.62	5.03	5.34	5.57	5.75	5.89	6.00
7	1.05	2.78	4.05	4.94	5.57	6.02	6.34	6.57	6.75	6.89	7.00
8	1.05	3.30	4.84	5.86	6.54	7.01	7.33	7.57	7.75	7.89	8.00
9	1.05	3.87	5.67	6.80	7.53	8.80	8.33	8.57	8.75	8.89	9.00
10	1.05	4.49	6.54	7.76	8.52	9.00	9.33	9.57	9.75	9.89	10.00
11	1.05	5.14	7.43	8.73	9.51	10.00	10.33	10.57	10.75	10.89	11.00
12	1.05	5.82	8.34	9.71	10.51	11.00	11.33	11.57	11.75	11.89	12.00
13	1.05	6.54	9.27	10.70	11.50	12.00	12.33	12.57	12.75	12.89	13.00
14	1.05	7.29	10.22	11.69	12.50	13.00	13.33	13.57	13.75	13.89	14.00
15	1.05	8.06	11.18	12.68	13.50	14.00	14.33	14.57	14.75	14.89	15.00
16	1.05	8.85	12.14	13.68	14.50	15.00	15.33	15.57	15.75	15.89	16.00

Table 6-2. Through-car equivalents, E_{L1}, for permitted left turns in a shared lane with two free queue.

Old	The Proportion of Left Turns in the Shared Lane, P_L										
E_{L1}	0	0.1	0.2	0.3	0.4	0.5	0.6	0.7	0.8	0.9	1
1.05	1.05	1.05	1.05	1.05	1.05	1.05	1.05	1.05	1.05	1.05	1.05
2	1.05	1.1	1.2	1.3	1.4	1.5	1.6	1.7	1.8	1.9	2.0
3	1.05	1.2	1.4	1.6	1.8	2.0	2.2	2.4	2.6	2.8	3.0
4	1.05	1.3	1.6	1.9	2.2	2.5	2.8	3.1	3.4	3.7	4.0
5	1.05	1.4	1.8	2.2	2.6	3.0	3.4	3.8	4.2	4.6	5.0
6	1.05	1.5	2.0	2.5	3.0	3.5	4.0	4.5	5.0	5.5	6.0
7	1.05	1.6	2.2	2.8	3.4	4.0	4.6	5.2	5.8	6.4	7.0
8	1.05	1.7	2.4	3.1	3.8	4.5	5.2	5.9	6.6	7.3	8.0
9	1.05	1.8	2.6	3.4	4.2	5.0	5.8	6.6	7.4	8.2	9.0
10	1.05	1.9	2.8	3.7	4.6	5.5	6.4	7.3	8.2	9.1	10.0
11	1.05	2.0	3.0	4.0	5.0	6.0	7.0	8.0	9.0	10.0	11.0
12	1.05	2.1	3.2	4.3	5.4	6.5	7.6	8.7	9.8	10.9	12.0
13	1.05	2.2	3.4	4.6	5.8	7.0	8.2	9.4	10.6	11.8	13.0
14	1.05	2.3	3.6	4.9	6.2	7.5	8.8	10.1	11.4	12.7	14.0
15	1.05	2.4	3.8	5.2	6.6	8.0	9.4	10.8	12.2	13.6	15.0
16	1.05	2.5	4.0	5.5	7.0	8.5	10.0	11.5	13.0	14.5	16.0

When the value of new through-car equivalents, $E_{L1(new)}$, for a shared lane permitted left turn is known, the new permitted saturation flow, $s_{p(new)}$, of a shared lane can be computed as follows:

$$s_{p \text{ (new)}} = \frac{s}{1 + P_L \ (E_{L1 \text{ (new)}} - 1)} \tag{6-6}$$

where

s = protected saturated flow rate (veh/sec); and

P_L = the proportion of left turns in the shared lane.

Estimation of Free Green, g_f, with Free Queue Parameter

The free green, g_f, originally described in the HCM needs to be modified when the free queue parameter is considered. When the green is initiated, the opposing queue begins to move. While the opposing queue is being served, left turns from the subject shared lane are effectively blocked. The portion of effective green blocked by the clearance of an opposing queue is referred as g_q in the HCM. Until the first left-turning vehicle arrives, however, the through vehicles on the shared lane are unaffected by left turners. The portion of effective green before the arrival of the first left-turning vehicle is referred to as free green, g_f, in the HCM. Basically, free green represents the time during which the through vehicles in the shared lane are not affected by a left turner when the green initiates.

Generally, signal timing models assume that the first permitted left turn at the stopline will block a shared lane. This is not always the case, as the through vehicles in the shared lane are often able to "squeeze" around one or more left turns or left-turning vehicles wait near

the intersection center. A reasonable value of free queues is between zero and two. The proper number of free queues can be observed from field. A left-turning vehicle in the free queue will not block the following vehicle in the shared lane, so the free green will increase. The proposed method to estimate the new free green with the existence of free queue is describe as follows.

Based on the number of opposing lanes, n_{opp}, and the relationship between g_q and g_f, the permitted saturation flow rate, s_p, can be determined as follows:

$$s_p = \frac{s}{1 + P_L (E_{L2} - 1)} \qquad \text{if } n_{opp} = 1 \text{ and } g_q > g_f \qquad (6\text{-}7a)$$

$$s_p = \frac{s}{1 + P_L (E_{L1(new)} - 1)} \qquad \text{others} \qquad (6\text{-}7b)$$

where

s = protected saturated flow rate;

P_L = proportion of left turns in the shared lane;

$E_{L1(new)}$ = new through-car equivalents for each left-turning vehicle during the unsaturated green period; and

E_{L2} = through-car equivalents for each left-turning vehicle during the period of $(g_q - g_f)$ when g_q is greater than g_f and the number of the opposing lane n_{opp} is equal to one.

Assume the average maneuver time (waiting time) for a LT vehicle in the free queue to leave is x seconds. This waiting time can be derived as follows:

$$\frac{1}{s_p} = \frac{(1-P_L)}{s} + P_L \; x$$

Therefore,

$$x = \frac{s - s_p + S_p \; P_L}{s \; s_p \; P_L} \tag{6-8}$$

The key to estimate the new g_f for permitted left turns in a shared lane with free queues is to estimate the time when a left turn arrival will block further flow in a shared lane. In order to estimate new g_f, the probability of blocking effect needs to be computed first which is the probability of at least one left turn arrival before one free queue space in the free queue location is available. If one free queue space in the free queue location is always available before one left turn arrives, no blocking effect will happen.

For the convenience of computation, "t" is defined as the average time allowed for a left-turning vehicle to go into the free queue location without blocking the further traffic flow. For example, the number of free queues available in a free queue location is two (n=2). The left-turning vehicle in the free queue location takes 8 seconds to leave (i.e. $x = 8$ seconds) on average. Then, t will be equal to 4 seconds ($= x/n = 8/2$). Assume the number of free queues is n $(0<n\leq2)$. t can be expressed as

$$t = x / n \qquad \text{if } n > 1$$

$$t = x \qquad \text{if } 0 < n \leq 1$$

Note that when n is less than one, the number of free queues will be assumed to be one first. Later, the free green will be modified based on the real number of free queues

according to its probability. This process will avoid a very large t when n is very small. During t seconds, the probability of left turn arrivals is P. According to the bunched arrival distribution, the probability P can be computed as the product of bunched cumulative distribution and the probability of left turn arrivals in a shared lane:

$$P = [1 - \varphi e^{-\lambda(t - \Delta)}] P_L \qquad (6\text{-}9)$$

where

Δ = minimum arrival (intra-bunch) headway (seconds);

φ = proportion of free (unbunched) vehicles; and

λ = a parameter calculated as

$$\lambda = \frac{\varphi q}{1 - \Delta q}$$

subject to $q < 0.98/\Delta$

where

q = total equivalent through arrival flow (vehicles/second) for all lane groups that actuated the phase under consideration.

During the maneuver time of x seconds for the left-turning vehicle, the probability of block effect due to left turn arrivals is assumed P'. P' can be computed by the following equations. Note that, at this stage the number of free queues, n, is still treated as one if it is less than one.

$$P' = P^n \qquad \text{if } n > 1 \qquad (6\text{-}10a)$$

$$P' = P \qquad \text{if } 0 < n \leq 1 \qquad (6\text{-}10b)$$

The new free green, g_f, can be computed as follows:

$$g_{f\,(new)} = g_{f\,(old)} + \frac{x}{p'} \qquad\qquad if\ n > 1 \qquad\qquad (6\text{-}11a)$$

$$g_{f\,(new)} = g_{f\,(old)} + n\,\frac{x}{p'} \qquad\qquad if\ 0 \le n \le 1 \qquad\qquad (6\text{-}11b)$$

In Equation 6-11b, the extended time of free green (x/p') is multiplied by n to account its occurrence probability of one free queue because it is assumed one in the previous computation. If free queues exist, the phase times of traffic-actuated operation may be influenced. The degree of difference between the phase times with and without free queues for a shared lane is mainly dependent on the combined effects of free green and through-car equivalents of a left-turning vehicle. The effect of the free queue parameter is especially important for a single shared lane.

The phase time analysis for free queue parameter is best illustrated with a simple example. Consider a trivial intersection with four single-lane approaches. All approaches are configured identically and carry the same traffic volume. In each approach, the portions of left turns, through and right turns are 0.2, 0.7 and 0.1, respectively. This is a simple two-phase fully-actuated operation. The minimum phase time for each approach is 15 seconds and the maximum phase time is 84 seconds. Detectors are 30 feet long and placed at the stopline. The allowable gap is 3 seconds. In each phase, the intergreen time is 4 seconds, and the lost time of 3 seconds is assumed.

Each approach volume varies from 100 to 800 vph, while the range of free queue is set from 0 to 2. Based on the proposed method, the phase time prediction for different free queues is shown in Figure 6-6. In this figure, the x axis represents the approach volume, the

y axis shows the number of free queues, and the vertical axis is the predicted phase from the

proposed analytical model. The effects of free queues may be easily observed from this three

dimensional surface diagram.
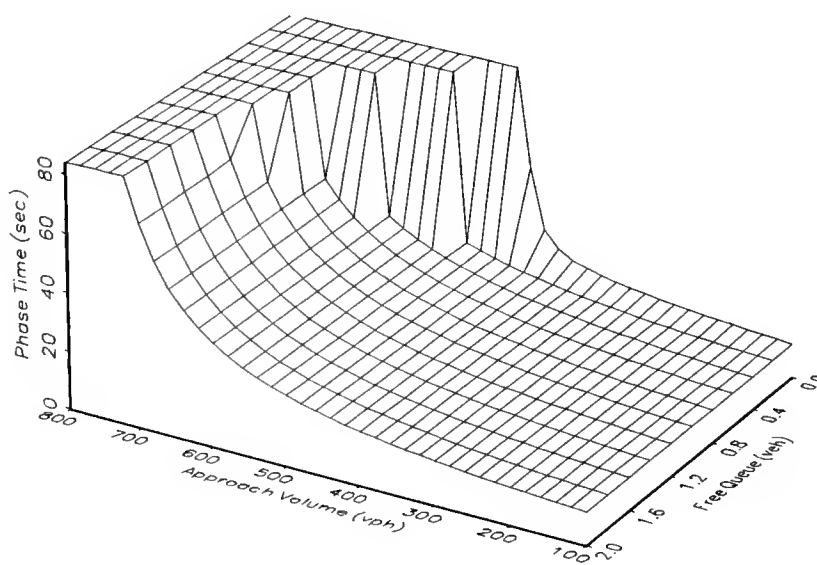
Figure 6-6. Phase time prediction for single shared lane with free queues.

In this example, left turns only occupy 20 percent of the total approach volume.

When approach volume is low, the headway between vehicles is large, and a left turn

maneuver is relatively easy to make. Therefore, the block effect caused by left turns is very

small. Theoretically, there will be nearly no difference of predicted phase times between

different free queues. This phenomenon can be shown in Figure 6-6 when approach volume

is below 400 vph. The left turn maneuver will become more and more difficult when the approach volume becomes heavier, because the number of acceptable gaps for left turns during the unsaturated portion of the opposing queue decreases. In other words, E_{L1} become large with the increase of the approach volume.

For the same number of free queues, the phase times will increase with the approach volume due to the increasing block effect by left turns in the shared lane. On the other hand, if the number of the free queues increases and the approach volume is fixed, the block effect is reduced because left-turning vehicles are able to wait in the free queue before turning left. The larger the free queue, the smaller the blocking effect.

These two phenomena can be clearly shown in Figure 6-6 when the volume is between 400 vph and 720 vph and the value of free queues is between 0 to 1.2. It is clear that the phase times will be mainly dependent on the combined effects of approach volume and free queues. In Figure 6-6, it is also easy to observe that the effect of free queue is reduced when the approach volume becomes very large. In this example, when volume exceeds 720 vph and the free queue exceeds 1.2, the phase times are always equal to the maximum phase time (84 seconds in this case). This indicates that the effect of the free queue is too small to prevent the phase time from reaching its maximum.

<u>Incorporation of the Analytical Model into the HCM Chapter 9 Procedure</u>

The HCM Chapter 9 Appendix II method is used to estimate the phase times for traffic-actuated operation. In the previous evaluation, the Appendix II method showed its limit to accurately predict the traffic-actuated phase times. The evaluation results indicated that the analytical model developed in this study can provide a much better prediction on

traffic-actuated signal timing than the Appendix II method. Thus, the analytical model may be used to replace the Appendix II model in the HCM Chapter 9 procedure.

The major difference in capacity computation between pretimed and actuated controlled intersections lies in the use of the effective green/cycle length (g/C) ratio. Unlike pretimed signals, the lane group g/C ratio for actuated operation does not stay constant but fluctuates from cycle to cycle. For actuated control, once the average g/C ratio of the lane group is known, the lane group capacity can be computed, as the product of the adjusted lane group saturation flow rate and its g/C ratio. Based on this basic method described in the HCM Chapter 9 for capacity computation, the analytical model can compute the average lane group g/C ratio and its capacity, which is listed in the output of the ACT3-48 program.

The traditional delay formulation used by virtually all analytical models is based on two components representing uniform delay and incremental delay respectively. The sum of the two components produces the computed delay per vehicle. Since the QAPs must be developed in detail by the proposed analytical model to determine the phase times, the value of the uniform delay term (i.e., the area contained within the QAP) may be computed by a simple extension to the existing model.

The detailed development of the QAP for any possible phase sequence and vehicle movement was presented earlier in this dissertation. The areas contained within the QAPs may be calculated readily from their geometry as an extension of the procedure now used in the supplemental worksheet for delay computation with compound left turn protection presented in the 1994 HCM update. The uniform delays can be determined using only those variables (volumes, saturation flow and signal timing) that are used by the existing HCM

Chapter 9 methodology. The uniform delay formulas developed in this study for each possible phase sequence associated with vehicle movement are shown in the Appendix. The ACT3-48 program is able to provide the uniform delay computation for each lane group. It can also provide lane group volume/capacity (v/c) ratios which may be very useful for the lane group incremental delay computation.

In summary, the phase times predicted from the analytical model can be used as an input to the HCM Chapter 9 procedure to estimate the capacity and delay of each lane group for traffic-actuated operation. The proposed analytical model has adopted the HCM approach as closely as possible in the treatment of traffic and the computation of capacity and delay. In addition, the worksheets developed in this study also provide a standard structure for presenting the results of computations in a common form that is compatible with the prescribed techniques. Therefore, the analytical model can be properly incorporated into the HCM Chapter 9 procedure to estimate capacity and delay. From the delay estimates, the level of service for each lane group and for the whole intersection can be determined

CHAPTER 7
CONCLUSIONS AND RECOMMENDATIONS

This dissertation has presented a comprehensive methodology and demonstrated a practical analytical procedure for the prediction of traffic-actuated signal timing for both isolated and coordinated modes. A computer program called ACT3-48 has been developed as a tool to implement the proposed analytical model and procedure. In comparison with the primitive technique presented in Appendix II to the Highway Capacity Manual (HCM) Chapter 9, the proposed analytical model has demonstrated its capability to provide a better estimate of actuated phase times than the HCM Chapter 9 Appendix II method. In comparison with simulation results and field data, the model has been shown to be a powerful tool to predict the traffic-actuated signal timing. The conclusions and recommendations addressed in this chapter are offered as a result of this study.

Conclusions

Three major conclusions of the research and their supporting considerations are presented below.

First, the proposed model can improve the analytical treatment of traffic-actuated control in the HCM Chapter 9 on signal timing prediction and the proposed methodology can be incorporated into the corresponding HCM procedure. This conclusion is supported by the following considerations:

146

1. This study considers the effects of actuated controller parameters and detector configurations. The proposed analytical model is sensitive to common variations in the actuated controller parameters and detector configurations.

2. The proposed analytical model considers all required inputs for actuated operation and predicts the traffic-actuated signal timing with strong theoretical basis. It can eliminate the major problems of the invalid assumption and the simplistic nature of the Appendix II technique in HCM Chapter 9.

3. The proposed analytical model has adopted the HCM approach as closely as possible. A set of worksheets has been developed to provide a structure for understanding the proposed technique and computational procedure. The ACT3-48 program developed in this study can also produce capacity and delay output; thus, it is appropriate to be incorporated into the HCM Chapter 9 procedure for traffic-actuated signal timing prediction.

Second, the proposed model can deal with possible phase sequences given a specified set of traffic volumes, actuated controller parameters, intersection configuration and detector placements. The following considerations support this conclusion:

1. The proposed analytical model considers all possible phase sequences.

2. For each specified phase sequence, the model developed in this study is functionally capable of providing reasonable estimates of operating characteristics such as average phase times and cycle length under normal range of traffic volumes, practical design of actuated controller parameters, intersection configuration and detector placements.

Third, the proposed analytical model can accurately and quickly predict the signal timing for traffic-actuated operation. The proposed model is analytically sound and the computational framework is robust. The following considerations support this conclusion:

1. The development of the traffic-actuated signal timing prediction model, in this study, is based on functionally and practically sound theories and concepts. The main theories and concepts include actuated operation logic, dual-ring operation logic, queue accumulation polygon concept (queuing theory), vehicle arrival headway distribution, circular dependency relationship and sequential process.

2. In the comparison of phase times and cycle length, between the analytical model and NETSIM simulation for fully-actuated operation based on a wide variety of conditions, the results show the proposed model and NETSIM simulation compare very favorably. These are confirmed by very high R square values.

3. In the limited comparison of phase times between the analytical model and actual field data for fully-actuated operation, the analytical model is able to achieve substantially the same results as field data.

4. This study proposes a procedure, which implements the analytical model for fully-actuated operation, to predict the phase times for coordinated semi-actuated operation. The results show that the procedure is capable of providing credible estimates of phase times for coordinated operation of a traffic-actuated controller. The phase times predicted based on the proposed procedure are very close to NETSIM estimates.

5. Most signal timing can be predicted by the ACT3-48 program in less than 10 seconds.

With regard to the refinements of the analytical model for the basic volume-density operation and for the incorporation of the free queue parameter, it is concluded that slight modification of the analytical model for fully-actuated operation can be used to predict the phase times and their corresponding cycle length for basic volume-density operation and for free queue scenarios.

Recommendations

The recommendations from the research described in this dissertation are divided into two parts. The first part addresses further improvement of the current analytical model and further investigation on the source of disparity between the proposed model and NETSIM. The second part suggests areas for further research.

Recommended Model Improvements

The proposed analytical model adopts the bunched exponential headway distribution to predict the vehicle extension time after an accumulated queue has been served. The bunched exponential headway distribution depends heavily on the traffic flow rate, but it is independent of link length. From the theoretical view and simulation observation, link length is a variable required to be considered in the bunched exponential headway distribution. Further study may focus on the examination of the impact of link length to the bunched exponential headway distribution and the proposed analytical model.

The length of a phase will depend heavily upon the probability of a gap extended in the traffic flow after an accumulated queue has been served. A vehicular arrival distribution

with a higher accumulated probability to actuate a detector to extend the allowable gap after the queue clearance will, in general, produces a longer phase time.

In the phase time comparison, it is found that, in general, NETSIM simulation produces longer phase times for medium and heavy volumes and shorter phase times for low volumes. The difference in arrival headway distributions between the NETSIM and bunched arrival models at the detector were found to be an important source of disparity of phase times between NETSIM and the proposed analytical model. They are also the easiest to explain. They are not, however, the only difference between the two techniques. There are some stochastic aspects of the operation that may not lend them well to deterministic approximations. There is also a significant divergence in the manner in which NETSIM and the analytical model treat traffic complexities such as permitted left turns from shared lanes.

It is anticipated that additional enhancements to NETSIM will appear in the near future. The new version of NETSIM should allow users to specify an arrival distribution. Further investigation should be conducted to compare phase time prediction between the proposed analytical model and any subsequent versions of NETSIM.

Recommended Future Research

Level of service of an intersection is directly related to its total delay value. The total delay formulation adopted by virtually all analytical models is equal to the summation of uniform delay and incremental delay. Based on the signal timing predicted by the analytical model developed in this study, the uniform delay for traffic-actuated operation can be estimated more accurately. Further research should focus on the development of the incremental delay formulation for traffic-actuated operation.

The phase time prediction model developed in this study covers basic volume-density operation. Further research may also expand the proposed analytical model to cover more complex volume-density operation and adaptive control strategies.

APPENDIX
UNIFORM DELAY FORMULAS

An analytical model describing the operation of a traffic-actuated signal has been developed in this study. The scope of this model is limited to the estimation of phase times, cycle lengths and volume/capacity ratios. Delay estimates are also required to assess the level of service (LOS) for each movement. Fortunately, the computational structure of the model lends itself very well to the estimation of delay.

The traditional delay formulation used by virtually all analytical models is based on two components, or terms, which are added together to produce the total delay per vehicle:

1. The uniform delay term, which determines the delay that would apply if all vehicles arrived in a completely uniform manner. This term is computed as the area under the queue accumulation polygon (QAP).

2. The incremental delay term, which adds a correction factor to compensate for randomness in the arrival patterns and the occasional oversaturation.

Since the QAPs must be developed in detail by the proposed analytical model to determine the phase times, the value of the uniform delay term (i.e., the area contained within the QAP) may be computed by a simple extension to the existing model. The detailed development of the uniform delay equations for computing the QAP areas of possible phasing alternatives is presented in this appendix.

There are ten distinctive shapes that may be taken by the QAP, each of which is associated with a specific phasing alternative. Each case is developed as a separate figure in this appendix. Each figure shows the shape of the QAP and presents the derivation of an equation that determines the uniform delay by computing the area of the associated polygon. Note that the minimum value of each accumulated queue for each case is zero. A summary of the phasing alternatives in Figures A-1 through A-10 is presented in Table A-1. The derivations are presented in a format similar to the format used in the supplemental worksheet now contained in HCM Chapter 9 for delay computations with compound left turn protection. In all cases, the delay may be determined using only those variables (volumes, saturation flow rates and signal timing) that are used by the existing Chapter 9 methodology.

Table A-1. Summary of phasing alternatives for the computation of uniform delay.

Figure	Description of Phasing Alternative
A-1	Single protected phase
A-2	Permitted left turns from an exclusive lane ($n_{opp} > 1$)
A-3	Permitted left turns from an exclusive lane ($n_{opp} = 1$)
A-4	Permitted left turns from a shared lane ($g_q > g_f$)
A-5	Permitted left turns from a shared lane ($g_f \leq g_q$)
A-6	Compound left turn protection: HCM Chapter 9 Case 1
A-7	Compound left turn protection: HCM Chapter 9 Case 2
A-8	Compound left turn protection: HCM Chapter 9 Case 3
A-9	Compound left turn protection: HCM Chapter 9 Case 4
A-10	Compound left turn protection: HCM Chapter 9 Case 5
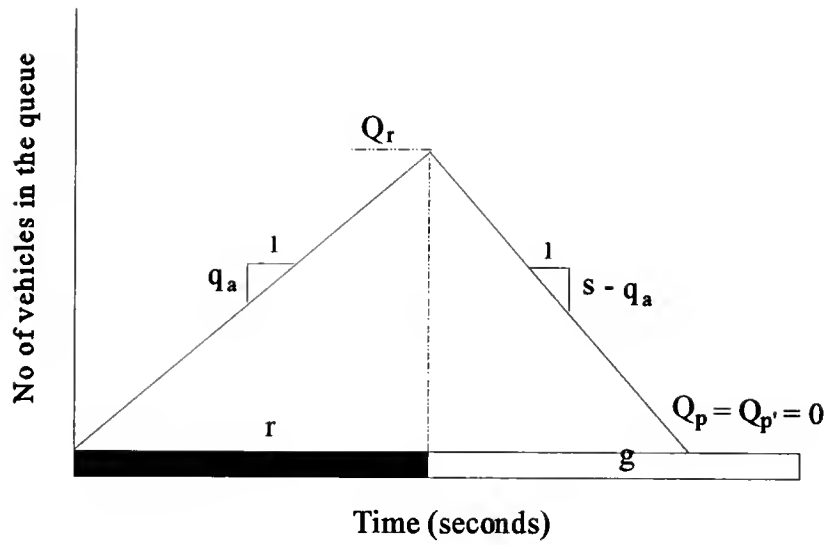
$$Q_r = r \, q_a$$

$$Q_q = Q_r$$

$$Q_p = Q_{p\prime} = 0$$

$$d_1 = \frac{0.5 \, [\, r \, Q_r + Q_r^2 \, / \, (s - q_a) \,]}{q_a \, C} \qquad \text{for isolated operation}$$

$$d_1 = \frac{0.5 \, [\, r \, Q_r + Q_r^2 \, / \, (s - q_a) \,]}{q_a \, C} \; \frac{(1 - P) \, f_p}{1 - (g \, / \, C)} \qquad \begin{array}{l}\text{for coordinated} \\ \text{phases 2 \& 6 only}\end{array}$$

Figure A-1. Uniform delay for single protected phase.
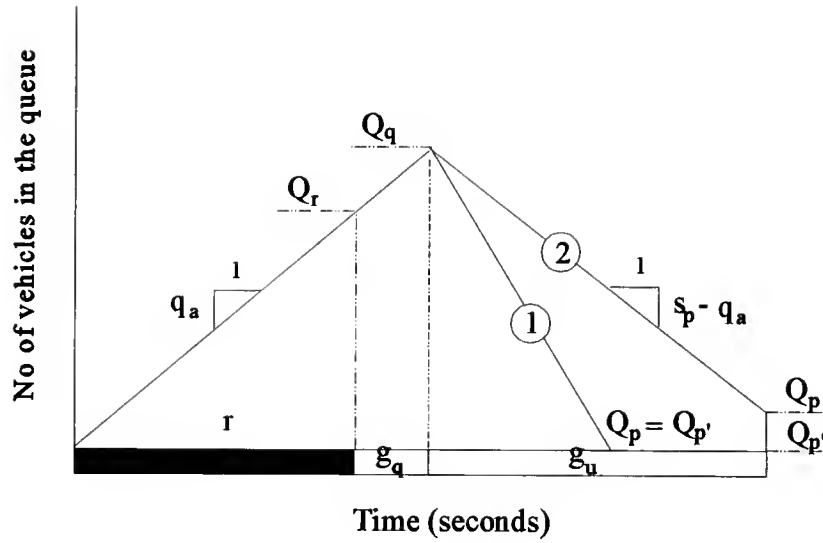
$$Q_r = r \, q_a$$

$$Q_q = Q_r + g_q \, q_a$$

$$QST = \frac{Q_q}{s_p - q_a}$$

Condition 1: $QST \le g_u$

$$Q_p = Q_{p'} = 0$$

$$d_1 = \frac{0.5 \left[(r + g_q) \, Q_q + Q_q^2 / (s_p - q_a) \right]}{q_a \, C}$$

Condition 2: $QST > g_u$

$$Q_p = Q_q - g_u (s_p - q_a)$$

$$Q_{p'} = 0$$

$$d_1 = \frac{0.5 \left[(r + g_q) \, Q_q + g_u (Q_q + Q_p) \right]}{q_a \, C}$$

Figure A-2. Uniform delay for permitted left turns from an exclusive lane ($n_{opp} > 1$).
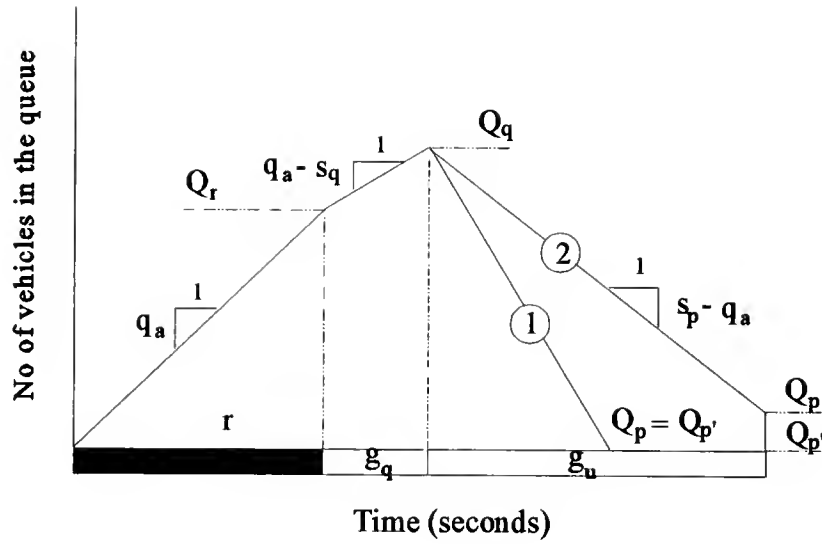
$$Q_r = r \; q_a$$

$$s_q = \frac{s}{E_{L2}}$$

$$Q_q = Q_r + g_q \; (q_a - s_q)$$

$$QST = \frac{Q_q}{s_p - q_a}$$

Condition 1: $QST \leq g_u$

$$Q_p = Q_{p'} = 0$$

$$d_1 = \frac{0.5 \; [\; (r + g_q) \; Q_q + Q_q^{\;2} \, / \, (s_p - q_a) \;]}{q_a \; C}$$

Condition 2: $QST > g_u$

$$Q_p = Q_q - g_u \; (s_p - q_a)$$

$$Q_{p'} = 0$$

$$d_1 = \frac{0.5 \; [\; (r + g_q) \; Q_q + g_u \; (Q_q + Q_p) \;]}{q_a \; C}$$

Figure A-3. Uniform delay for permitted left turns from an exclusive lane ($n_{opp} = 1$).

The figure shows a queue diagram with "No of vehicles in the queue" on the vertical axis and "Time (seconds)" on the horizontal axis. Labeled points include Q_r, Q_f, Q_q, $Q_p = Q_{p'}$, and $Q_{p'}$. Slopes labeled q_a, $s - q_a$, $s_p - q_a$. Time segments labeled r, g_f, g_q, g_u. Points ① and ② are circled.
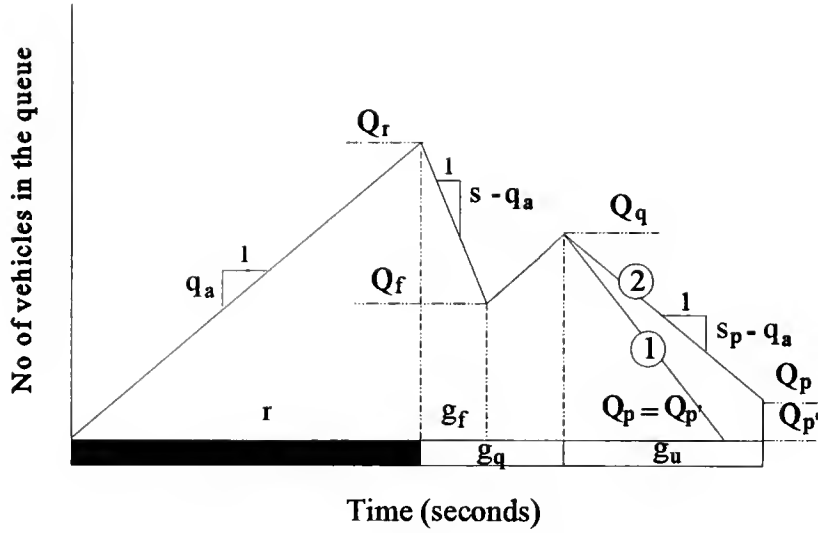
$$Q_r = r\, q_a \qquad\qquad QST = \frac{Q_q}{s_p - q_a}$$

$$Q_f = Q_r - g_f\,(s - q_a)$$

$$Q_q = Q_f + (g_q - g_f)\, q_a \qquad\qquad \text{if } n_{opp} > 1$$

$$Q_q = Q_f + (g_q - g_f)\left(q_a - \frac{s}{1 + P_L\,(E_{L2} - 1)}\right) \qquad \text{if } n_{opp} = 1$$

Condition 1: $QST \le g_u$

$$Q_p = Q_{p'} = 0$$

$$d_1 = \frac{0.5\,[\, r\,Q_r + g_f\,(Q_r + Q_f) + (g_q - g_f)\,(Q_f + Q_q) + Q_q^{\,2} / (s_p - q_a)\,]}{q_a\, C}$$

Condition 2: $QST > g_u$

$$Q_p = Q_q - g_u\,(s_p - q_a)$$

$$Q_{p'} = 0$$

$$d_1 = \frac{0.5\,[\, r\,Q_r + g_f\,(Q_r + Q_f) + (g_q - g_f)\,(Q_f + Q_q) + g_u\,(Q_q + Q_p)\,]}{q_a\, C}$$

Figure A-4. Uniform delay for permitted left turns from a shared lane ($g_q > g_f$).

$$Q_r = r\, q_a \qquad\qquad QST = \frac{Q_q}{s_p - q_a}$$

$$Q_f = Q_r - g_f\, (s - q_a)$$

$$Q_q = Q_r - g_q\, (s - q_a)$$

Condition 1: $QST \leq g_u$

$$Q_p = Q_{p'} = 0$$

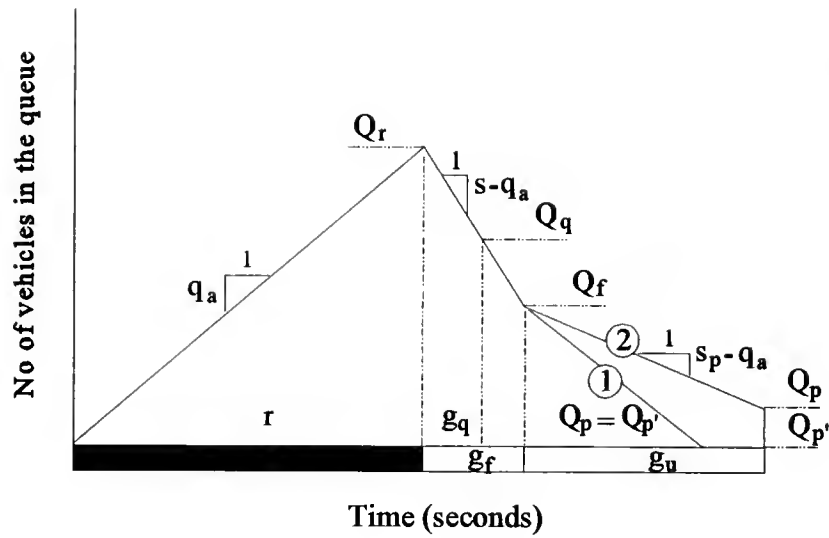$$d_1 = \frac{0.5\ [\ r\, Q_r + g_f\, (Q_r + Q_f) + Q_f^2\ /\ (s_p - q_a)]}{q_a\, C}$$

Condition 2: $QST > g_u$

$$Q_p = Q_f - g_u\, (s_p - q_a)$$

$$Q_{p'} = 0$$

$$d_1 = \frac{0.5\ [\ r\, Q_r + g_f\, (Q_r + Q_f) + g_u\, (Q_f + Q_p)]}{q_a\, C}$$

Figure A-5. Uniform delay for permitted left turns from a shared lane ($g_q \leq g_f$).

$$Q_r = r \, q_a$$

$$QST = \frac{Q_q}{s_p - q_a}$$

$$Q_q = g_q \, (q_a - s_q)$$

$$s_q = 0 \qquad\qquad\qquad\qquad\qquad \text{if } n_{opp} > 1$$

$$s_q = \frac{s'}{E_{L2}} \qquad (\text{where } s' = s / 0.95) \qquad \text{if } n_{opp} = 1$$

Condition 1: $QST \le g_u$

$$Q_p = Q_{p'} = 0$$

$$d_1 = \frac{0.5 \, [\, r \, Q_r + Q_r^2 / (s - q_a) + g_q \, Q_q + Q_q^2 / (s_p - q_a) \,]}{q_a \, C}$$

Condition 2: $QST > g_u$

$$Q_p = Q_q - g_u \, (s_p - q_a)$$

$$Q_{p'} = 0$$

$$d_1 = \frac{0.5 \, [\, r \, Q_r + Q_r^2 / (s - q_a) + g_q \, Q_q + g_u \, (Q_q + Q_p) \,]}{q_a \, C}$$

Figure A-6. Uniform delay for compound left turn protection (Case 1).

$$Q_r = r \ q_a$$

$$Q_{p''} = Q_r - g \ (s - q_a)$$

$$Q_q = Q_{p''} + g_q \ (q_a - s_q)$$

$$s_q = 0 \qquad\qquad \text{if } n_{opp} > 1$$

$$s_q = \frac{s'}{E_{L2}} \qquad (\text{where } s' = s / 0.95) \qquad \text{if } n_{opp} = 1$$

$$QST = \frac{Q_q}{s_p - q_a}$$

Condition 1: $QST \leq g_u$

$$Q_p = Q_{p'} = 0$$

$$d_1 = \frac{0.5 \ [\ r \ Q_r + g \ (Q_r + Q_{p''}) + g_q \ (Q_{p''} + Q_q) + Q_q^2 \ / \ (s_p - q_a) \ ]}{q_a \ C}$$

Condition 2: $QST > g_u$

$$Q_p = Q_q - g_u \ (s_p - q_a)$$

$$Q_{p'} = 0$$

$$d_1 = \frac{0.5 \ [\ r \ Q_r + g \ (Q_r + Q_{p''}) + g_q \ (Q_{p''} + Q_q) + g_u \ (Q_q + Q_p) \ ]}{q_a \ C}$$

Figure A-7. Uniform delay for compound left turn protection (Case 2).

$$Q_r = Q_{p'} + r \, q_a$$

$$Q_q = g_q \, (q_a - s_q)$$

$$s_q = 0 \qquad \qquad \text{if } n_{opp} > 1$$

$$s_q = \frac{s'}{E_{L2}} \qquad \text{(where } s' = s / 0.95) \qquad \text{if } n_{opp} = 1$$
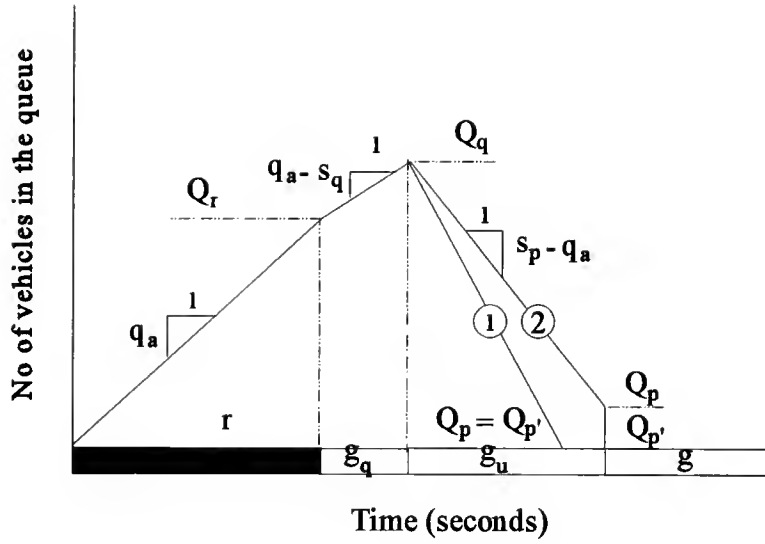
$$Q_p = Q_q - g_u \, (s_p - q_a)$$

$$Q_{p'} = Q_p - S_a$$

$$\text{where} \qquad S_a = \text{Min} \, (\text{Sneakers}_{max} \, , \, Q_p)$$

$$d_1 = \frac{0.5 \, [\, r \, (Q_{p'} + Q_r) + Q_r^2 / (s - q_a) + g_q \, Q_q + g_u \, (Q_q + Q_p) \,]}{q_a \, C}$$

Figure A-8. Uniform delay for compound left turn protection (Case 3).

$$Q_r = r \, q_a$$

$$Q_q = Q_r + g_q \, (q_a - s_q)$$

$$QST = \frac{Q_q}{s_p - q_a}$$

$$s_q = 0 \qquad \text{if } n_{opp} > 1$$

$$s_q = \frac{s'}{E_{L2}} \qquad (\text{where } s' = s / 0.95) \qquad \text{if } n_{opp} = 1$$

Condition 1: $QST \leq g_u$

$$Q_p = Q_{p'} = 0$$

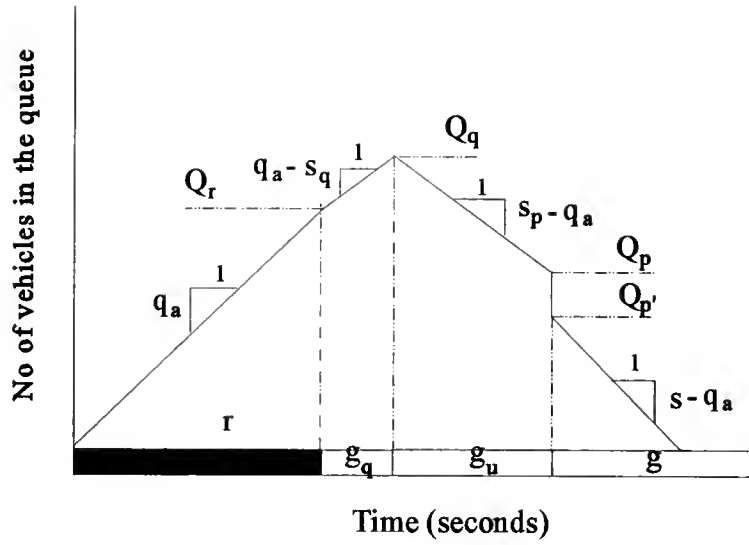$$d_1 = \frac{0.5 \, [\, r \, Q_r + g_q \, (Q_r + Q_q) + Q_q^2 / (s_p - q_a) \,]}{q_a \, C}$$

Condition 2: $QST > g_u$

$$Q_p = Q_q - g_u \, (s_p - q_a)$$

$$Q_{p'} = 0$$

$$d_1 = \frac{0.5 \, [\, r \, Q_r + g_q \, (Q_r + Q_q) + g_u \, (Q_q + Q_p) \,]}{q_a \, C}$$

Figure A-9. Uniform delay for compound left turn protection (Case 4).

$$Q_r = r \, q_a$$

$$Q_q = Q_r + g_q \, (q_a - s_q)$$

$$s_q = 0 \qquad\qquad\qquad\qquad\qquad \text{if } n_{opp} > 1$$

$$s_q = \frac{s'}{E_{L2}} \qquad (\text{where } s' = s / 0.95) \qquad \text{if } n_{opp} = 1$$

$$Q_p = Q_q - g_u \, (s_p - q_a)$$

$$Q_{p'} = Q_p - S_a$$

$$\text{where} \qquad S_a = \text{Min (Sneakers}_{max} , Q_p)$$

$$d_1 = \frac{0.5 \, [\, r \, Q_r + g_q \, (Q_r + Q_q) + g_u \, (Q_q + Q_p) + Q_p{}^2 / (s - q_a) \,]}{q_a \, C}$$

Figure A-10. Uniform delay for compound left turn protection (Case 5).

BIBLIOGRAPHY

1. Highway Capacity Manual, Special Report 209, TRB, National Research Council, Washington, D.C., 1985.

2. Lin, Feng-Bor, "Estimating Average Cycle Lengths and Green Intervals of Semiactuated Signal Operations for Level-of-Service Analysis," Transportation Research Record 1287, TRB, National Research Council, Washington D.C., 1990-1991, pp.119-128.

3. Lin, Feng-Bor, "Applications of 1985 Highway Capacity Manual for Estimating Delay at Signalized Intersections," Transportation Research Record 1225, TRB, National Research Council, Washington D.C., 1989, pp. 18-23.

4. Li, Jing, N. M. Rouphail and R. Akçelik., "Overflow Delay Estimation for a Simple Intersection with Fully-actuated Signal Control," Presented at Transportation Research Board 73rd Annual Meeting, Washington D.C., January 1994.

5. Prevedouros, P. D, "Actuated Signalization: Traffic Measurements and Capacity Analysis," ITE 1991 Compendium of Technical Papers, Institute of Transportation Engineers.

6. Courage, K. G. and R. Akçelik, "A Computational Framework for Modeling Traffic-Actuated Controller Operations," Working Paper NCHRP 3-48-1, Transportation Research Center, University of Florida, Gainesville, 1994.

7. Lin, Feng-Bor, "Estimation of Average Phase durations for Full-Actuated Signals," Transportation Research Record 881, TRB, National Research Council, Washington D.C., 1982, pp. 65-72.

8. Lin, Feng-Bor and F. Mazdeyasna, "Delay Model of Traffic-Actuated Signal Controls," Transportation Research Record 905, TRB, National Research Council, Washington D.C., 1983-1984, pp. 33-38.

9. Akçelik, R., "Analysis of Vehicle-Actuated Signal Operations," Working Paper WD TE 93/007, Australian Road Research Board, Victoria, Australia, 1993.

10. Akçelik, R., "Estimation of Green Times and Cycle Time for Vehicle-Actuated Signals," Presented at Transportation Research Board 73rd Annual Meeting, Washington D.C., January 1994.

11. Orcutt, F. L., "A Primer for Traffic Signal Selection," Public Works-City, County and State, March 1975, pp. 76-80.

12. National Electrical Manufactures Association, "Traffic Control System," Standards Publication No. TS1, Washington D.C., 1976.

13. Vodrazka, W. C., C. E. Lee and H. E. Haenel, "Traffic Delay and Warrants for Control Devices," HRB Record Vol. 366, 1971, pp. 79-91.

14. Gerlough, D. L. and F. A. Wagner, "Improved Criteria for Traffic Signal at Individual Intersections," NCHRP Report 32, TRB, National Research Council, Washington D.C., 1976.

15. Bang, K. and L. Nilsson, "Traffic Signal Control with Long Loop detectors," Traffic Engineering and Control, Vol. 11, No. 11, March 1970, pp. 525-527.

16. Cribbins, P. E. and C. A. Meyer, "Choosing Detectors and Placing Them Right," Traffic Engineering, Vol. 45, No. 1, January 1975, pp. 15-18.

17. Webster, F. V., "Traffic Signal Settings," Road Research Paper No. 39, Scientific and Industrial Research, HMSO, London, 1958.

18. Miller, A. J., "Settings for Fixed-Cycle Traffic Signals," Operations Research Quarterly, Vol. 14, No. 4, 1963, pp. 373-386.

19. Newell, G. F., "Properties of Vehicle-Actuated Signals: I. One-Way Streets," Transportation Science, Vol. 3, No. 1, February 1969, pp. 30-52.

20. Newell, G. F. and E. E. Osuma, "properties of Vehicle-Actuated Signals: II Two-Way Streets," Transportation Science, Vol. 3, No. 2, May 1969, pp.99-125.

21. Staunton, M. M., "Vehicle Actuated Signal Controls for Isolated Locations," AN FORAS FORBARTHA, The National Institute for Physical Planning and Construction Research, No. RT-159, Dublin, Ireland, September 1976.

22. Bang, K. L., "Optimal Control of Isolated Traffic Signals," Traffic Engineering and Control, Vol. 17, No. 7, July 1976, pp. 288-292.

23. Tarnoff, P. and P. S. Parsonson, "Selecting Traffic Signal Control at Individual Intersections," NCHRP Report 233, TRB, National Research Council, Washington D.C., June 1981.

24. Lin, Feng-Bor, "Optimal Timing Setting and Detector Lengths of Presence Mode Full-Actuated Control," Transportation Research Record 1010, TRB, National Research Council, Washington D.C., 1985, pp. 37-45.

25. Kell, J. H. and T. J. Fullerton, "Manual of Traffic Signal Design", Prentice-Hall, Englewood Cliffs, N. J., 1982.

26. Bullen, A. G. R., N. Hummon, T. Bryer and R. Nekmat, "EVIPAS:A Computer Model for the Optimal Design of a Vehicle-Actuated Traffic Signal," Transportation Research Record 1114, TRB, National Research Council, Washington D.C., 1987, pp. 103-110.

27. Messer, C. J. and M. Chang, "Traffic Operation of Basic Traffic-Actuated Control Systems at Diamond Interchanges," Transportation Research Record 1114, TRB, National Research Council, Washington D.C., 1987, pp. 54-62.

28. Courage, K. G. and J. Z. Luh, "Development of Guidelines for Implementing Computerized Timing Design at Traffic Actuated Signals, Final Report Volume 1," Isolated Intersection Implementation, Transportation Research Center, University of Florida, Gainesville, February 1989.

29. Bullen A. G. R., "The Effects of Actuated Signal Settings and Detector Placement on Vehicle Delay," Presented at Transportation Research Board 68th Annual Meeting, Washington, D.C., January 1989.

30. Kell, J. H. and T. J. Fullerton, Manual of Traffic Signal Design, 2nd Edition. Institute of Transportation Engineers, Prentice-Hall, Englewood Cliffs, N. J., 1991.

31. Bonneson, J. A. and P. T. McCoy, "A Methodology for Evaluating Traffic Detector Designs," Presented at Transportation Research Board 72nd Annual Meeting, Washington D.C., January 1993.

32. Jovanis P. P. and J. A. Gregor, "Coordination of Actuated Arterial Traffic Signal System," Journal of Transportation Engineering, Vol. 112, No. 4, July 1986.

33. Courage, K. G. and C. E. Wallace, "Development of Guidelines for Implementing Computerized Timing Design at Traffic Actuated Signals, Final Report Volume 2," Arterial System Implementation, Transportation Research Center, University of Florida, Gainesville, February 1989.

34. Chang, E. Chin-Ping and J. Koothrappally, "Field Verification of Coordinated Actuated Control," Presented at Transportation Research Board 73rd Annual Meeting, Washington D.C., January 1994.

35. Luh, J. Z. and K. G. Courage, "Late-Night Traffic Signal Control Strategies for Arterial Systems," Transportation Research Record 1287, TRB, National Research Council, Washington D.C., 1990-1991, pp. 205-211.

36. Lin, Feng-Bor and M. C. Percy, "Vehicle-Detector Intersections and Analysis of Traffic-Actuated Signal Controls," Transportation Research Record 971, TRB, National Research Council, Washington D.C., June 1984, pp. 112-120.

37. Lin, Feng-Bor and S. Chen, "Relationships between Queuing Flows and Presence Detectors," ITE Journal Vol. 55, No. 8, August 1985.

38. Lin, Feng-Bor, "Evaluation of Queue Dissipation Simulation Models for Analysis of Presence-Mode Full-Actuated Signal Control," Transportation Research Record 1005, TRB, National Research Council, Washington D.C., 1984, pp. 46-54.

39. Chang, Gang-Len and J. C. Williams, "Estimation of Independence of Vehicle Arrival at Signalized Intersections: A Modelling Methodology," Transportation Research Record 1194, TRB, National Research Council, Washington D.C., 1988, pp. 42-47.

40. Chang, Gang-Len and A. Kanaan, "Variability Assessment for TRAF-NETSIM," Journal of Transportation Engineering, Vol. 116, No. 5, September/October, 1990, pp. 636-657.

41. Cowan, R. J., "Useful Headway Models," Transportation Research, Vol. 9, No. 6, 1975, pp. 371-375.

42. Troutbeck, R. J., "Does Gap Acceptance Theory Adequately Predict the Capacity of a Roundabout," Proc. 12th ARRB Conf. 12 (4), 1984, pp. 62-75.

43. Troutbeck, R. J., "Average Delay at an Unsignalized Intersection with Two Major Stream Each Having a Dichotomised Headway Distribution," Transportation Science, Vol. 20, No. 4, 1986, pp. 272-286.

44. Troutbeck, R. J., "Current and Future Australian Practices for the Design of Unsignalized Intersections," In: Intersections Without Traffic Signals (Edited by W. Brilon), Proceedings of an International Workshop (Bochum, West Germany), Springer-Verlag, Berlin, 1988, pp.1-19.

45. Troutbeck, R. J., "Evaluating the Performance of a Roundabout," Special Report DR 45, Australian Road Research Board, Victoria, Australia, 1989.

46. Troutbeck, R. J., "Roundabout Capacity and the Associated Delay," In: Transportation and Traffic Theory (Edited by M. Koshi), Prodeedings of Eleventh International Symposium on Transportation and Traffic Theory (Yokohama, Japan). Elsevier, New York, 1990, pp. 39-57.

47. Troutbeck, R. J., "Recent Australian Unsignalized Intersection Research and Practices," In: Intersection without Signal II (Edited by W. Brilon), Prodeedings of Eleventh International Workshop (Bochum, West Germany), Springer-Verlag, Berlin, 1991, pp. 239-257.

48. Nemeth, Z. A. and J. R. Mekemson, "Comparison of SOAP and NETSIM: Pretimed and Actuated Signal Controls," Transportation Research Record 905, TRB, National Research Council, Washington D.C., 1983-1984, pp. 84-89.

49. Akçelik, R., "The Highway Capacity Manual Delay Formula for Signalized Intersections," ITE Journal, Vol.58, No.3, March 1988, pp. 23-27.

50. Hagen, L. T. and K. G. Courage, "Comparison of Macroscopic Models for Signalized Intersection Analysis," Transportation Research Record 1225, TRB, National Research Council, Washington D.C., 1989, pp. 33-44.

51. May, A. D. and E. Gedizlioglu and L. Tai, "Comparative Analysis of Signalized Intersection Capacity Methods," Transportation Research Record 905, TRB, National Research Council, Washington D.C., 1983-1984, pp. 118-127.

52. EZVIPAS 1.0 User Guide, Viggen Corporation, McLean, VA, 1993.

53. Akçelik, R. and E. Chung, "Calibration of the Bunched Exponential Distribution of Arrival Headways," Road and Transport Research, Vol. 3, No.1, 1994, pp. 42-59.

54. Courage, K. G., "Remote Monitoring of Arterial Traffic Control System Operation," Transportation Research Center, University of Florida, Gainesville, 1990.

55. SAS Language Guide for Personal Computers. Release 6.03 Edition, SAS Institute, Inc., Cary, N.C., 1988.

56. Jiang Chian-Chi and K.G. Courage, "Modeling Coordinated Operation at Traffic-Actuated Intersections," Working paper NCHRP 3-48-7, Transportation Research Center, University of Florida, Gainesville, May 1995.

57.   Courage, K. G., D. B. Fambro, R. Akçelik, P-S Lin, M. Anwer, "Capacity Analysis of Traffic-Actuated Intersections," NCHRP 3-48 Draft Interim Report, TRB, National Research Council, Washington D.C., January, 1995.

BIOGRAPHICAL SKETCH

Pei-Sung Lin was born in Hsinchu, Taiwan, on January 2, 1964. He attended elementary and junior high schools in Hsinchu. After passing the competitive senior high school entrance examination, he was admitted to the Hsinchu Senior High School as the number two student among more than 5,000 participants.
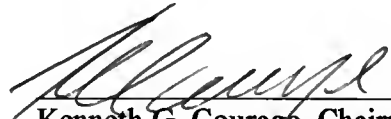
In September 1982, he was admitted to the Department of Civil Engineering at the National Chung-Hsing University. In September 1989, he attended the Graduate School of the University of Texas at Austin. His specialized area was in transportation engineering. He was awarded the Master of Science in August 1991. During the course of his studies, he was a research assistant and participated in two research projects for the Texas State Department of Highway and Public Transportation. During the course of his academic training, he developed his interests in research.

In September 1992, he entered the Graduate School of the University of Florida where he pursued the degree of Doctor of Philosophy in civil engineering, specializing in transportation. In 1993, he was a graduate assistant in the Technology Transfer Center and then he worked as a technical assistant in the Center for Microcomputers in Transportation (McTrans Center) for transportation software testing and maintenance. In November 1993, he won the first place of 1993 Florida ITE Past President Paper competition. In January

1994, he was honored to participate in the National Cooperative Highway Research Program (NCHRP) project 3-48 concerning capacity of traffic-actuated signalized intersections. During his studies at the University of Florida, he received an award for his academic achievement of earning a cumulative 4.0 grade point average from the Office of International Studies and Programs.

Mr. Pei-Sung Lin was married to Hui-Min Wen when he studied at the University of Florida. He is a student member of Institute of Transportation Engineers.

I certify that I have read this study and that in my opinion it conforms to acceptable standards of scholarly presentation and is fully adequate, in scope and quality, as a dissertation for the degree of Doctor of Philosophy.
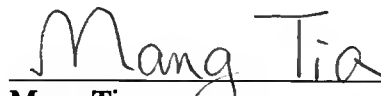
Kenneth G. Courage, Chairman
Professor of Civil Engineering

I certify that I have read this study and that in my opinion it conforms to acceptable standards of scholarly presentation and is fully adequate, in scope and quality, as a dissertation for the degree of Doctor of Philosophy.

Charles. E. Wallace
Professor of Civil Engineering

I certify that I have read this study and that in my opinion it conforms to acceptable standards of scholarly presentation and is fully adequate, in scope and quality, as a dissertation for the degree of Doctor of Philosophy.
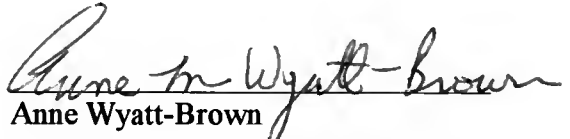
Mang Tia
Professor of Civil Engineering

I certify that I have read this study and that in my opinion it conforms to acceptable standards of scholarly presentation and is fully adequate, in scope and quality, as a dissertation for the degree of Doctor of Philosophy.
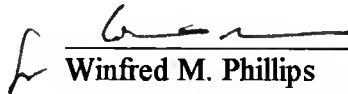
Sherman X. Bai
Assistant Professor of Industrial & System Engineering

I certify that I have read this study and that in my opinion it conforms to acceptable standards of scholarly presentation and is fully adequate, in scope and quality, as a dissertation for the degree of Doctor of Philosophy.

Anne Wyatt-Brown
Assistant Professor of Linguistics

This dissertation was submitted to the Graduate Faculty of the College of Engineering and to the Graduate Council, and was accepted as partial fulfillment of the requirements for the degree of Doctor of Philosophy.

December 1995

Winfred M. Phillips
Dean, College of Engineering

Karen A. Holbrook
Dean, Graduate School